Response to reviewers on "Glacial cycles simulation of the Antarctic Ice Sheet with PISM – Part 1: Boundary conditions and climatic forcing" by Torsten Albrecht et al.

We would like to thank the reviewers Johannes Sutter and Lev Tarasov for the very constructive criticism of our manuscript. These reviews have considerably improved the manuscript for which we are grateful.

We were able to address all requests. In particular, we reorganized the manuscript content for better readibility and added a summary of the sensitivity results as additional table as basis for a better motivated ensemble parameter selection. We also included information on the used bedrock thermal model.

In order to facilitate the reading of this document, the referee's comments are given in **blue** and in **black** the author's response.

Response to Referee 1 Johannes Sutter (johannes.sutter@awi.de)
()

We thank Johannes Sutter for his excellent suggestions and thoughtful comments.

The study by Albrecht et al. is an impressive compendium of Antarctic Ice Sheet ensemble simulations covering the response of the ice sheet to different forcing settings and ice sheet model parameterizations. This manuscript is poised to become standard literature for people starting to use the Parallel Ice Sheet Model (PISM) as well as for scientist which already use PISM. The scope of the manuscript fits well into the topics covered by The Cryosphere and I think it is a nice entry into the ice sheet modelling literature.

That being said, the manuscript needs some additional work to improve the readability and to clarify the main "take-aways" for the reader. Due to its holistic scope and length it is sometimes difficult to follow the line of thought. Also typos and the german-style syntax sometimes hampers the reader to fully grasp the content of the manuscript. In isolation these points are very minor but clustered throughout the manuscript they make it difficult to enjoy the overall high quality of this work.

I will provide some general remarks which I deem necessary to be addressed followed by minor comments. Please also find comments and corrections to the manuscript in the annotated attached pdf.

Once again, we would like to thank the reviewer for his very constructive assessment and suggestions for improvement, they really improve the readability of manuscript considerably. We are glad that he considers the study worthy for publication in The Cryosphere (TC).

1. The manuscript truly has an epic length and discusses the impact of different model parameterisations, forcing approaches as well as specific research questions regarding e.g. Termination I. In theory the manuscript could be actually split into two publications, one covering the uncertainties intrinsic to the choice of model parameterisations and climate forcings, and one investigating specifically the response of the AIS to the latter

in glacials and Terminations, specifically Termination I. I assume the authors would like to abstain from splitting the manuscript in two, so I suggest reordering the discussion of the results into a part covering the effect of different parameterisations and forcings (e.g. individual forcings versus combined forcings) and a part specifically addressing the intricacies of glacial termination and the impact of model parameterisations and forcings during that period.

We very much understand the reviewer's impression, but as this study consists already of two parts (sensitivity experiments in part 1 and ensemble analysis in part 2), we preferred to reorganize the manuscript with focus on the model description and on the model parameter selection for the ensemble study in the companion paper (Albrecht et al., 2019b). The selection is mainly based on two criteria, the reproduction of the present-day state within an uncertainty range and the LGM ice volume sensitivity to parameter change, while the paramter choice also covers the four uncertainty classes and both Antarctic parts. We totally agree, that in particular the last deglaciation is of particular interest for the community, such that we would like to discuss this aspect in more detail in a separate study.

2. Model results are almost exclusively illustrated as integrated variables (ice volume or SLE ice volume). It would be nice to see some illustrations of ice sheet geometry as modelled for the LIG, LGM and present day, either within the manuscript or as e.g. supplementary videos.

We understand that so much more can be learned about the model's sensitivity to the choice of parameters and boundary conditions with a more detailed look to certain Antarctic regions. Yet, this is boyond the scope of this study, which focusses on a first estimate of relative parameter sensitivity, as selection criterion for the ensemble analysis in the companion paper (Albrecht et al., 2019b).
In fact, there is already a movie of the reference simulation available in the assets of this manuscript submission covering LIG, LGM and PD (see https://doi.org/10.5446/41779). As the reference simulation corresponds to the best fit simulation in the companion paper (Albrecht et al., 2019b) there are also some more plots in the corresponding Sect. 3.3 covering LGM, last deglaciation and present-day. We have already mentioned this in the introduction section:
*„The sensitivity of the modeled ice volume above flotation to different choices of parameters and boundary conditions is evaluated as the difference to a baseline simulation (Movie: Albrecht, 2019) that is consistent with the model configuration of the best fit ensemble simulation presented in the companion paper (Albrecht et al., 2019, **see plots in Sect. 3.3**).*"

3. Currently, there is a study in TCD by Tigchelaar et al. (https://doi.org/10.5194/tc-2019-83) addressing the effect of isolated forcings versus combined forcings on late Quaternary (ca. last 400 kyr) ice sheet evolution. A similar discussion can be found in condensed form in Section 4.5 of this manuscript. It would be nice to include a comparison to the findings in Tigchelaar et al. as to put the results presented here in perspective.

Yes, we noticed the study by Tigchelaar et al. (2019), published in TCD just one week after our submission. We have added a short paragraph to Sect. 4.5:

„Another recent study using the PSU-ISM ice sheet model also finds a dominance of

atmospheric and sea-level forcing on the Antarctic ice volume, over the last four glacial cycles (Tigchelaar et al., 2019), which together drive glacial-interglacial ice volume changes of 12–14 m SLE, while ocean temperature forcing is almost negligible, also during interglacials. Here, we do not want to go into the details of this study, which uses a comparably coarse output of an Earth System Model of intermediate complexity for the atmospheric and ocean forcing instead of a scaling with ice core temperature reconstructions. As a key result, Tigchelaar and colleagues find much smaller individual ice volume changes, which amount to less than half of the full ice volume response. In our simulations, however, the individual response to sea-level forcing (and surface temperature forcing) as well as the sum of all individual forcings exceed the combined response. This is partly due to the fact, that precipitation forcing (up to 50% less during glacial climate) provides a strong negative effect on the ice volume in full forcing case, which seems to be weaker in the "atm" forcing in Tigchelaar et al. (2019, ca. 15% in Fig. 8). If we consider the LGM and present-day state as rather stable states, a certain perturbation threshold need to be hit to initiate the (non-linear) transition (Termination I) into the other state. In our simulations this threshold can be reached with individual forcings, while in the other study the combined superposition is required.“

Minor comments:
In general, throughout the manuscript you often omit articles ("e.g. the") which makes some sentences hard to read. I marked the spots which where most obvious to me (attached annotated pdf) but maybe I missed a couple.

Thanks, we revised and rephrased the manuscript accordingly.

It would be helpful to know which "baseline" parameter set was used in the parameter sensitivity experiment shown in the various volume line-plots. Is it the one highlighted (in brackets) in Table 1? I guess you put this Table almost to the end of the manuscript as to provide the reason for your parameter selection in the preceeding sections. I would prefer to see such a Table at the very beginning of the paper as to get a quick overview of which parameters have been investigated and which are the optimal combination for paleo-studies with PISM. Some readers might not get to page 38 and miss the table altogether.

We appreciate the reviewer's perspective. Yes, the parentheses are the reference values. We have shifted the table to the PISM introduction and added this (baseline) information to the caption. We have also added a second Table to the end of the results section summarizing the sensitivity stastistic for all varied parameters and boundary conditions.

Check your use of past tense, you almost never use it, I tried to mark all instances in the annotated pdf.

Thanks, we changed this in the manuscript.

You mostly discuss glaciation timescales, glacial maximum ice volume and glacial termination while only shortly touching on the effects of different parameterisations and forcings on interglacial ice volume and extent. Is there a specific reason for this? Also, in your simulations MIS5e ice volume seems to be very similar to your simulated present day ice volume. I think it would be worth discussing this briefly in the manuscript.

LIG is indeed an interesting time period covered by the two-glacial-cycle (2GC) simulations. We found that WAIS collapse at LIG, as the most likely candidate for additional ice mass loss in comparison to PD (as in Sutter et al., 2016), is prohibited in all our simulations. However, discussing the required conditions for WAIS collapse at LIG would fill a separate study.

We find relatively low sensitivity to (warmer than present) ocean forcing as we do not interpolate melt rates over the grounding line. Additionally, the used precipitation scaling with temperature forcing seems to compensate for the mass losses by sub-shelf melting (Fig. 25, light and dark blue). There is also another feedback at play (precipitation scaling with surface elevation change), which seems to stabilize grounding line retreat (we have appended a corresponding simulation to Fig. 25, light orange). Till water availability and till friction angle seem to play an important role as well. The optimized till friction angles yields intermediate values of up to 20° in the inner WAIS, while the parameterization with respect to bed-topography suggest minimal till friction angles in this deep marine region (e.g. 5°) which increases the risk for collapse (as in Fig. 13).

We have discussed parts of it in the companion study, and have added a paragraph to the revised ocean forcing section *and to the basal paramter section*:

„Ocean forcing likely plays a key role in warmer than present-climates. However, we do not see this effect in our simulations during the Last Interglacial. Although ocean and surface temperatures rise by 1-2 K above present we find similar ice volumes as for present-day, in all our simulations. Precipitation scaling and the till properties seem to play an important role in stabilizing WAIS and preventing from collapse. However, a thorough investigation of necessary model settings for WAIS collapse during LIG would fill a separate study.“

„Till friction angle is an important uncertain parameter for possible WAIS collapse. As no (partial) WAIS collapse is induced in the simulations, we find very similar ice volumes for last interglacial and present day.“

p8, l214-216 Doesn't your study from last year (Kingslake et al. 2018) show sensitivity specifically of the Ross Sea grounding line to the Eigencalving parameterization (Extended Data Figure 7)? I guess it is a question of the ice sheet state and memory effects whether the calving parameterization can play a role or not.

The effect of the eigencalving constant K in both this study and in the previous study (Kingslake, Scherer, Albrecht et al., 2018) is quite similar. For the reference value $K=1\times10^{17}$ m s and larger we do not see much influence on the grounding line and ice volume history, as the eigencalving rate is mainly limited by the minor eigenvalue of the strain rate tensor. For smaller values (e.g. $K=1\times10^{16}$ m s) we find generally smaller calving rates and the ice shelf front can advanced up to the edge of the continental shelf (where an additional calving condition applies), rather independent of climate conditions. This adds some more buttressing and hence causes slightly higher interglacial ice volumes. In fact, a lower K value seems to initiate earlier deglaciation in both studies, which may be a result of existing ice shelves in the LGM state, which become unstable in response to rising sea-level and ocean temperatures. We added some more discussion on this issue and linked to the previous study.

*„For a smaller value of 1×10^{16} m s**, in contrast,** estimated calving rates tend to be smaller than terminal ice shelf flow and thus calving front expands up to the edge of the continental shelf**. The additional buttressing supports a slightly larger present-day ice volume, while in turn the more extended LGM ice shelves can respond***

effectively to increasing sea level and ocean temperatures, leading to slightly earlier deglaciation (Kingslake, Scherer, Albrecht et al., 2018) ."

Naturally for such an extensive manuscript, the discussion sections is covering a lot of ground which makes it difficult to structure. Maybe one or two sentences at the beginning of the discussion preparing the reader with respect to the structure would be helpful (e.g. in the following we summarize the main findings of our study with regard to the impact of different parameterisation and climate forcing choices on the evolution of the Antarctic Ice Sheet during the last glacial cycles analysed above.).

We now provide an overview over the manuscript structure and contents at the end of the introduction. And we rephrased the beginning of the conclusions: „*In this study we have run PISM simulations of the Antarctic Ice Sheet over the last two glacial cycles ~~and investigated the sensitivity of ice volume history to variations in~~*. **In the following we summarize the main findings of our analysis with regard to the impact of different** *model parameter settings, boundary conditions and climate forcing* **choices on the evolution of the Antarctic Ice Sheet.**"

We also added a transition sentence just before the first results section 2: „*In the following sections we will discuss different choices of model parameterizations, boundary conditions and climatic forcings on the sea-level relevant Antarctic Ice Sheet history over the last two glacial cycles.*"

References

Albrecht, T., Winkelmann, R., and Levermann, A.: Glacial cycles simulation of the Antarctic Ice Sheet with PISM – Part 2: Parameter ensemble analysis, The Cryosphere Discuss., https://doi.org/10.5194/tc-2019-70, in review, 2019b.

Kingslake, J., R. P. Scherer, T. Albrecht, J. Coenen, R. D. Powell, R. Reese, N. D. Stansell, S. Tulaczyk, M. G. Wearing, and P. L. Whitehouse. "Extensive retreat and re-advance of the West Antarctic Ice Sheet during the Holocene." *Nature*558, no. 7710 (2018): 430.

Sutter, J., Gierz, P., Grosfeld, K., Thoma, M., & Lohmann, G. (2016). Ocean temperature thresholds for Last Interglacial West Antarctic Ice Sheet collapse. *Geophysical Research Letters*, *43*(6), 2675-2682.

Tigchelaar, Michelle, Axel Timmermann, Tobias Friedrich, Malte Heinemann, and David Pollard. "Nonlinear response of the Antarctic ice sheet to Quaternary sea level and climate forcing." The Cryosphere Discuss., https://doi.org/10.5194/tc-2019-83, in review, 2019.

Response to Referee 2 Lev Tarasov (lev@mun.ca)
()

We thank Lev Tarasov for his helpful suggestions and very detailed and helpful review.

This large paper explores PISM sensitivities to various parametric, forcing, and boundary condition uncertainties for the AIS glacial cycle context. Aside from a need for consolidation and organizational/editorial work and some missing critical information about the model, for me the underlying weakness stems from the choice of journal. I take the Cryosphere to be about the science, ie understanding the world around us. Models are a tool for this, but in this "cookbook", the model has become the dominant focus.

We understand the reviewer's suggestion to consider a more model-focussed journal such as GMD instead of The Cryosphere (TC) and we agree that the model sensitivity has received the dominant focus in this study. Although, we actually learn many new things from this study, for instance when we compare individual and combined effects of climatic and sea-level forcing. Also previous glacial model descriptions have been published in TC with quite some impact (e.g. Briggs et al. (2013), Winkelmann et al. (2011)). We believe that TC is the perfect journal to reach the growing scientific community, who uses the PISM for various applications to actually gain a better understanding of the cryosphere within the climate system.

There are also a few key implicit assumptions that are never justified, eg the choice of only 4 ensemble parameters. Is the relevant uncertainty in the climate forcing over the last 2 glacial cycles for the whole Antarctic ice sheet really reducible to a single parameter? Is the uncertainty in basal drag representation well captured by a single parameter? This is effectively an implicit claim of this paper for which I'm curious to see what kind of justification can be provided (aside from the choice to use an inefficient full factorial sensitivity analysis with its resulting computational limits).

The reviewer raises an important limitation of the ensemble design regarding the reduced selection of relevant parameters, which we have now discussed in much more detail in the companion paper in Albrecht et al. (2019b). Our first intension was to allow for a close comparison to the (full factorial sampling) ensemble analyses by Pollard et al. (2016, 2017). Yet, they used a different model and different model parameterizations and varied mainly oceanic and solid Earth parameters.
In our study, the parameter selection criteria are mainly the sensitivity of both present-day and LGM ice volume to parameter change (we made that clearer in the manuscript). Another aspect was to have one representing parameter for each uncertainty class, as well as a balanced representation of the two Antarctic parts (WAIS and EAIS). Regarding climate forcing, we showed that the parameter PREC fulfilled best the selection criteria, although other climate-related parameters may also have a relevant impact, i.e. for deglaciation. For the basal sliding parameterization we find the largest uncertainties. In fact, we could have additionally tested different paramterizations implying an even larger uncertainty. Pollard et al. (2016, 2017) found the sliding coeffcient underneath modern ice shelves to be the most relevant of their ensemble paramters. We have run an additional basal ensemble, as discussed in the Appendix A of the companion paper (Albrecht et al.,

2019b) and found for variation of a similar till parameter on the continental shelf a much stronger variability in the aggrgated scores, than for the PPQ parameters. However, to what extent the one selected paramter PPQ can represent the uncertainty of the basal processes was not so clear when running the sensitivity experiments presented here. This is something we can learn from the ensemble analysis (including paleo data scoring), in particular when taking into account a more refined parameter space.

Furthermore, the main reliance on a single metric (ice volume evolution) masks many other potential sensitivities in the model (eg grounding line position for different basins, regional ice thickness at LGM for various ice core sites,...). Though other aspects are at times discussed and a few ice sheet thickness snapshots are shown, without a detailed comparative table of all tested parameters and various metric values, it's hard to see any clear justification for the chosen parameters.

The usage of a single aggregated metric provides certainly a very limited view. But in order to avoid confusion and regarding the number of uncertain model parameters, we decided in part 1 to compare the modeled ice volume sensitivity with a reference simulation (with focus on present-day and LGM states), which provides a first one-dimensional estimate of parameter relevance. This is an excellent suggestion to add a comparative table for the main selection criteria, we used (see Table 2 with means and standard deviations in revised manuscript). However, using statistical means over a few samples can provide only a rough comparison of parameter sensitivity. For this relatively limited approach we have at least a chance to attribute anomalies to a range of physical parameter effects. In part 2 (Albrecht et al., 2019b), we actually do a second step and consider the combined affects of parameter variation on the Antarctic ice volume history, but with a closer look to certain key regions.

The submission states that they "identify relevant model parameters and motivate plausible parameter ranges" but I find the approach weak and shallow. I would submit that at the minimum, ensemble parameter selection (in good part by appropriate sensitivity analysis) should show that within observational/proxy uncertainties, the model + ensemble parameters can "bound reality" and capture relevant uncertainties. This is not explicitly done. And given available proxies, the comparative description of "reality" should be much more than just the ice volume time series.

We understand that this sentence suggests to find „all" relevant parameters. We make this clearer in the manuscript, that we select one representative parameter for each group of uncertainty, namely climate forcing, basal sliding, as well as ice and Earth dynamics, such that the selection criteria with respect to the Antarctic ice volume are hit. From the sensitivity analysis we can infer a best guess of the individual parameter range, such that the modern observed ice volume can be re-produced within some uncertainty. For the ensemble, however, we chose the parametric range large enough to account for possible effects of parameter interaction. We reformulated the last paragraph of the abstract:

„For each of the different model uncertainty groups with regard to climatic forcing, ice and Earth dynamics and basal processes, we select one representative model parameter that captures relevant uncertainties and motivate corresponding parameter ranges that bound the observed ice volume at present. The four selected parameters are systematically

varied in a parameter ensemble analysis, which is described in a companion paper."

This paper would strongly benefit from some consolidation (few will read this many pages), and a summary table with various metrics comparing the glacial cycle sensitivity to the various possible parameters discussed. This table would help justify the choice of final ensemble parameters.
Wrt paper content/consolidation, as a general rule, think of who your intended audience is. For the Cryosphere, it has to be more than the the few dozen of us doing glacial cycle AIS modelling. Include what is relevant to that audience and stick the rest in a supplement for the smaller community who will be interested in all the details (keeps page charges down as well...). This problem is also evident in the overly detailed conclusions section. Again, very few readers are going to care about the detailed sensitivity range of your model setup to your 4 chosen ensemble parameters. That information would be much more usefully presented in a summary table with a more complete set of metrics.

As already stated above, we very much apreciate the reviewer's suggestion for a parameter sensitivity range overview table and added such a table to the revised manuscript. We also consolidated the main manuscript content, such that it should be more suitable for a broader range of TC readers.

I did like the approach of section 4.3 (ocean temperature forcing is a challenge), but I'm surprised no discussion is raised about associated uncertainties, assumptions, and limitations. The biggest assumption is that the critical stabilization ratio of mid−depth Antarctic ocean temperature and global mean temperature anomaly from a single datapoint (ie from a single model) appropriately reflects the real ocean response.

This is certainly a good point, and we added some more details to the manuscript.

"A comparison to reconstructions with a GCM in the TraCE-21ka project (Liu et al., 2009) shows that short warming periods above present level can occur at intermediate depth, e.g. during ACR around 14 kyr BP, which can not be adequately resolved with our approach. The GCM ocean data are bounded below by the pressure melting point...
The here presented parameterization assumes that ocean water masses at depth below 500 m can access ice shelf cavities and induce melting, which is certainly very simplified regarding the complex topography flow patterns around Antarctica. Also, we used data from a simplified sensitivity experiment with ECHAM5/MPIOM, for a much warmer than present climate, which implies various model uncertainties. We had to make assumptions about a suitable response function, which is fitted to model data that are averaged over certain regions and ocean depths, implying further uncertainties."

However, the glacial-interglacial ice sheet volume response in our experiments turns out to be not very sensitive to the actual choice of the ocean temperature forcing, which might be different with a closer look into the deglaciation or warmer-than-present periods.

If the central purpose of this paper is to be a "cookbook for the

growing comunity of PISM users" then I would think GMD would be more
appropriate for this paper. This would mitigate some (but not all) of
my issues raised here.

We have discussed the preference for the TC journal already above.

This paper would also benefit from more attention to punctuation,
appropriate completeness of figure captions, and consistent
description of symbols when first introduce. A reviewer is not meant
to be a copy editor, so I have only identified example infractions of
this in my detailed comments below.

We did not mean to upset the reviewer with our oversight mistakes. We went through the
manuscript and double-checked symbols, figure captions and formulations.

specific comments

l.26: „Coupled climate−ice sheet systems models are computationally too expensive in
order to run many long simulations"
depends on the complexity of the climate model and what is meant by "long", cf
Bahadory and Tarasov, GMD 2018

Definitely true, we were thinking of GCM complexity, but we are happy to emphasize this
option in combination with EMICs:

„*Coupled climate-ice sheet systems models* **can be** ~~are~~ *computationally* ~~too~~ *expensive in
order to run* ~~many long~~ **hundreds of full glacial-cycle** *simulations*, **depending on their
complexity (e.g., Bahadory and Tarasov, 2018, using a model of intermediate
complexity with about 1 kyr per day on one core)**.*"*

l.34: „parameters need to be constrained and calibrated (Briggs et al., 2014)"
that wasn't a calibration, just a large ensemble analysis (cf Tarasov et al, EPSL 2012 for
more of a sense what a full calibration entails)

Yes, we replaced „and calibrated" by „*with observational data* ".

l.75: „Here we use the non−conserving hydrology model"
pretty crude to call this a model −> Here we use the non−conserving sub−glacial
hydrology parametrization

Ok. It is actually the off-mode of the implemented mass-conserving sub-glacial (routing)
hydrology model in PISM (Bueler & van Pelt, 2015), but we agree to call this mode
„parameterization" here.

l. 81: „PISM uses a generalized version of the Lingle−Clark bedrock deformation model
(Bueler et al., 2007), assuming an elastic lithosphere, a resistant asthenosphere and a
spatially−varying viscous halfspace below the elastic plate (Whitehouse, 2018)."
What aspect of the viscous half−space is spatially varying? Viscosity, thickness, ...?

In deed, this seems to be wrong and has been changed to:

*„PISM uses a **modified** ~~generalized~~ version of the Lingle-Clark bedrock deformation model (Bueler et al., 2007), assuming an elastic lithosphere **and** a resistant asthenosphere ~~and a spatially-varying~~ **with** viscous **flow in the** half-space below the elastic plate (Whitehouse, 2018)."*

I.83: „The computationally−efficient bed deformation model has been improved to account for changes in the load of the ocean layer around the grounded ice sheet, due to changes in sea−level and ocean depth."
how is sea−level being computed?

We use the global mean sea-level height as forcing, which affects the ice via the flotation crierion and hence the grounding line position. In order to account for changes in ocean load, we compute the ocean layer thickness with respect to changes in bed topography and global mean sea-level stand. There is no self-consistent sea-level equation solved.

We added *„**global mean** sea-level **height**"* to the mansucript to avoid false expectations.

I. 90: „PISM paleo simulations are initiated with a spin−up procedure for prescribed ice sheet geometry, in which the three−dimensional enthalpy field can adjust to mean modern climate boundary conditions over a 200 kyr period."
given the thermodynamic timescale of the Antarctic ice sheet, it makes no sense to equilibrate against " mean modern climate boundary conditions" when that is not the mean boundary condition over the last 200 kyr.

Yes, this has not been the best model choice. But this aspect is covered in Sect. 5.1: „Energy spin-up procedure and intrinsic memory" (now moved to Sect. 1.3 in the revised manuscript). The difference for the ice volume reconstruction, however, is within the „intrinsic" uncertainty of up to 1m SLE.

I. 110: „For consistency reasons with the used PISM version, we use ocean water density here"
I see no justification for this. This should be fixed (and should be easy to fix).

Yes, this change has been already merged into the development branch of PISM (https://github.com/pism/pism/issues/412) for the PISM output, but as the difference in sea-level equivalent ice volume is less than 2.4%, we did not want to throw away previous simulations results.

I. 111: „In fact, a density of 1000 kg m^-3 should be used instead as ice melts to fresh water"
Actually, this is not quite correct either given the non−linearity of the equation of state for seawater. But it is a much better approximation than using the nominal density of seawater.

Yes, we have already had the same thoughts, and found a difference by using the non-linear equation of state vs. adding salinity fluxes (V*S) of less than 2e-4 psu, when the entire Antarctic Ice Sheet were melted to the ocean. (http://fermi.jhuapl.edu/denscalc.html). We added to the manuscript: *„... (which is a good approximation of the equation of state of the freshened ocean water)."*

l. 122: „such that the flow law fitting exponent is no fixed physical constant.“
not clear what the intended meaning is here. Do you mean to say that the the effective exponent is empirical since it depends on different processes that have different exponents?

No, we wanted to say that **„n comes with significant uncertainties“** and is not a fundamental universal physical constant. We rephrased this accordingly.

l. 131: „In the model, the same effect is achieved when adjusting the SIA enhancement factor ESIA= 2.0 divided by 50,000 Pa yields 4.0x10^-5 instead“
awkward wording, intent not clear especially since it's not clear where 4.0x10^-5 came from

We have omitted this sentence as it describes just a technical workaround how A=A(n=4) can be simply adjusted in PISM.

l. 162: „However, the simulated ice volume seems to increase by 3-5 m SLE for doubling vertical resolution (see red line in Fig. 2), as less temperate ice is formed in the lowest layers of the ice sheet“
This is disconcerting. Any ideas why? Does the thermodynamic solver have a sub−iteration to ensure the CFL condition is not broken? What kind of switch is used to turn on basal sliding?

There is no switch in PISM, as SSA stress balance is calculated in the entire ice domain as a sliding law for given basal shear stress. Hence we have basal sliding everywhere (Bueler & Brown, 2009). For the advection-conduction-reaction problem of the conservation of energy within the ice domain, PISM uses a BOMBPROOF numerial scheme (https://pism-docs.org/sphinx/technical/bombproof.html), which is conditionally-stable according to the CFL criterion, which is included in the PISM adaptive timestepping technique. Truncation error is O(Δz^2). But it is a known fact that vertical resolution of O(1m) seems to be required for capturing temperate ice adequately in the enthalpy model (Kleiner et al., 2015). The implementation of the conservation of energy in PISM will be overhauled by next year with a vertical coordinate system that will improve accuracy with much higher resolution at the surface and the base of the ice sheet.

l. 179: „SIA enhancemnet generally produces thicker grounded ice.“
−> thinner

True, this has been changed accordingly.

l. 207: „Hence, ice at the calving front thinner than 75m is removed“
Is this condition imposed during each ice dynamic timestep? Or when precisely ?

Calving in PISM is generally applied in each timestep after the mass-transport is applied, but before the surface and basal mass balance terms are calculated. The removal of thin ice tongues of less than 75m is rather for technical (SSA convergence) than for physical reasons.

figure 4
captions should explain any non−obvious figure keys (eg "no oceankill")

Yes, this is a PISM-specific term of a model option. We have renamed it to "no deep-ocean-calv" and defined it in both the text and figure caption.

General figures: the red and orange colours will be hard to differentiate by anyone with weak eyesight. Please choose a stronger contrasting colour and/or add textures.

OK, we used the d3 categorial 10 color scheme, and switched to categorial 20 and updated all figures accodingly (https://github.com/d3/d3-3.x-api-reference/blob/master/Ordinal-Scales.md#category20). This implies more light/dark graduation and a smaller number of different colors (i.e. no red – orange, or red – green combination).

l. 218: „We have shown that sea−level changes drive grounding line migration"
as have many others. And with no citation, should only state "we show below"

Well, this may be a relict of reordering the manuscript and has be changed accordingly.

l. 219: „In fact sea−level changes at the grounding line are not only caused by global mean sea−surface height change but also by local changes in the sea floor and bed topography."
incorrect, global mean sea−surface height change −> local sea−surface height change

Yes, the local sea-level is what matters at the grounding line, and we changed this accordingly. But the global mean sea-surface height is the driving force that is applied to the whole model domain uniformly.

l. 220: „but also by local changes in the sea floor and bed topography"
what is the difference between sea floor and bed topography? −> bed topography

„Sea floor" was used here to distinguish between ocean and ice load region, but we omitted it according to the reviewer's suggestion.

l. 228: „The formulation closely approximates the approach used within many GIA models (Whitehouse, 2018), which are defined to account for the response of the solid Earth and the global gravity field to changes in the ice and water distribution on the entire Earth's surface (Whitehouse et al., 2019).
Provide a citation to support claim that ignoring geoidal spatial variations and use of half−space approximation gives a "close approximation" to full solution of sealevel equation with a full visco−elastic model with radially varying viscosity or otherwise this drop claim. Also, be more precise than "closely approximates". What does that really mean?

We agree that this formulations was somewhat misleading. We actually have compared the simulated vertical bed displacement for an Antarctic deglaciation scenario (which is similar to the reference simulation) with results of the GIA model used by Pippa Whitehouse, who co-authored a previous PISM study. We rephrased as follows:

„The Earth model can be initilized with a present-day uplift map (Whitehouse et al., 2012) **and reproduces plausible uplift pattern and magnitudes for a given load history (Kingslake et al., 2018, personal communication Pippa Whitehouse). Yet, it is still a simplification of the** *approach used within many GIA models (Whitehouse, 2018), which are defined to account for the response of the solid Earth and the global gravity field to*

changes in the ice and water distribution on the entire Earth's surface (Whitehouse et al., 2019)."

l. 232: „account for vertical displacement"
−> account for vertical bed displacement

Added.

l. 251: „we presented simulations"
−> we present simulations

Changed.

l. 261: „We have deactivated the elastic part of the Earth model in our reference simulation, as the numerical implementation was flawed. Instead we have used PISM v1.1, which considers only grounded ice thickness changes as loads, with additionally fixed elastic part, in order to evaluate the ice sheet volume's sensitivity to changes in the flexural rigidity parameter value"
Now I'm not clear what exact GIA model is used. You first claim to include changing ocean load but here you state that you do not.

There are several components in the GIA model, which have been changed since the last PISM version. First, the elastic part has been fixed in PISM v.1.1 (https://github.com/pism/pism/pull/435). As we used an older PISM version for the experiments, we ran only the elastic sensitivity experiment with the newer PISM version. Second, for the viscous part, PISM has accidently used ice thickness (including floating ice) as load in the GIA model. That has been fixed for the presented experiments, such that both changes in grounded ice thickness and ocean thickness are considered as loads. Only the grounded ice part of this fix entered into the stable PISM v1.1 (https://github.com/pism/pism/commit/4b5e14037), as is was obviously wrong, while the ocean load part still requires proper numerical tests cases before it can be merged to the main PISM development branch. We reordered this paragraphin the manuscript:

„In order to evaluate the ice sheet volume's sensitivity to changes in the flexural rigidity parameter value, we have used PISM v1.1 instead, with additionally fixed elastic part. Yet, PISM v1.1 considers considers only grounded ice thickness changes as loads, and not the ocean thickness in the reference."

l. 329: „with fp=7%/K a precipitation change factor with temperature"
from Clausius−Clapeyron or?

Right, has been added to the revised manuscript: *„...with f_p=7%/K a precipitation change factor **according to Clausius-Clapeyron relationship** with temperature..."*

is there a bed thermodynamic model or not? If so, please detail. If not, justify why not included

Yes, there is a bed thermal unit, see details below.

l. 383: „In our PISM simulations the Mohr−Coulomb criterion (Cuffey and Paterson, 2010)

determines the yield stress c as a function of small−scale till material properties and of the effective pressure Ntil on the saturated till"
I'm confused, previously you state that the basal drag exponent q is an ensemble parameter, but yield stress is only meaningful for q=0 (Coloumb plastic) basal drag.

The basal drag exponent q is an (ensemble) parameter in the generalized „pseudo-plastic" sliding relationship (Eq. 7), in which τ_c is called the Mohr-Coulomb yield stress (Eq. 8), and here actually valid for all exponents $0 \leq q \leq 1$. This implies that basal shear stress can be larger than the Coulomb yield stress in fast-flowing regions ($u > u_{thr}$) for $q > 0$, in contrast to purely plastic sliding for $q = 0$, when $|\tau_b| \leq \tau_c$ and $|u| > 0$. In fact, purely plastic behavior of till must be assumed to derive τ_c values from in situ measurements.

*„In our PISM simulations the Mohr-Coulomb failure criterion (Cuffey and Paterson, 2010) determines the yield stress τ_c **in Eq. (7) (valid for** $0 \leq q \leq 1$ **)**.."*

l. 450: eq 9
what do the constants \delta, \epsilon_o, C_c represent?

*„...while all other parameters are constants (adopted from Bueler and van Pelt, 2015**, see Table 1 for parameter meaning and values**)."*

l. 474: The effective pressure cannot exceed the overburden pressure, i.e., Nmax til = P0 (for details see Bueler and van Pelt, 2015, Sect. 475 3.2),
this follows by definition, so I don't understand why references are provided.

Omitted reference.

l. 475: „we find a lower limit Nmintil = \delta P0,"
So would anyone "find". This directly follows from eq 9.

Modified to: *„..., while in the case of saturated till layer (s=1) **Eq. (9) yields** a lower limit..."*

l. 512: In particular the so−called meltwater pulse 1a
remove "so−called". Or do you want to start stating "so−called Last Glacial Maximum"....?

Omitted.

l. 543: „As WDC temperature rise occurred somewhat earlier than at EDC the Antarctic Ice Sheet responds with higher deglaciation rate (cf. grey in blue line)."
readability of this paper would benefit from more punctuation

Yes, we addressed this in the revised manuscript and separate each message into one sentence with actual numbers:

*„**In our simulations, the Antarctic Ice Sheet volume responds with several thousand years delay to the surface temperature forcing. The LGM minimum in surface temperatures reconstructions happened around 22kyr BP in the WDC data, while**

largest ice volume is simulated at 14kyr BP. The main temperature rise at WDC occurred between 18kyr and 12kyr BP contributing to initial deglaciation at around 12kyr BP with major retreat between 8kyr and 4kyr BP. At EDC location the reconstructed temperature rise happened about 1kyr later with more variability leading to a more gradual deglaciation between 12kyr and 2kyr BP. Comparisons with other ice core temperature reconstructions, however, suggest a superimposed **lapse rate** effect ~~of~~ due to surface height change during deglaciation at WDC **location** (Werner et al., 2018)."

l. 552: „4.3 Ocean temperature forcing"
this section would really benefit from a comparative repeat of the analysis with the ocean temperature results from the TRACE (Liu and Otto−Bleisner) deglaciation GCM model run that are freely avaiable.

This idea seems great, as the response function analysis in Sect. 4.3 has only been applied to warmer than present conditions. For comparison, we have plotted the WDC temperature anomaly and associated ocean temperature anomaly estimate in intermediate water depth against ocean temperature data (mean over regions south of 66°S) from the TraCE-21ka deglaciation GCM (https://www.earthsystemgrid.org/project/trace.html), and added the corresponding graph to Figs. 22 and 30.

Generally, we find in the GCM data similar response trough the Holocene period as in our parameterization, while the temperature dip at ACR is much more pronounced in the GCM data (Fig. R1). For colder glacial conditions another discrepancy arises, as ocean temperatures in the data are bounded below by pressure melting temperature (in Fig. R1 for anomaly -1.8C). The PICO module can handle such ocean temperature forcing for colder than present climates and bounds ocean temperatures in each basin below by pressure meltung temperature.
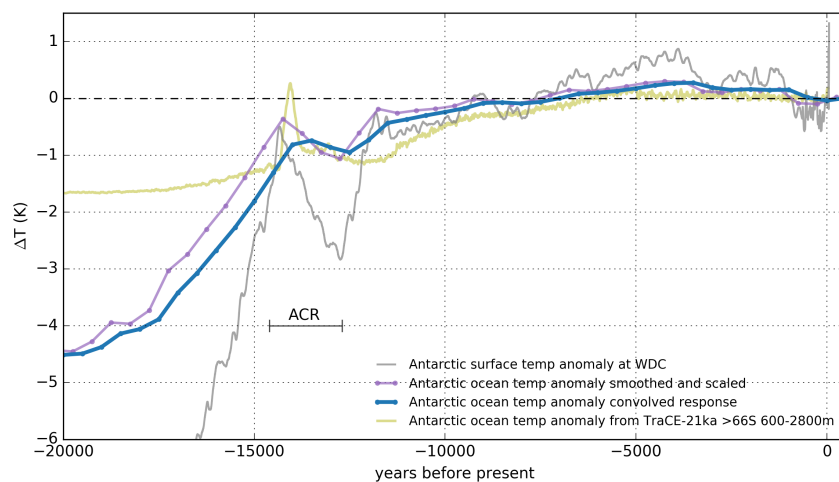
Fig. R1: Surface temperature anomaly over the last 22 kyr as reconstructed from WAIS Divide Core (WDC, grey) and indermediate depth ocean response estimate (blue) as described in Sect. 4.3, compared to scaled timeseries (purple) and to TraCE-21ka (Liu et al., 2009; https://www.earthsystemgrid.org/project/trace.html) ocean model anomaly between 600m and 2800m depth (olive).

We have also performed the response function analysis with these TraCE-21ka data, but we could not find a meaningful response function, as the analysis is suited to step forcing experiments. But we were able to calculate the convolved ocean response estimate from TraCE-21ka global mean surface temperature (with the previous fitting paramters), which is similar to the one derived from WDC reconstructions, and which can also not adequately

resolve the variability around ACR (1K warming followed by 1K cooling), at least for 500 yr bin size (Fig. R2).
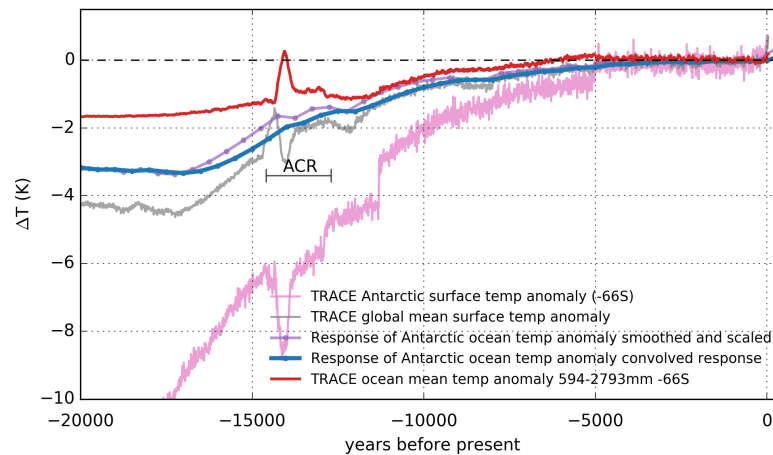
Fig. R2: TraCE simulated surface temperature anomaly over the last 20 kyr as global mean (grey) and mean over the Antarctic region south of 66S latitude (rose), as well as ocean model anomaly between 600m and 2800m depth (red, Liu et al., 2009). In violet the smoothed (500yr bins) and scaled timeseries (factor 0.75) as well as the estimated ocean response ($1/x^2$) in blue.

l. 635: „We hence choose PREC as relevant climate forcing"
what is PREC? Not shown in any provided equation
later page:
l. 659: „The simulations hence suggest that the precipitation scaling parameter fp is highly relevant for the ice sheet's extent at glacial maximum and will be considered as ensemble parameter PREC in Albrecht et al. (2019)."
repeat of early, but now you explain what PREC is. Please clean up paper organization.

Thanks for pointing out this inconsistent declaration of this key parameter. We switched the two sentences.

l. 663: „5.1 Energy spin−up procedure and intrinsic memory"
I can't interpret your spin−up experiments without knowing what kind of bed thermodynamics is implemented though I suspect you have none given that a full (eg 3−5 km deep) bed thermodynamics components would likely show more sensitivity to the spinup climate forcing.

„PISM uses a bedrock thermal model (1-D heat equation with bedrock thermal conductivity of 3.0 W m-1 K-1, bedrock thermal density = 3300 kg m^-3 and bedrock thermal specific heat capacity = 1000.0 J / (kg K)), similar to Ritz et al., 1996, with upper lithosphere thickness of 2 km discretized in 20 equidistant layers and geothermal heatflux applied as constant boundary condition to calculate the heatflux into the ice at the ice-bedrock interface depending on ice base temperature." We added this information to the revised mansucript and the following Fig. R3:
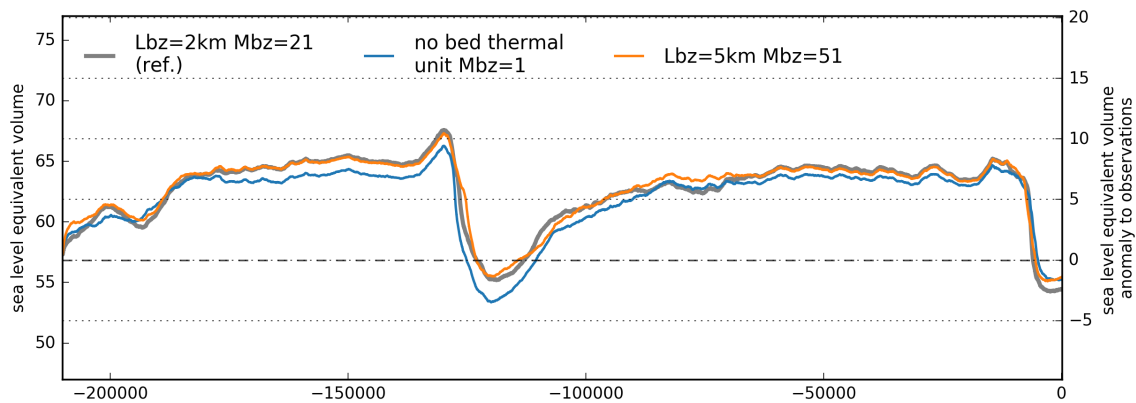
Fig. R3: Timeseries of sea-level relevant ice volume for different bedrock thermal layer thicknesses (Lbz), with 2km with 100m vertical resolution in the reference (grey). In comparison, a 5km thick thermal bedrock layer (orange) has only little influence on the ice volume history, while in the absence of a bed thermal unit (blue) ice volume tends to be 1-2 m SLE smaller.

l. 665: „As the three−dimensional enthalpy field carries the memory of past climate conditions, a more realistic spin−up climatic boundary condition may be achieved when the temperature reconstruction of the previous glacial cycles"
"may be" −> "would be"

Changed.

l. 710: „A timeseries of well−dated sediment data of iceberg−rafted debris (Weber et al., 2014) suggest that the main retreat of the Antarctic Ice Sheet occurred 14.6 kyr BP, as a consequence of MWP1a."
The RAISED consortium of glacial geologists concluded otherwise (Bentley et al, QSR 2014) so this inference remains an open question and this should be made clear.

*„**It remains an open question how much Antarctic deglaciation contributed to the the MWP1a.** A timeseries of well-dated sediment data of iceberg-rafted debris (Weber et al., 2014) suggest that the main retreat of the Antarctic Ice Sheet occurred at 14.6 kyr BP, ~~as a consequence of~~ **synchronously with** MWP1a**, while the RAISED Consortium concluded on an a later retreat with a relatively small Antarctic contribution to MWP1a (Bentley et al., 2014). „***

l. 813: „we find for geothermal heat flux maps from different available sources comparably little difference in modeled LGM ice volume, in contrast to previous studies"
Again I can't evaluate this without knowing what kind of bed thermal model is used.

See discussion above.

l. 835: „...and air temperature PISM−PICO simulates similar LGM states. However, the onset of deglaciation and hence present−day ice volume can differ by a few meters SLE. This means that, compared to the other forcings, ocean temperature forcing is of minor relevance for glacial cycle simulations."
You seem to forgetting about the Eemian, where sub−shelf melt may play a critical role in partial to near complete WAIS collapse or some such which is what is inferred to be required to explain the sealevel high−stand then.

We agree with the referee that ocean forcing may have played a critical role in major ice volume changes during the Last interglacial. However, in this paragraph of the conclusions we refer to Fig. 23 and hence to the sensitivity of ice volume history to chosen temperature reconstructions and involved parameters. As WDC temperature reconstuction covers only the last 67 kyr we find consequently no differences in the ice volume response before that time, except for the (60%) scaled time series. We changed the manuscript to:

„However, the onset of deglaciation and hence present-day ice volume can differ by a few meters SLE. This means that, compared to the other forcings, **we find low sensitivity of the ice volume history to the selection of** *ocean temperature forcing* **in our** *is of minor relevance for glacial cycle simulations. Hence, we have not varied PICO parameters in this study,* **although ocean forcing in general may play a key role for ice sheet retreat during interglacials.**

In fact, in our simulations (also in the ensemble) we do not find (partial nor complete) WAIS collapse during the Last Interglacial. This is most likely related to the basal friction paramterization, as the optimization algorithm for the till friction angle (Sect. 3.4.2) suggest values of up to 25° in the deepest marine sections of WAIS, which corresponds to relatively high yield stress of the till and hence thicker ice in this region (in agreement with present-day data), which seems to prevent from collapse. In constrast, till friction optimization suggests angles of 1° or 2° in ice stream regions to allow for sufficient ice flux, e.g. in Siple Coast. Other PISM studies (e.g. Golledge et al., 2015; Feldmann & Levermann, 2015; Sutter et al., 2016; Feldmann et al., 2019) may find more sensitivity in WAIS to enhanced ocean melt by using 4-5° till fricition angle in the entire marine sections of WAIS. But also basal melt interpolation and availablity of till water at the grounding line may have enhanced grounding line sensitivity in those experiments.

l. 844: „From the discussed model settings and boundary conditions we select four relevant parameters representative for each of the different sections"
misleading wording. I take it you mean "we select a total of four relevant parameters, one each for the 4 different sections" but I'm not clear what 4 sections you are talking about. Be explicit.
given all the uncertainties in the physics and forcing of the glacial cycle AIS along with the size of the AIS, I'm surprised you only choose 4 ensemble parameters, with no justification for such a small size.

We corrected for the misleading wording accordingly by adding:
„...one each for the different sections (Sect. 2: Ice sheet and Earth model parameters, Sect. 3: Boundary conditions and input datasets and Sect. 4: Climatic Forcing)."

References

Albrecht, T., Winkelmann, R., and Levermann, A.: Glacial cycles simulation of the Antarctic Ice Sheet with PISM – Part 2: Parameter ensemble analysis, The Cryosphere Discuss., https://doi.org/10.5194/tc-2019-70, in review, 2019b.

Briggs, R., Pollard, D., & Tarasov, L. (2013). A glacial systems model configured for large ensemble analysis of Antarctic deglaciation. *The Cryosphere*, 7(6), 1949-1970.

Bueler, E., & Pelt, W. V. (2015). Mass-conserving subglacial hydrology in the Parallel Ice Sheet Model version 0.6. *Geoscientific Model Development*, *8*(6), 1613-1635.

Bueler, E., & Brown, J. (2009). Shallow shelf approximation as a "sliding law" in a thermomechanically coupled ice sheet model. *Journal of Geophysical Research: Earth Surface*, *114*(F3).

Feldmann, J., & Levermann, A. (2015). Collapse of the West Antarctic Ice Sheet after local destabilization of the Amundsen Basin. *Proceedings of the National Academy of Sciences*, *112*(46), 14191-14196.

Feldmann, J., Levermann, A. & Mengel., M. (2019). Stabilizing the West Antarctic Ice Sheet by surface mass deposition. *Science Advances*, *5*(7),

Golledge, N. R., Kowalewski, D. E., Naish, T. R., Levy, R. H., Fogwill, C. J., & Gasson, E. G. (2015). The multi-millennial Antarctic commitment to future sea-level rise. *Nature*, *526*(7573), 421.

Kleiner, T., Rückamp, M., Bondzio, J. H., & Humbert, A. (2015). Enthalpy benchmark experiments for numerical ice sheet models. *The Cryosphere*, *9*(1), 217-228.

Liu, Z., Otto-Bliesner, B. L., He, F., Brady, E. C., Tomas, R., Clark, P. U., ... & Erickson, D. (2009). Transient simulation of last deglaciation with a new mechanism for Bølling-Allerød warming. *Science*, *325*(5938), 310-314.

Ritz, C., A. Fabre, and A. Letréguilly. "Sensitivity of a Greenland ice sheet model to ice flow and ablation parameters: consequences for the evolution through the last climatic cycle." *Climate Dynamics* 13.1 (1996): 11-23.

Sutter, J., Gierz, P., Grosfeld, K., Thoma, M., & Lohmann, G. (2016). Ocean temperature thresholds for Last Interglacial West Antarctic Ice Sheet collapse. *Geophysical Research Letters*, *43*(6), 2675-2682.

Winkelmann, R., Martin, M. A., Haseloff, M., Albrecht, T., Bueler, E., Khroulev, C., & Levermann, A. (2011). The Potsdam parallel ice sheet model (PISM-PIK)–Part 1: Model description. *The Cryosphere*, *5*(3), 715-726.

Manuscript prepared for The Cryosphere
with version 2014/09/16 7.15 Copernicus papers of the LaTeX class copernicus.cls.
Date: 7 November 2019

Glacial cycles simulation of the Antarctic Ice Sheet with PISM - Part 1: Boundary conditions and climatic forcing

Torsten Albrecht [1], Ricarda Winkelmann [1,2], and Anders Levermann [1,2,3]

[1]Potsdam Institute for Climate Impact Research (PIK), Member of the Leibniz Association, Potsdam, Germany
[2]Institute of Physics and Astronomy, University of Potsdam, Potsdam, Germany
[3]Lamont-Doherty Earth Observatory, Columbia University, New York, USA

Correspondence to: T. Albrecht (albrecht@pik-potsdam.de)

Abstract. Simulations of the glacial-interglacial history of the Antarctic Ice Sheet provide insights into dynamic threshold behavior and estimates of the ice sheet's contributions to global sea-level changes, for both the past, present and future. However, boundary conditions are weakly constrained, in particular , at the interface of the ice-sheet and the bedrock. Also climatic forcing covering the last glacial cycles is uncertain as it is based on sparse proxy data.

We use the Parallel Ice Sheet Model (PISM) to investigate the dynamic effects of different choices of input data, e.g. for modern basal heat flux or reconstructions of past changes of sea-level and surface temperature. As computational resources are limited, glacial-cycle simulations are performed using a comparably coarse model grid of 16 km and various parameterizations, e.g. for basal sliding, iceberg calving or for past variations of precipitation and ocean temperatures. In this study we evaluate the model's transient sensitivity to corresponding parameter choices and to different boundary conditions over the last two glacial cycles . It hence and provide estimates of involved uncertainties. We also discuss isolated and combined effects of climate and sea-level forcing. Hence, this study serves as a 'cookbook' for the growing community of PISM users. We identify relevant model parameters and motivate plausible parameter ranges for a Large Ensemble

For each of the different model uncertainties with regard to climatic forcing, ice and Earth dynamics and basal processes, we select one representative model parameter that captures relevant uncertainties and motivate corresponding parameter ranges that bound the observed ice volume at present. The four selected parameters are systematically varied in a parameter ensemble analysis, which is described in a companion papercompanion paper.

1 Introduction

Process-based models provide the tools to reconstruct the ~~ice sheet's history and to improve our~~ history of the Antarctic Ice Sheet leading to a better understanding of involved processes and thresholds ~~and to better anticipate possible future pathways~~ regarding the ice sheet's evolution in the past as well as in the future (Pattyn, 2018). However, ice sheet ~~simulations involve~~ modeling involves various sorts of uncertainties. The stress balance and thickness evolution of the ice sheet is approximated and discretized, which implies different sorts of model-internal errors that should vanish for finer model grids (Gladstone et al., 2012; Pattyn et al., 2013). Parameterizations of physical processes at the interfaces of the ice with bedrock, ocean or atmosphere, such as basal friction, isostatic rebound, sub-shelf melting or accumulation of snow at the ice surface, involve uncertain model parameters (e.g., Gladstone et al., 2017). Certain feedback mechanisms associated with self-sustained calving may be relevant for much warmer than present climates, but not for the last glacial cycles (Edwards et al., 2019). Coupled climate-ice sheet systems models ~~are computationally too~~ can be computationally expensive in order to run ~~many long simulations~~ hundreds of full glacial-cycle simulations, depending on their complexity (e.g., Bahadory and Tarasov, 2018, using a model of intermediat complexity with about The climatic history can be instead approximated with the ~~modern climate mean~~ averaged modern climate scaled by temperature anomaly time series. Those anomalies can be based on single ice cores reconstructions, which can involve significant methodological uncertainties though (Cuffey et al., 2016; Fudge et al., 2016). Uncertainties are also large for available indirect observations of boundary conditions, e.g. for the bed topography (Sun et al., 2014; Gasson et al., 2015) or till properties underneath the ice sheet and ice shelves (Brondex et al., 2017; Falcini et al., 2018).

In order to gain confidence in model reconstructions and hence in future model projections, uncertain model parameters need to be constrained ~~and calibrated~~ with observational data (Briggs et al., 2014) using a ~~Large Ensemble~~ parameter ensemble analysis (Pollard et al., 2016), as demonstrated in a systematic way in a ~~companion paper~~ companion paper (Albrecht et al., 2019). This study motivates choices of boundary conditions and climatic parameterizations for application in large-scale paleo ice-sheet simulations and provides an assessment of the associated sensitivity of the model's response. Therefore, we run simulations of the entire Antarctic Ice Sheet with the Parallel Ice Sheet Model (Winkelmann et al., 2011; The PISM authors, 2017) and describe a spin-up procedure for uncertain state variables, such as the three-dimensional enthalpy field or the till friction angle at the base. The hybrid of two shallow approximations of the stress balance and the comparably coarse resolution of 16 km enable computationally efficient simulations of ice sheet dynamics over the last two glacial cycles, each lasting for about 100,000 years ~~(or 100 kyr, Lisiecki, 2010)~~ (100 kyr, Lisiecki, 2010).

Section 1.1 describes the ice sheet model and Sect. 2 assesses the sensitivity for parameter variations of the ice sheet model dynamically coupled to an Earth model. Sections 3 and 4 describe the used boundary conditions and climatic forcing, respectively, and discuss how they contribute to the sea-level relevant ice volume history. ~~The~~ Although not the primary focus of this study, the analysis

is complemented by perturbation experiments ~~in Sect.~~ concerning the onset of the last deglaciation in Appendix A. In the conclusions we identify a subset of ~~the most relevant parameters~~ four relevant parameters, one for each of the uncertainty classes, as used in the ~~Large Ensemble~~ ensemble analysis in a ~~companion paper~~ companion paper (Albrecht et al., 2019) .

1.1 PISM

The Parallel Ice Sheet Model (PISM[1]) is an open-source three-dimensional ice-sheet model (Winkelmann et al., 2011; The PISM authors, 2017) that is used in a growing community for sea-level projections (e.g. Winkelmann et al., 2015; Golledge et al., 2015, 2019) and regional studies (e.g. Mengel and Levermann, 2014; Feldmann and Levermann, 2015; Mengel et al., 2016). It uses a hybrid combination of two stress balance approximations for the deformation of the ice, the Shallow ~~Ice-Shallow~~ Ice - Shallow Shelf Approximation (SIA-SSA), that guarantees a smooth transition from vertical-shear-dominated flow in the interior via sliding-dominated ice-stream flow to fast plug flow in the floating ice shelves (Bueler and Brown, 2009), while neglecting higher-order modes of the flow. Driving stress at the grounding line is discretized using one-sided differences (Feldmann et al., 2014). Using a sub-grid interpolation scheme (Gladstone et al., 2010) the grounding line location simply results from the flotation condition, without additional flux conditions imposed. Basal friction ~~and basal melt~~ is interpolated accordingly. Thus, grounding-line migration is reasonable well represented in PISM (compared to full Stokes), even for coarse ~~resolution~~ resolutions (Pattyn et al., 2013; Feldmann et al., 2014). Ice ~~deforms~~ deformation ($\dot{\epsilon}$) in response to deviatoric stresses τ (and effective stress $\tau_e = \tau_e(\tau)$) can be described according to the Glen-Paterson-Budd-Lliboutry-Duval flow law ~~connecting strain rates $\dot{\epsilon}$ and deviatoric stresses τ for~~ with enhancement factor E ~~,~~ and flow law exponent n ~~and ice~~ ,

$$\dot{\epsilon}_{ij} = \mathrm{E} \cdot A(T, \omega)\, \tau_e^{n-1}\, \tau_{i,j}. \tag{1}$$

Ice softness A ~~, that~~ depends on both liquid water fraction ω and temperature T (Aschwanden et al., 2012) ~~,~~

$$\dot{\epsilon}_{ij} = \mathrm{E} \cdot A(T, \omega)\, \tau^{n-1}\, \tau_{i,j}.$$

. PISM simulates the three-dimensional polythermal enthalpy conservation for given surface temperature and basal heat flux to account for melting and refreezing processes in temperate ice (Aschwanden and Blatter, 2009; Aschwanden et al., 2012). The energy conservation scheme also accounts for the production of sub-glacial (and transportable) water (Bueler and van Pelt, 2015), which affects basal friction via the concept of a saturated and pressurized sub-glacial till. ~~With a modeled distribution of yield stress this allows for~~ The strength of the till below the ice sheet is strongly controlled by water pressure (Cuffey and Paterson, 2010) . A time-dependent basal substrate rheology

---

[1] http://www.pism-docs.org, see also ~~Code~~ note on 'code and data availability ~~Sect. 5~~'

scheme allows meltwater generated at the ice-sheet bed to saturate and weaken the subglacial till layer (Tulaczyk, S. et al., 2000; de Fleurian et al., 2018) . The resulting reduced basal traction allows grounded ice to accelerate. This can, in turn, cause dynamic thinning, a reduction in driving stress and ultimately a reduced ice stream flow later on. In PISM, the hydrology-related effective pressure

$$N_{\text{til}} = N_0 \left(\frac{\delta P_0}{N_0} \right)^s 10^{(e_0/C_c)(1-s)}, \tag{2}$$

accounts for the overburden pressure $P_0 = \rho_i g H$ for given ice thickness H, and the fraction of effective water thickness in the till layer s, while all other parameters are constants (adopted from Tulaczyk, S. et al., 2000; Bueler an... Till water in till pore spaces is modeled in our PISM simulations as a boundary layer with an effective thickness of water content W with respect to a maximum amount of basal water $W_{\text{til}}^{\text{max}} = 2\,\text{m}$ and enters as fraction s in Eq. (11). For $0 \le s \le 1$ the effective pressure in Eq. (11) is hence bounded by $\delta P_0 \le N_{\text{til}} \le P_0$. We use a non-conserving hydrology model that connects W_{til} to the basal melt rate M_b (Tulaczyk, S. et al., 2000) , where ρ_w is the density of water and C_d is a fixed drainage rate,

$$\frac{\partial W_{\text{til}}}{\partial t} = \frac{M_b}{\rho_w} - C_d. \tag{3}$$

Sliding in PISM is of nonlinear Weertman-type for sliding over rigid bedrock (Fowler, 1981; Schoof, 2010) , where the basal shear stress $\boldsymbol{\tau}_b$ (tangential sliding) is related to the SSA sliding velocity $\boldsymbol{u}_b$ in the form

$$\boldsymbol{\tau}_b = -\tau_c \frac{\boldsymbol{u}_b}{u_0^q |\boldsymbol{u}_b|^{1-q}}, \tag{4}$$

with $0 \le q \le 1$ the positive sliding exponent and $|\boldsymbol{u}_b| > 0$. Therein, the Mohr-Coulomb failure criterion (Cuffey and Paterson, 2010) determines the yield stress τ_c in (valid for all $0 \le q \le 1$) as a function of small-scale till material properties (till friction angle ϕ) and of the effective pressure N_{til} on the saturated till,

$$\tau_c = \tan(\phi) \, N_{\text{til}}. \tag{5}$$

With a modeled distribution of yield stress this allows for grow-and-surge instability (Feldmann and Levermann, 2017; Bakker et al., 2017). Here we use the non-conserving hydrology model, where the till water content in each grid cell is balanced by basal melting and a constant drainage rate.

Iceberg formation at ice shelves is parameterized based on spreading-rates (Levermann et al., 2012). Ice shelf melting is calculated using the Potsdam Ice-shelf Cavity mOdel (PICO), that considers ocean properties in front of the ice shelves and simulates vertical overturning circulation in the ice-shelf cavity (Reese et al., 2018).

PISM uses a generalized modified version of the Lingle-Clark bedrock deformation model (Bueler et al., 2007), assuming an elastic lithosphere , and a resistant asthenosphere and a spatially-varying viscous with viscous flow in the half-space below the elastic plate (Whitehouse, 2018). The computationally-efficient bed deformation model has been improved to account for changes in the load of the ocean layer around the grounded ice sheet, due to changes in global mean sea-level height and ocean depth.

125   A continental-scale representation of modern bed topography is obtained from the Bedmap2 dataset (Fretwell et al., 2013) and modern uplift rates as initial condition from Whitehouse et al. (2012). We simulate the entire Antarctic continent with 16 km grid resolution compatible with the definition of the initMIP model intercomparison project (Nowicki et al., 2016).

    PISM paleo simulations are initiated with a spin-up procedure ~~for prescribed~~ using a fixed ice sheet
130 geometry, in which the three-dimensional enthalpy field can adjust to mean modern climate boundary conditions over a 200 kyr period. Full glacial dynamics are then simulated over the last two glacial cycles with a forcing starting in the penultimate interglacial (210 kyr BP, ~~before present~~ 'before present', defined for reference year 1950 AD) and run until the year 2000 AD ~~(-50yr BP)~~. The sensitivity of the modeled ice volume above flotation to different ~~choice~~ choices of parameters and bound-
135 ary conditions is evaluated as the difference to a baseline simulation (see Movie in Supplementary Asset) that is consistent with the model configuration of the best fit simulation presented in a ~~companion paper~~ companion paper (Albrecht et al., 2019, see plots in Sect. 3.3) .

1.2   Volume above flotation

In order to compare ice volume histories we calculate the associated contribution to global mean sea-
140 level in units of 'm SLE'. Be aware that many studies just convert grounded ice volume (in units of 'million km^3') into more handy units of sea-level equivalents (using conversion factors between 2.4 and 2.8), without subtracting the portion of the ice volume that is grounded below flotation. If this fraction of ice resting on deep submarine beds is lost, its mass converts to water required to fill the same basin (almost) without changing sea-level (Goelzer et al., 2019) . Analogous to the 'volume
145 above flotation' by the SeaRISE model intercomparison (Bindschadler et al., 2013, Eq. 1), we define here

$$
\begin{aligned}
V_{\mathrm{SLE}} &= \frac{\rho_i}{\rho_o}\,\mathrm{sum}\,(H\,c_a)/A_o \quad \text{if} \quad H > \max\,(10, h_{\mathrm{f}})\\
&- \mathrm{sum}\,[(z_{\mathrm{sl}} - b)\,c_a]/A_o \quad \text{if} \quad H > \max\,(10, h_{\mathrm{f}}) \quad \text{and} \quad h_{\mathrm{f}} > 0,\\
h_{\mathrm{f}} &= \frac{\rho_o}{\rho_i}\,(z_{\mathrm{sl}} - b)\,,
\end{aligned}
\tag{6}
$$

where H is the full ice thickness above a threshold of 10 m (ice-free standard definition in PISM), h_{f} the flotation height, c_a is the area distribution among grid cells (corrected for stereographic projec-
150 tion), $z_{\mathrm{sl}} - b$ is the water depth for current sea level z_{sl} and bedrock topography b and $\rho_o = 1028\,\mathrm{kg\,m^{-3}}$ and $\rho_i = 910\,\mathrm{kg\,m^{-3}}$ are the densities of sea water and ice, respectively (see also Table 1). For consistency reasons with the used PISM version, we use ocean water density here. In fact, a density of $1000\,\mathrm{kg\,m^{-3}}$ should be used instead ~~as ice melts to fresh water~~ (which is a good approximation of the equation of state of the freshened ocean water). Hence, the anomaly $\Delta V_{\mathrm{SLE}}(t)$ is calculated from the
155 total Antarctic ice above flotation for current sea level forcing z_{sl} and evolving bedrock topography b, divided by global ocean area $A_o = 3.61 \times 10^{14}\,\mathrm{m^2}$, relative to the value for the modern observed ice sheet (Bedmap2; Fretwell et al., 2013).

1.3 Energy spin-up procedure and intrinsic memory

In the introduction to PISM (Sect. 1.1) we have briefly described a spin-up procedure, which results
in a three-dimensional enthalpy field that is in balance with the modern climate boundary conditions
(see Sect. 3). We thereby assume that present-day conditions have been similar to those in the
penultimate interglacial (210 kyr BP). As the three-dimensional enthalpy field carries the memory
of past climate conditions, a more realistic spin-up climatic boundary condition might be achieved
when the temperature reconstruction of the previous two glacial cycles (423–210 kyr BP, see Sect. 4.2)
or the long-term mean over this period were used as anomaly forcing, while the ice sheet geometry
remains fixed at present-day observations (Bedmap2; Fretwell et al., 2013) . In the case of a simulation
over the last four glacial cycles (423 kyr BP), in which the ice geometry can evolve, we can assume
an even more realistic enthalpy distribution. Here we investigate to what extent the choice of the
temperature forcing in the enthalpy field spin-up can affect subsequent full-dynamics simulations
over the last two glacial cycles until present.

Three simulations are conducted with identical model settings and climate forcing, but different
initial energy states. The modeled ice volumes converge at Last glacial Maximum (LGM, 15 kyr
BP) with less than 0.2 m SLE difference among the simulations, but they differ for present-day
conditions by up to 2 m SLE (see blue and light blue lines in Fig. 1, at time 0 BP). This The reference
simulations, based on the initial state that was spun-up with comparably warm constant modern
climate, tends to show earlier and stronger deglaciation than the other simulations using glacial
climate or mean glacial climate for the thermal spin up. Also the full-physics simulation with glacial
climate over four glacial cycles converges against the reference simulation and reveals about 1 m
SLE differences to the reference ice volume evolution at present day (orange line in Fig. 1).

In order to evaluate how long the memory to the initial thermal state lasts, we continue the
simulations with repeated glacial climate forcing but different present-day geometries for another
2×210 kyr. Instead of converging ice volume timeseries we find 1-2 m SLE divergence during
interglacial states. As deglaciation reveals a nonlinear threshold behavior it can amplify small differences
in LGM ice sheet geometry. Ice thickness variations of up to 1,000 m at the final interglacial state
(see Fig. 2, at time 420 kyr after present) are found mainly in the large ice shelf basins of Ross
(Siple Coast), Amery and Ronne-Filchner Ice Shelf in the Weddell Sea, mostly determined by the
migration of the grounding line. Hence, the remaining standard deviations of about 1 m SLE (for
this small sample) can be interpreted as model-internal uncertainty and should be kept in mind when
comparing and evaluating ensembles of Antarctic ice volume reconstructions. Comparably small
differences in initial conditions (that can potentially be amplified) could be also related to numerical
settings, such as number of used CPU for parallel simulations.

Figure 2: Maximum difference in present-day ice thickness of three simulations of the Antarctic Ice Sheet after three rounds of two-glacial-cycle simulations with identical model settings, but for different initial enthalpy states (cf. final state in Fig. 1). In particular the Siple Coast (Ross) and Amery trough shows more than 1 km difference in ice thickness between the final states.

In the following sections we will discuss different choices of model parameterizations, boundary conditions and climatic forcings on the sea-level relevant Antarctic Ice Sheet history over the last two glacial cycles. Find a summary of the corresponding sensitivities at Last Glacial Maximum and present-day state in Table 2.

2 Ice sheet and Earth model parameters

PISM solves a coupled system of model equations for the conservation of energy, momentum and mass. Model equations are discretized using a regular rectangular grid of 16 km resolution. Equations of stress balance are simplified using a hybrid of the shallow approximations SIA and SSA, which allows PISM to run glacial cycles simulations simulations. In order to close the equation system, ice sheet models commonly use a flow law (Eq. (2)), which relates ice flow to stresses. It is a result of empiric measurements and statistics for rather idealized conditions, such that the flow law fitting exponent ~~is no fixed physical constant~~n comes with significant uncertainty. Enhancement factors compensate for unresolved rheological effects, e.g. anisotropy. In this section we want to understand effects of ice sheet and Earth model parameter variations on the transient glacial cycle ice sheet response.

Parameter	Value	Units	Physical meaning
ϱ_i	910	kg m^{-3}	Ice density
ϱ_o	1028	kg m^{-3}	Seawater density
ϱ_w	1000	kg m^{-3}	Water density
g	9.81	m s^{-2}	Gravitational acceleration
A_o	3.61×10^{14}	m^2	Surface area of world ocean
c_a	2.2–2.7×10^8	m^2	Projected grid cell area for 16 km resolution
E_{SIA} (ESIA)	1–7 (2)		Enhancement factor for SIA stress balance
E_{SSA}	0.3–1.0 (0.6)		Enhancement factor for SSA stress balance
n	2–4 (3)		Exponent in Glen's flow law
K	0.1-10 (1)$\times 10^{17}$	m s	Eigencalving constant
H_{cr}	0–225 (75)	m	Thickness calving threshold
η (VISC)	0.1–10 (0.5)$\times 10^{21}$	Pa s	Earth upper mantle viscosity
D	0.5–10 (5)$\times 10^{24}$	N m	Flexural rigidity of lithosphere
q (PPQ)	0–1 (0.75)		Basal friction exponent in Eq. (11)
ϕ	1–70	°	Till friction angle
ϕ_{min}	0.5–5 (2)	°	Minimal till friction angle in marine parts
u_0	100	m yr^{-1}	Threshold velocity in sliding law Eq. (11)
N_0	1000	Pa	Reference effective pressure
e_0	0.69		Reference void ratio at N_0
C_c	0.12		Till compressibility
W_{max}	2	m	Maximum water thickness in till
C_d	0.001–0.01 (0.001)	m yr^{-1}	Till drainage rate
δ	0.02–0.1 (0.04)		Lower bound of hydrology-related effective pressure as fraction of overburden pressure, δP_0
f_p (PREC)	2–10 (7)	% K^{-1}	Relative precipitation change with air temperature
f_o	0.75		Amplification factor ocean to global mean temperature
f_s	1.8		Amplification factor Antarctic to global mean temperature
τ_x	3000	yr	Typical response time in intermediate ocean temperature

Table 1: Physical constants and parameter values used in this study, grouped in ice and Earth dynamics, basal sliding and sub-glacial hydrology, as well as climatic forcing. For varied parameters, the range is indicated, with the reference value in parentheses.

2.1 Ice flow enhancement factors

Enhancement factors account for unresolved effects of grain size, fabric and impurities and have often been used as tuning parameter in ice sheet modeling entering the constitutive flow law (Eq. (2)) that balances strain rates and stresses within the ice sheet. Value 1 means 'no enhancement', but

generally enhancement factors for the SSA tend to be smaller than 1 and larger than 1 for the SIA. Anisotropic ice-flow modeling suggests E_{SSA} values between 0.5 and 0.7 for ice shelves and between 0.6 and 1 for ice streams, while for SIA enhancement should lie between 5 and 6 (Ma et al., 2010). Previous model ensembles that consider isotropic ice flow use values down to E_{SSA} =0.3 (for E_{SIA} =1) in (Pollard and DeConto, 2012a, PSU-ISM) or up to E_{SIA} =9 (for E_{SSA} =0.8) in (Maris et al., 2014, ANICE model), both for 20 km resolution. PISM seems to favor enhancement factors closer to 1 (e.g. E_{SSA} =0.5–0.6 and E_{SIA} =1.2–1.5 in Golledge et al. (2015) for 10–20 km resolution).

Figure 3 shows the effects of ice flow enhancement factors on the simulated Antarctic Ice Sheet history. SIA enhancement generally produces thinner grounded ice. Compared to the reference simulations with E_{SIA} =2 the model simulates for E_{SIA} =1 more than 5 m SLE thicker and for E_{SIA} =5 about 6 m SLE thinner ice sheets, both at glacial and interglacial states (dark and light blue). The effect of E_{SSA} variation is most predominant for ice sheet growth and for deglaciation, when ice flow across the grounding line influences its migration and stabilization (Schoof, 2007b). For E_{SSA} =1 (orange) we find earlier retreat and hence 1–2 m SLE thinner modern ice sheets than for E_{SSA} =0.6 (grey reference). For lower values of E_{SSA} =0.3 (light orange), in contrast, deglaciation is limited and modern ice volumes are more than 5 m SLE thicker than observations. Small values for the SSA enhancement factor produce slower and thicker ice streams and ice shelves. However, as that the SIA enhancement factor, 'ESIA', has a larger influence on the ice sheet's volume on glacial scales, we find it a more suitable ice-internal parameter candidate for the ensemble analysis in Albrecht et al. (2019).

2.2 Ice rheological flow law exponent

Generations of ice sheet modelers used variants of Glen's flow law (Eq. (2)) as the constitutive relationship between stress and internal flow with the rheological exponent $n = 3$. According to an analysis of data in Greenland by Bons et al. (2018) the ice rheological exponent for the SIA stress balance should be rather $n = 4$. For the same strain rates at a reference pressure of 50 kPa, we would need to adjust the ice softness factor A accordingly. In the model, the same effect is achieved when adjusting the SIA enhancement factor ESIA= 2.0 divided by 50,000 Pa yields $4.0 \cdot 10^{-5}$ instead.

We have tested the effect of the flow law exponent $n = 4$ (and $n = 2$ to cover the range according to Goldsby and Kohlstedt (2001)) in comparison to the reference simulation and find only small differences in the ice volume time series during glacials and moderate differences in interglacial periods, with on average less than 0.9 m SLE difference (Fig.4). However, the flow law exponent for the SSA has much stronger effects on ice volume with 2–7 m SLE less Antarctic ice volume for $n = 4$ and significantly earlier deglaciation, while for $n = 2$ deglaciation is damped effectively.

Figure 3: ~~Simulation~~ Ice volume above flotation for simulations over the last two glacial cycles with ~~different flow law exponents in the SIA stress balance, varying from 2–4 (orange, grey, green). Enhancement factor has been adjusted such that stress balances compares at 50kPa. The impact of the choice of the exponent~~ varied enhancement factors for ~~the~~ SIA and SSA stress balance~~on the simulated ice volume above flotation is rather small. In contrast, variation of the SSA flow law exponent strongly affects~~ Lower E_{SIA} lead to thicker grounded ice ~~sheet growth and~~ sheets, while larger E_{SSA} cause faster deglaciation ~~(red~~ and ~~blue)~~slightly thinner modern ice sheets.

figs/fig04.pdf

2.3 Model grid resolution

Resolution is a key parameter which determines the misfit between the model results based on discretized model equations and the associate analytical solutions. Analytical solutions for the coupled system of ice sheet model equations, however, can only be found for simplified flow line configurations. For the more realistic case we can get some impression of resolution requirements if we run regression tests to show that grid refinement leads to a convergence of the model solution . Resolution (Cornford et al., 2016) . The horizontal resolution of the boundary data in turn , for instance, can control key parameters of ice stream flow, such as basal roughness (Falcini et al., 2018). We Here we also test for the vertical resolution of the three-dimensional enthalpy field here, which is highest at the ice sheet's base and lowest at the top of the computational domain using a quadratic spacing. The enthalpy formulation allows the transition from cold to temperate ice (Aschwanden et al., 2012), which can form temperate ice layers of up to a few hundred meters.

We find that for our reference parameters and 16 km resolution a similar ice volume history can be reconstructed as for 8 km resolution, while computation costs are about a factor of 10 higher (see Fig. 5). For much coarser grids of the order of 30 km or more (Briggs et al. (2014) used 40 km) we find that relevant ice streams dynamics cannot be resolved any more in an adequate way (Aschwanden et al., 2016). In Fig. 5 we find how resolution can effect glacial-interglacial ice volume history with more than 5m SLE difference, resulting in very different modern ice sheet configurations (see blue line lines in Fig. 5). In fact, also for coarse resolution resolutions we may find solutions that are closer to the reference simulation, e.g. by choosing different enhancement factors.

For the vertical grid we define highest in the reference simulation narrowest grid spacing at the base with a resolution of around 20 m in the reference simulation. Coarser vertical resolution (doubled spacing) does not change the simulation result much (green orange line in Fig. 5). For finer resolution, in contrast, shear heating and the formation of temperate ice is expected to be better resolved and the simulation results should converge. However, the simulated ice volume seems to increase by 3–5m SLE for doubling vertical resolution (see red light orange line in Fig. 5), as less temperate ice is formed in the lowest layers of the ice sheet. Benchmark experiments with respect to an analytical enthalpy solution (Kleiner et al., 2015) suggests adequate convergence for vertical resolution finer than 1 m at the base (see violet line in Fig. 5). Simulated volume above flotation over two last glacial cycles with reference resolution of 16km (grey), fine grid resolution of 8km (blue) and relatively coarse resolution of 32km (orange) resulting in different Antarctic Ice Sheet histories. Refined vertical resolution of 10m (red) and 1m (violet) at the base is compared to the reference simulation with 20m and with coarse resolution of 40m (green).

2.4 Ice flow enhancement factors

Enhancement factors account for unresolved effects of grain size, fabric and impurities and have often been used as tuning parameter in ice sheet modeling entering the constitutive flow law (Eq.) that balances strain rates and stresses within the ice sheet. Value 1 means 'no enhancement', but generally enhancement factors for the SSA tend to be smaller than 1 and larger than 1 for the SIA. Anisotropic ice-flow modeling suggests E_{SSA} values between 0.5 and 0.7 for ice shelves and between 0.6 and 1 for ice streams, while for SIA enhancement should lie between 5 and 6 (Ma et al., 2010) . Previous model ensembles that consider isotropic ice flow use values down to E_{SSA} =0.3 (for E_{SIA} =1) in (Pollard and DeConto, 2012a, PSU model) or up to E_{SIA} =9 (for E_{SSA} =0.8) in (Maris et al., 2014, ANICE model) , both for 20km resolution. PISM seems to favor enhancement factors closer to 1 (e.g. E_{SSA} =0.5–0.6 and E_{SIA} =1.2–1.5 in (Golledge et al., 2015) for 10–20km resolution).

Figure 3 shows the effects of ice flow enhancement factors on the simulated Antarctic Ice Sheet history. SIA enhancemnet generally produces thicker grounded ice. Compared to the reference simulations with E_{SIA} =2 the model simulates for E_{SIA} =1 more than 5m SLE thicker and for E_{SIA} =5 about 6m SLE thinner ice sheets, both at glacial and interglacial states (blue and orange). The effect of E_{SSA} variation is most predominant for ice sheet growth and for deglaciation, when ice flow across the grounding line influences its migration and stabilization (Schoof, 2007b) . For E_{SSA} =1 (green) we find earlier retreat and hence 1–2m SLE thinner modern ice sheets than for E_{SSA} =0.6 (grey reference). For lower values of E_{SSA} =0.3 (red), in contrast, deglaciation is limited and modern ice volumes are more than 5, although this comes with much higher computational costs and memory requirements. For the used set of model parameters, such a high vertical resolution yields a present-day state close to LGM, which is 14 m SLE thicker than observations. This is because larger values of the SSA enhancement factor produce faster ice streams and thinner ice shelves. We hence find the SIA enhancement factor, 'ESIA', a suitable ice-internal parameter candidate for the ensemble analysis in a companion paper. observed. This finding emphasizes the fact that resolution is a relevant model parameter that should be taken into account in model tuning. Ice volume above flotation for simulations over two last glacial cycles with varied enhancement factors for SIA and SSA stress balance. Larger E_{SIA} lead to thicker grounded ice sheets, while larger E_{SSA} cause faster deglaciation and slightly thinner modern ice sheets.

2.4 Iceberg calving

Currently, calving constitutes almost half of the observed mass loss from the Antarctic Ice Sheet (Depoorter et al., 2013). PISM provides different schemes for iceberg calving. For floating ice shelves we use the strain-rate based *eigencalving* parameterization, which accounts for the average tabular iceberg calving flux depending on ice shelf flow and confinement geometry (Levermann et al., 2012; Albrecht and Levermann, 2014). The minor eigenvalue of the horizontal strain rate basically determines where calving can occur, e.g. in the expansive flow regions beyond a critical arch, between

315 outer pinning points of ice rises or mountain ridges (Doake et al., 1998; Fürst et al., 2016). The average eigencalving rate is the product of the minor and major eigenvalue of the horizontal strain rate scaled with a constant.

In our simulations we use a reference parameter value of K$= 1 \times 10^{17}$m s. For a much larger value of 1×10^{18}m s the calving front tends to retreat, but limited by the location of the compressive

320 arch. ~~Smaller~~ As smaller ice shelves exert less buttressing on the ice flow~~and we find s~~, we hence find slower ice sheet growth for glacial climate conditions (see Fig. 6), but negligible effects on deglaciation or interglacial ice volume. For a smaller value of 1×10^{16}m s, in contrast, estimated calving rates tend to be smaller than terminal ice shelf flow and thus calving front expands up to the edge of the continental shelf. The additional buttressing supports a slightly larger present-day ice volume,

325 while in turn the more extended LGM ice shelves can respond effectively to increasing sea level and ocean temperatures, leading to slightly earlier deglaciation (as already discussed in Kingslake et al., 2018) .

In our simulations we define a ~~maximal~~ maximum extent for ice shelves where the present ocean floor drops below 2 km depth, assuming that ice shelves can only exist on the shallow continental shelf ("deep-ocean-calv"). Additionally we avoid very thin ice shelves below 75 m, as enthalpy field

330 evolution and hence the ice flow can not adequately be represented for only a few vertical grid layers. Hence, ice at the calving front thinner than 75 m is removed. Both calving conditions are applied mainly for numerical reasons (adaptive time stepping) to avoid thin ice tongues, but they have negligible influence on the simulated ice volume history.

For higher lower bounds of terminal ice thickness of 150 m or ~~evenm~~ even 225 m, as often used

335 in other model studies, we find slower ice sheet growth but negligible effect on deglaciation and interglacial ice volume (see Fig. 6). As eigencalving supports ice shelves within confinements we find that the effects of ice shelf extent beyond its compressive arch is of relatively low relevance for the glacial-interglacial ice sheet history. This is in contrast to previous model ensembles, who diagnosed high sensitivity of simulation results to varied calving parameters using different calving

340 parameterizations (Briggs et al., 2013; Pollard et al., 2016)

Figure 5: Ice volume ~~histories over two glacial cycles~~ above flotation for ~~different parameter values~~ simulations with horizontal reference resolution of ~~eigencalving constant~~ 16 km (grey), fine grid resolution of 8 km (light blue) and relatively coarse resolution of 32 km (blue) resulting in different Antarctic Ice Sheet histories. Refined vertical resolution of 10 m (light orange) and ~~calving thickness~~ 1 m (~~green and red~~violet) ~~compared to~~ at the base yields larger ice volumes than the reference simulation with 20 m (grey) ~~. Defining a maximum extent of the ice along the edge~~ or for coarse resolution of ~~the continental shelf has only negligible effect on the sea-level relevant ice volume~~ 40 m (~~violet~~orange).

2.5 Mantle viscosity and flexural rigidity

We have shown that sea-level changes drive grounding line migration (in particular in deglaciation processes) through the flotation criterion (see Sect. 4.1). In fact, sea-level changes at the grounding line are not only caused by ~~global mean~~ local sea-surface height change but also by local changes in the ~~sea floor and~~ bed topography. PISM incorporates an Earth model that reflects the deformation of an elastic plate overlying a viscous half-space, based on Lingle and Clark (1985). A key advantage ~~this approach has~~ of this approach over traditional Elastic Lithosphere Relaxing Asthenosphere (ELRA) models is that the response time of the ~~sea floor~~ bed topography is not considered a constant, but depends on the wavelength of the load perturbation for a given Asthenosphere viscosity (Bueler et al., 2007). Calculations are carried out using the computationally efficient Fast Fourier Transform to solve the biharmonic differential equation for vertical bed displacement in response to (ice) load changes σ_{zz} (Bueler et al., 2007, Eq. 1). The Earth model can be initilized with a present-day up-lift map (Whitehouse et al., 2012) ~~. The formulation closely approximates~~ and reproduces plausible uplift pattern and magnitudes for a given load history (Kingslake et al., 2018, personal communication Pippa Whitehouse). Yet, it is still a simplification of the approach used within many GIA models ~~(Whitehouse, 2018)~~ (Whitehouse, 2018), which are defined to account for the response of the solid Earth and the global gravity field to changes in the ice and water distribution on the ~~entire~~ Earth's surface (Whitehouse et al., 2019). With our modification of PISM's Earth model approach we can also account for vertical bed displacement in response to spatially varying water-load changes. However, ~~our Earth~~ the model is not ~~yet~~ able to account for self-consistent gravitational effects associated with local sea-level variations or the rotational state of the Earth (Gomez et al., 2013; Pollard et al., 2017).

We investigate two relevant parameters of the Earth model with regard to both the viscous and the elastic part. ~~.~~ *Mantle viscosity* affects model behaviour because it defines the rate and pattern of the deformation of the ice-sheet's bed and the sea floor. ~~Antarctic Ice Sheet models typically use mantle viscosity of 1×10²¹~~ GIA modeling indicates a viscosity range of viscosities of $10^{20} - 10^{21}$ Pa s ~~.~~ ~~Our reference simulation uses a mantleviscosity~~ for the upper mantle, while the lower mantle is less constrained with $10^{21} - 10^{23}$ Pa s (Whitehouse, 2018). Our PISM simulations do not distinguish between upper and lower mantle, not between East or West Antarctic Ice Sheet (EAIS and WAIS respectively). We choose a reference value of 5×10^{20} Pa s ~~to account for the weaker~~, but for the relatively weak mantle beneath the WAIS even lower values are likely (Gomez et al., 2015), for some regions mantle viscosity values of $< 10^{20}$ Pa s have been suggested (Hay et al., 2017; Barletta et al., 2018).

In our glacial-cycle simulations an even lower mantle viscosity of 1×10^{20} Pa s results in delayed deglaciation and thicker present-day ice sheets than for the reference value of 5×10^{20} Pa s (cf. ~~grey and blue~~ blue and grey in Fig. 7a). As the bed at the grounding line responds faster to unloading for lower viscosities, grounding line retreat is hampered accordingly. In contrast, more viscous mantles

of 25–100$\times 10^{20}$ Pa s result in slower ice sheet growth but in faster deglaciation and hence lower present-day ice volumes above flotation (~~orange and green~~ light blue and orange in Fig. 7a). Within ~~a plausible range~~ the range of $10^{20} - 10^{21}$ Pa s the effect of mantle viscosity on grounding line retreat and re-advance since last deglaciation has been discussed in ~~Kingslake et al. (2018) .~~ a PISM study by Kingslake et al. (2018) . In Appendix A2, we highlight the influence of further model decisions on grounding line sensitivity and thus on the onset of deglacial retreat, although this is not the focus of this study.

The bed deformation model in PISM up to v1.0 considered all changes in ice thickness H as loads[2], including changes in ice shelf thickness, although this does not make physical sense. Here we ~~presented~~ present simulations that consider changes in load of the grounded ice sheet and of the ocean layer within the computational domain with load per unit area defined as

$$\sigma_{zz} = \rho_i \left[\max \left(H - h_f, 0.0 \right) + h_f \right], \tag{7}$$

with h_f the flotation height as defined in Eq. (6). Be aware that since PISM v1.1 the bed deformation model has been fixed and only the grounded ice sheet changes are considered as load.

Our simulations that considers changes in ocean loads yields up to 3 m SLE higher ice volumes above flotation at glacial maximum, while interglacial ice volumes are comparable (*cf.* grey and red lines in Fig. 7a and violet line in Fig. 7b, which excludes both ocean and ice shelf loads as in PISM v1.1). Also, deglaciation is delayed by a few thousand years.

Flexural rigidity is associated with the thickness of the elastic lithosphere and has an influence on the horizontal extent to which bed deformation responds to changes in load. We have deactivated the elastic part of the Earth model in our reference simulation, as the numerical implementation was flawed. ~~Instead~~ In order to evaluate the ice sheet volume's sensitivity to changes in the flexural rigidity parameter value, we have used PISM v1.1 ~~, which~~ instead, with an additional fixed elastic part[3]. Yet, PISM v1.1 considers considers only grounded ice thickness changes as loads, ~~with additionally fixed elastic part[4], in order to evaluate the ice sheet volume's sensitivity to changes in the flexural rigidity parameter value~~ and not the ocean thickness in the reference. As most dynamic changes on glacial cycles occur in West Antarctica previous studies based on gravity modelling suggest appropriate values lying within the range of 5×10^{23} N m and 5×10^{24} N m (Chen et al., 2018). The PISM default value marks the upper end of this range, assuming a thickness of 88 km for the elastic plate lithosphere (Bueler et al., 2007).

~~For this range extended~~ Extending this range to 1×10^{25} N m, which is more than an order of magnitude, we find differences in ice volume above flotation of up ot 4 m SLE, with ~~enhanced~~

---

[2]until commit https://github.com/pism/pism/commit/4b5e14037 from April, 2018

[3]https://github.com/pism/pism/pull/435

[4]

increased temporal variability, see Fig. 7b. Compared to the reference simulation without the elastic part, we find earlier deglacial retreat but similar glacial and interglacial volumes.

Figure 7: Simulations over two last glacial cycles with varying Earth model parameters for the viscous (a) and the elastic part (b). Mantle ~~viscosity~~ viscosities with a range over two orders of magnitude cause slower ice sheet growth but faster decay for increasing viscosity~~, with up to 5m SLE difference in ice volumes~~. ~~Flexural~~ Tested flexural rigidity ~~that ranges~~ over a ~~ranges of~~ more than one order of magnitude yields smaller difference in simulated ice ~~volumes above flotation~~volume response, but ~~enhanced~~ increased variability. Be aware that for the lower panel a different PISM v1.1 has been used, with a fixed elastic model~~. PISM v1.1 accounts~~, but only accounting for changes in grounded ice loads~~only and reduces glacial volume by a few meters SLE (violet in~~, explaining lower ~~panel) as compared to~~ glacial volumes than the reference ~~(grey in upper panel), while modern ice volumes are similar. If only changes in ice load are considered (including changes in ice shelf thickness as in PISM v1.0, but no changes~~ in the ~~load of the ocean water load) then glacial ice volume is estimated up to 6m SLE lower (red in~~ upper panel~~)~~.

3   Boundary conditions and input datasets

3.1   Air temperature

415   Air temperature is an important surface boundary condition for the enthalpy evolution which is thermodynamically-coupled to the ice flow. The annual and summer mean temperature distribution is required in the Positive-Degree-Day scheme (PDD) to ~~estimates~~ estimate surface melt and runoff rates, assuming a sinusoidal yearly temperature cycle (Huybrechts and de Wolde, 1999, Eqs. C1-3). Hitherto, surface temperatures for Antarctica have been often parameterized based

420   on a multiple regression fit to reanalysis data, e.g. as a function of latitude lat and surface elevation h. This provides a temperature field that adjusts to a changing geometry with a prescribed lapse rate and is hence convenient for paleo time-scale simulations. Using ERA Interim C20 data ~~(Simmons, 2006)~~ (Dee et al., 2011) multiple regression fit of summer mean temperatures (January) provides a temperature distribution with a RMSE of 2.2 K over the entire ice sheet, while for annual

425   mean temperatures the RMSE is 4.1 K. Temperatures are considerably overestimated by up to 11 K over the large Ronne and Ross ice shelves and in large parts of inner East Antarctica, while temperatures in dynamically relevant regions along the West Antarctic Divide are underestimated by up to -5 K.

Regarding the comparably shallow ice shelves with less than 100 m surface height, this surface-

430   height dependent parameterization estimates temperature close to those on the sea surface, although observed climatic conditions on the large ice shelves are much colder than those on the ocean~~(probably effects of albedo and catabatic winds). ,~~ where sea ice can be absent in summer. Typically, the Antarctic ice sheet and shelves inhibit a negative radiation budget that efficiently cools the surface (?) .

435   As a correction we assume that the ice shelves' surface (and all other icy regions below 1000 m altitude for consistency) is as cold as at 1000 m altitude to achieve a better fit to ERA-Interim surface temperature data. Furthermore, the climate ~~in~~ of the much larger East Antarctic Ice Sheet is more isolated than the climate in West Antarctica which can be accounted for with a longitudinal dependence lon and symmetry axis through the West Antarctic Divide (110°W), as

440   $$T_{\mathrm{aml}} = 37.5 - 0.0095 \cdot \max(h, 1000) - 0.644 \cdot lat + 2.145 \cdot \cos(lon + 110°) \tag{8}$$

$$T_{\mathrm{sml}} = 15.7 - 0.0083 \cdot \max(h, 1000) - 0.196 \cdot lat + 0.225 \cdot \cos(lon + 110°). \tag{9}$$

Summer temperatures T_{sml} are well represented by Eq. (9) with a RMSE of 2.1 K over the entire ice sheet and a particularly good match in the large ice shelves and East Antarctica. Annual mean temperatures T_{aml} parameterized by Eq. (8) are overestimated by less than 5 K both in the inner

445   East Antarctic Ice Sheet and the large ice shelves of Ross and Ronne-Filchner (see Fig. 8), while temperatures in the West Antarctic Ice Sheet are underestimated by less than 1 K (RMSE 3.1 K).

Figure 8: Comparison of ERA Interim annual mean temperatures (a) with ~~parameterization of multiple regression fit according to~~ Eq. (8), with 110°W-longitude indicated as blue-dashed line (b). Inner parts of the West Antarctic Ice Sheet are less than 1 K too cold (d), while temperatures in the shallow ice shelves of Ross and Ronne are overestimated by up to 5 K (cf. panels c and f). Root-mean-square-errors of temperatures in grounded and floating ice sheet regions are 3.0 K and 4.1 K respectively (e).

Figure 9: Comparison of ERA Interim summer (January) mean temperatures with parameterization of Eq. (9). Root-mean-square-errors of temperatures in grounded and floating ice sheet regions are 2.0 K and 3.1 K respectively, with temperatures in the large ice shelves close to observations.

The annual mean and summer air temperatures enter the PDD scheme, to calculate melt rates and runoff at the surface. We assume melt rates of snow and ice of 3.0 and 8.8 mm for each day and per each degree above freezing point, assuming a daily temperature variability represented by a normally distributed white noise signal with a 5 K standard deviation.

In order to evaluate the transient effects of the choice of the modern climate boundary conditions we run two-glacial cycle paleo simulation with a climatic forcing that is introduced in the following sections of the paper. Here we compare the simulated histories of the ice sheet's 'volume above flotation '-with respect to different modern surface temperatures and PDD settings. ~~Lower~~ A lower temperature standard deviation in the PDD scheme of 2 K instead of 5 K has no influence on glacial volume but it can delay deglaciation slightly. Generally, the effect of the PDD scheme for Antarctic paleo simulations seems of minor relevance , (see Fig. 10). Even if we omit the PDD scheme and use a more realistic annual mean temperature pattern from Racmo2.3p2 (Wessem et al., 2018) or ERA-

Interim ~~(Simmons, 2006)~~ (Dee et al., 2011) , simulated ice volumes differ ~~most~~ at most by up to
460   2 m SLE from the parameterized surface temperature (Sect. 3.1) for interglacial and modern climate
forcing~~with up to 2m SLE~~.
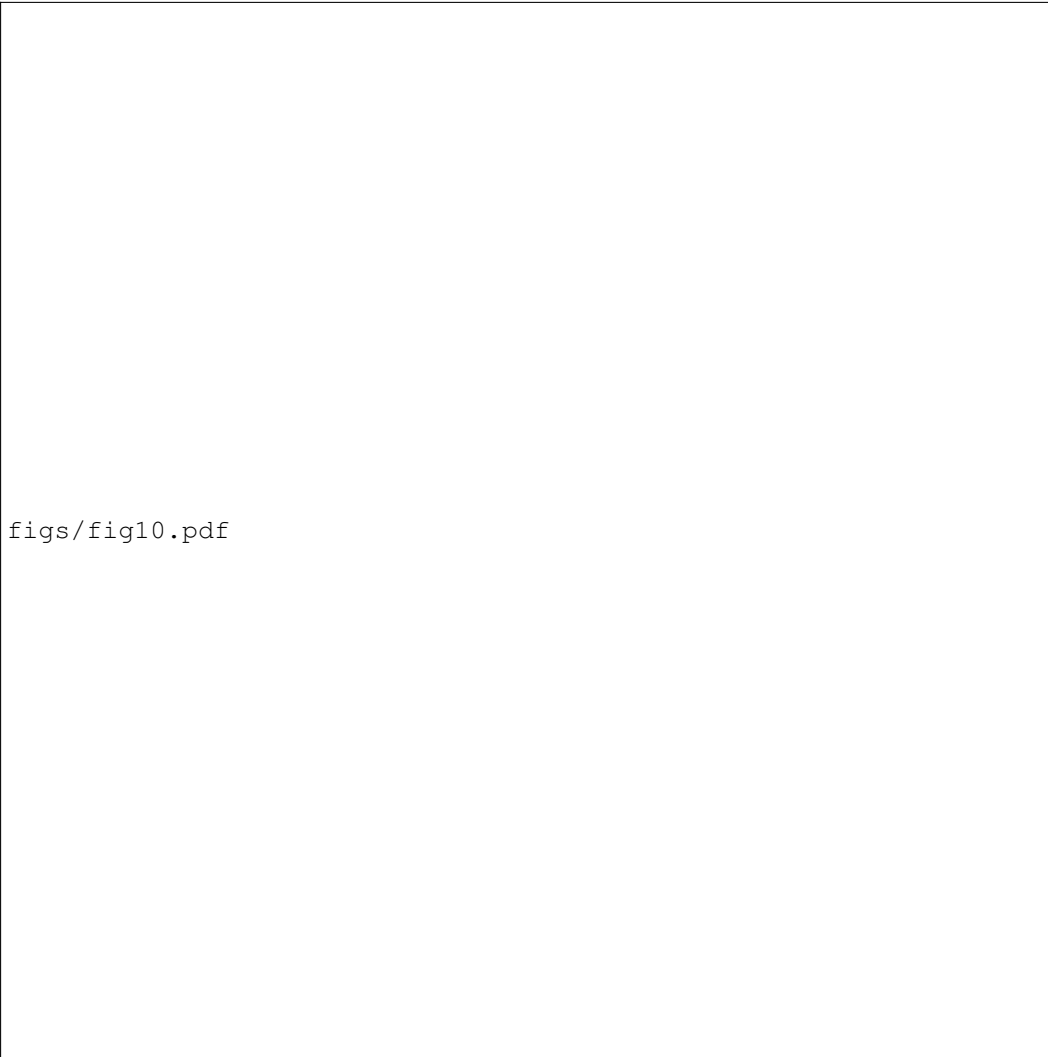
Figure 10: ~~Sensitivity of simulated glacial cycles ice~~ Ice volume ~~to~~ above flotation for variation
of PDD standard deviation and for different ~~surface temperatures~~ modern mean temperature
distributions. The sensitivity is low for different PDD ~~standard deviations~~ parameters of 5 K (ref-
erence in grey), 2 K and when off (blue and light blue respectively), also for interglacials. ~~More~~ For
more realistic annual mean surface temperatures from Racmo2.3p2 (Wessem et al., 2018) or ERA-
Interim ~~(Simmons, 2006) but~~ (Dee et al., 2011) without PDD applied show slightly more difference
in ~~volume above flotation at the onset of~~ simulated volumes for glacial ice sheet growth and ~~in~~ at
interglacials (orange and light orange respectively).

3.2 Precipitation

The distribution of mean precipitation over the Antarctic continent is related to temperatures, but its pattern is strongly determined by the moisture transport over the ice and mountain surface, such that parameterizations as for the temperature (see previous Sect. 3.1) are rather unrealistic. ~~A more realistic near-surface climate, surface mass balance and surface energy balance has been simulated with a resolution of 27km using a~~ We use a more realistic precipitation field from the regional atmospheric climate model ~~forced with re-analysis data for the recent past~~ RACMO2.3p2 (Wessem et al., 2018) (mean over CMIP5 reference period 1986-2005), ~~such as~~ which was forced with re-analysis data for the recent past. RACMO2.3p2 ~~(Wessem et al., 2018) , which~~ incorporates all relevant physical processes at the ice surface ~~.~~ simulated with a resolution of 27 km. Similar as for the temperature parameterization we apply a lapse correction ~~for the~~ to the RACMO precipitation field for changing surface elevation Δh ~~, which is defined~~ to account for the elevation desertification effect (DeConto and Pollard, 2016) , which we define as

$$\Delta P(\Delta h) = P_0 \exp\left(f_p \,\Delta T(\Delta h)\right) = P_0 \exp\left(f_p \,\gamma_T \,\Delta h\right). \tag{10}$$

with f_p=7%/K a precipitation change factor according to Clausius-Clapeyron relationship with temperature and γ_T=7.9 K/km the temperature lapse rate. This correction ensures that topographical changes have an influence on local precipitation through their effect on local surface temperature. However, as re-analysis and regional climate models tend to underestimate present-day precipitation in the interior of the East Antarctic Ice Sheet, simulated ice volume may be biased towards lower than observed values (Van de Berg et al., 2005).

3.3 Basal heat flux

Geothermal heat flux is one of the most poorly known boundary conditions that controls ice flow (Pittard et al., 2016). It can keep basal ice relatively warm, and thus less viscous than colder ice above. PISM uses a bedrock thermal model (1-D heat equation, similar to Ritz et al. (1996)), with storage in an upper lithosphere thickness of 2 km discretized in 20 equidistant layers and geothermal heatflux applied as constant boundary condition to calculate the heatflux into the ice at the ice-bedrock interface depending on ice base temperature. In combination with enhanced supply of melt-water at the ice sheet base it supports rapid ice flow by sliding over the bed and deformation of the subglacial sediments (see previous Sect. 3.4.2). Various maps with substantially different ~~pattern~~ patterns derived from satellite magnetic and seismological data have been made available for the whole Antarctic continent[4] and were used in ice-sheet model simulations for longer then a decade now (Shapiro and Ritzwoller, 2004; Fox Maule et al., 2005; Purucker, 2013; An et al., 2015). Due to their sparse data coverage and significant methodological uncertainty some modelers decided using a simplified two-valued heat-flux pattern that distinguishes the geology of the East and West Antarc-

---

[4]https://blogs.egu.eu/divisions/cr/2018/03/23/image-of-the-week-geothermal-heat-flux-in-antarctica-do-we-really-know-anything/

tic plate (Pollard and DeConto, 2012a). In our ~~simulations~~ reference simulation we use the latest high resolution heat flux map by Martos et al. (2017), which is derived from spectral analysis of the most advanced continental compilation of airborne magnetic data.

For the different Antarctic basal heat flux data sets we compare PISM simulated quasi-equilibria after 50 kyr with constant boundary conditions and find only little differences with ~~about 21~~around 43 m RMSE between the resulting ice thickness distributions (Fig. 11).

Figure 11: PISM present-day equilibrium results after 50 kyr ~~simulation~~ for different basal heat flux fields (upper row) affecting the near-ground ice temperatures and hence the ice thickness, here shown for the first result as anomaly to Bedmap2 (first panel in lower row) or relative to the first PISM result. First three columns show the results for the magnetic reconstructions by Martos et al. (2017) (as in the reference), Purucker (2013) and Fox Maule et al. (2005). ~~Column~~ Columns 4 to 5 ~~shows~~ show the seismic reconstructions by An et al. (2015) and Shapiro and Ritzwoller (2004), and last column for comparison a two-valued field as used in Pollard and DeConto (2012a), separating East and West Antarctica. The overall effect of the choice of geothermal heatflux on present-day equilibrium ice thickness ~~equilibrium is comparably small with~~ measures up to ~~50~~100 m ~~ice thickness anomaly~~ RMSE for Purucker (2013) , while for the other tested setups it differs only in individual spots ~~in West Antarctica and~~ with a RMSE of ~~around 21~~40–45 m.

Here we compare the simulated histories of ~~ice sheet~~ 'the ice sheet's volume above flotation '-with respect to the different basal heat flux boundary conditions. The overall effect on ice volume history seems rather small for glacial climate with a variation of ~~1.7~~about 3 m SLE~~in the present-day result, except for An et al. (2015) with 6~~, with the lowest mean heatflux of 54 ~~m SLE above the reference~~ mW m^{-2} Purucker (2013) yielding generally largest ice volumes and vise versa for the hightes mean heatflux of 67 mW m^{-2} Martos et al. (2017) (see Fig. 12a). The transient sea-level relevant volume shows most variance during ~~deglaciation~~interglacials, when in some relevant regions of West Antarctica, such as Siple Coast, grounding line migration is delayed and the local anomaly in ice thickness reaches up to 500 m. ~~On average ice volume differse laess than 1.6~~Largest differences are found for the present-day state with a range of simulated ice volumes of 8 m SLE~~and, compared~~. Compared to other uncertainties discussed in this study, e.g. with regard to friction-related parameters (see next Sect. 3.4), we evaluate the choice of basal heat flux distribution of low relevance for the total ice volume history. However, in another PISM ensemble study that covers the last 2 million years with a focus on ice domes and deep ice cores during interglacials, geothermal heat flux becomes the most relevant uncertain boundary condition (Sutter et al., 2019).

Figure 12: (a) Simulation ~~over two glacial cycles with~~ results for different basal heat flux distribu-
tions (Martos et al., 2017; Purucker, 2013; Fox Maule et al., 2005; An et al., 2015; Shapiro and

3.4 Basal friction

Subsurface boundary conditions and their influence on basal sliding are key in the understanding of Antarctic ice flow, in particular subglacial topography, basal morphology (e.g. presence of sediments) and subglacial hydrology (Siegert et al., 2018)~~, and how they influence basal sliding~~.

3.4.1 Pseudo plastic exponent

In PISM~~basal sliding is of nonlinear Weertman-type for sliding over rigid bedrock (Fowler, 1981; Schoof, 2010), where the basal shear stress τ_b (tangential sliding) is related to the SSA sliding velocity u_b in the form~~

$$\tau_b = -\tau_c \frac{u_b}{u_0^{\,q}\,|u_b|^{1-q}}\,,$$

~~with $0 \leq q \leq 1$ the positive sliding exponent .~~, basal sliding is parameterized according to the Eq. (11) with sliding exponent q. Value $q = 0$ represents ~~plastic~~ purely-plastic (Coulomb) deformation of the till where ice is flowing over a rigid bed with filled cavities (Schoof, 2005, 2006). Many studies use $q = 1/3$ (Schoof, 2007a; Pattyn et al., 2013; Gillet-Chaulet et al., 2016) or a linear sliding relationship between basal velocity and basal shear stress for $q = 1$, as most commonly adopted for inversion methods (Larour et al., 2012; Gladstone et al., 2013; Yu et al., 2017). Note, that u_b results from solving the non-local SSA stress balance (Bueler and Brown, 2009, Eq. 17) in which τ_b appears as one of the terms that balance the driving stress. The PISM default sliding velocity threshold is $u_0 = 100\,\mathrm{m\,yr}^{-1}$, where basal shear stress is independent of q.

Over the valid range of q we find ~~in transient simulations~~ a spread of reconstructed ice volumes of up to 12 m SLE (see Fig. 13) ~~, while larger~~ in transient simulations. Larger values lead to thinner ice sheets, in particular at interglacial states. ~~We choose the pseudo-plastic q~~ Due to its large impact on ice volume the pseudo plastic exponent q or 'PPQ' ~~as relevant basal~~ is a key parameter in the large ensemble analysis in ~~a companion paper~~ the companion paper to this study (Albrecht et al., 2019) .
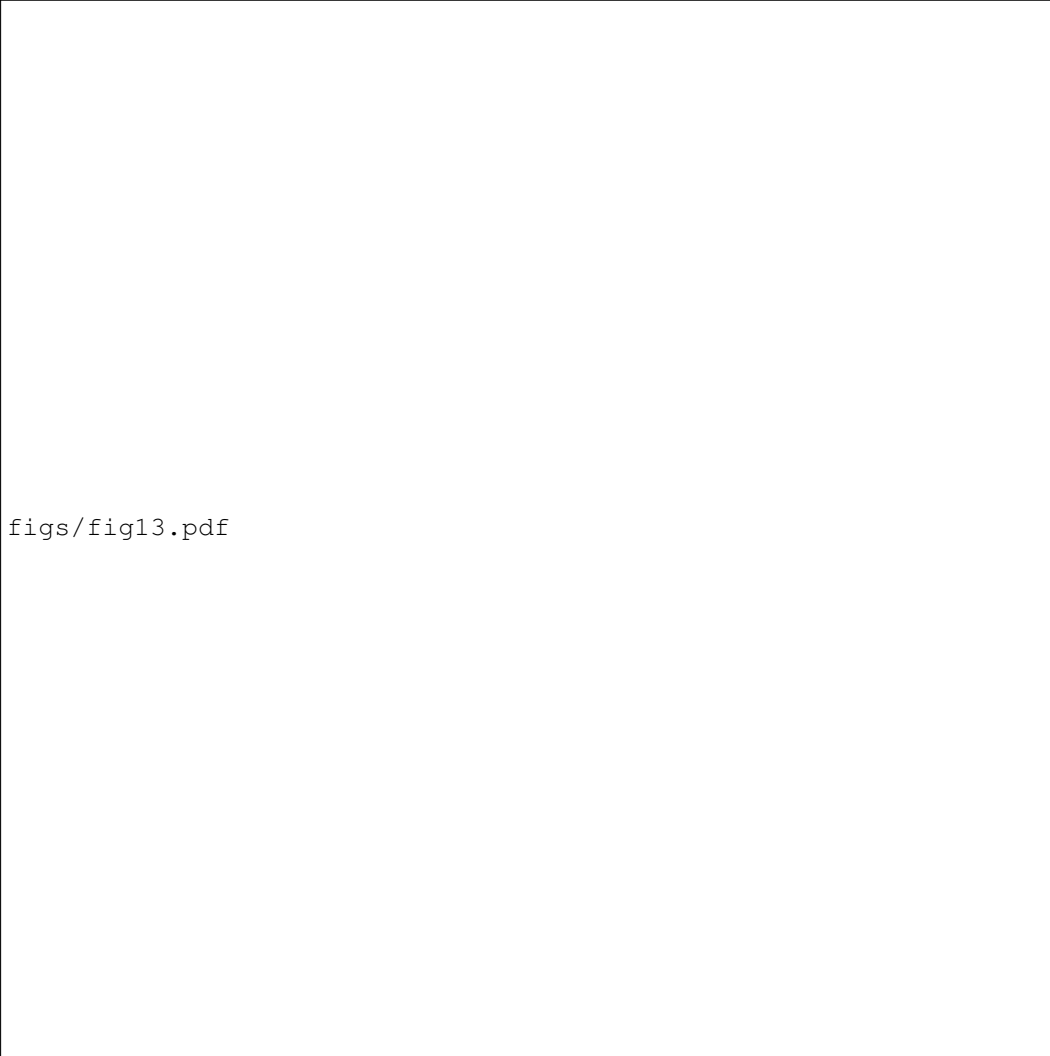
Figure 13: Antarctic ice volume history over the last two glacial cycles for different values of the basal sliding exponent q in Eq. (11). Between plastic (blue) and linear (~~red~~light orange) ice volume above flotation can vary by up to 12 m SLE for interglacial periods, on average by 6 m SLE. Generally, smaller values of q lead to slower ice flow and hence to larger ice volumes.

3.4.2 Till properties

~~In our PISM simulations the Mohr-Coulomb criterion (Cuffey and Paterson, 2010) determines the yield stress τ_c as a function of small-scale till material properties and of the effective pressure N_{til} on the saturated till,~~

$\tau_c = \tan(\phi) \, N_{til}.$

~~Till~~The till friction angle ϕ is a shear strength parameter for the till (in Eq. (11)) associated with the ~~roughness~~geology of the bed and can be parameterized in PISM as a piecewise-linear function of bed

elevation (Martin et al., 2011), assuming that marine basins and ice stream fjords have a rather loose ~~till~~ sediment material, while ~~it is~~ being denser in the rocky regions above the sea-level. The till friction angle is weakly confined (observational range in ice streams is 18-40° in Cuffey and Paterson, 2010) and

550 we assume $\phi_{min} = 2°$ in the marine basins lower than -500 m, $\phi_{max} = 45°$ above 500 m and a linear gradient between those two levels.

First, we run 50 kyr equilibrium simulations with constant boundary conditions and compare to a spatially equal distribution of till friction angle with $\phi = 30°$ ~~(see Fig. 14)~~(Cuffey and Paterson, 2010, see Fig. 14). The simulation shows a general overestimation of ice thickness with anomalies of more than 800 m

555 in West Antarctica and an overall RMSE of 372 m for the constant till friction angle. The anomalies are negative in large parts of the East Antarctic Ice Sheet and at WAIS Divide using the piece-wise linear parameterization, with a RMSE of about 296 m. This suggests that estimates of till friction angle in parts of the sub-marine basins are too low, while along Siple Coast and in the Transantarctic Mountains values seem too high. Nevertheless, the dependence on fjord-topography supports

560 narrowly confined structures of simulated ice streams, which is observed in many Antarctic regions.

These simulation results are compared with those using a till friction angle field that has been optimized to fit the observed grounded surface elevation (or ice thickness) from Bedmap2 (Fretwell et al., 2013)~~, not observed velocities.~~ We followed the simple inversion method by Pollard and

565 DeConto (2012b), but we inverted for the till friction angle ϕ rather than for the basal sliding coefficient τ_c. In PISM the effective pressure N_{til} in Eq. (11) is physically determined by the subglacial hydrology model, while Pollard and DeConto (2012b) use basal temperature as a surrogate. As we run the simulation forward in time for constant boundary conditions the till friction angle is adjusted in every grounded grid cell every 500 years in incremental steps of $\Delta\phi$ that are proportional to

570 the misfit to observed surface elevation (divided by 200 m) and bounded by $-0.5° <= \Delta\phi <= 1°$. Since the surface elevation is underestimated in the inner parts of the East Antarctic Ice Sheet by a couple of hundred meters (~~eventually~~ due to underestimated ~~accumulation~~precipitation forcing), retrieved till friction angles ~~reaches~~ reach the maximum value of $\phi_{i_{max}} = 70°$ which enhances yield stress by about an order of magnitude. In contrast, in Siple Coast the minimum values of $\phi_{i_{min}} = 2°$

575 compensates for overestimated ice thickness (see lower rows in Fig. 14). Thus, the RMSE of ice thickness can be significantly reduced to 141 m (or even 123 m for $\phi_{i_{min}} = 0.5°$) and the modeled ice volume is only 0.5% below observation. The retrieved distributions of till friction angles are rather independent of initial conditions and iteration parameters (not shown here). But this method may overcompensate for inconsistent model boundary conditions or not adequately represented pro-

580 cesses.

For the transient response of the ice sheet's volume to the different distributions of till friction angle, we find similar glacial ice volumes for the depth-dependent parameterization and the optimization, while in contrast interglacial ice volumes differ considerably (cf. ~~orange~~ light blue and grey in Fig. 15a). For the spatially constant till friction angle of $30°$ underneath the grounded ice sheet and $2°$ on the ocean floor, we simulate similar glacial cycle volume histories as for the parameterizations (blue). In fact, we find a larger shift in ice sheet volume for variations of till friction angle on the ocean floor. ~~Ice volume histories over two glacial cycles for different parameterizations of till friction angle. Volumes at Last Glacial Maximum are similar for same $\phi_{min} = 2$ in the marine ice sheet sections, but deglaciation is omitted in the depth-dependent parameterization (orange). For a smaller $\phi_{min} = 1$ we find generally smaller ice volumes, as discussed in the next section.~~

Till properties under modern ice shelves

Friction (and also bed topography) at the ocean bed underneath the modern ice shelves is weakly constrained, as the optimization algorithms only applies to modern grounded regions (e.g., Pollard and DeConto, 2012b; Morlighem et al., 2017). Friction coefficient on the continental shelf has been thus chosen as one of the ensemble parameters in Pollard et al. (2016, 2017). In PISM the till friction angle accounts for the flow properties of the substrate and enters the yield stress definition ~~with its tangent as~~ $\tan(\phi)$ (see Eq. (11)). As sandy sediments are prevalent in the ice shelf basins low values of ϕ are likely ~~(Halberstadt et al., 2018) . On the other hand~~ in these regions (Halberstadt et al., 2018) . Additionally, till friction angle in the ice shelf basins is a crucial parameter, which determines the thickness of the extended ice sheet for LGM conditions and hence the potential contribution to the global sea-level change.

Modeled LGM ice volumes increase by up to 2–4 m SLE per $1°$ change in minimal till friction angle (see Fig.15b). Compared to observations we detect much higher volumes above flotation at present-day for $\phi_{min} \geq 3°$. At the same time, relative volume changes ~~from LGM to~~ between the LGM and modeled modern state become slightly smaller for rougher basins. This effect may be related to the effect of friction on the rate of grounding line retreat. Till friction angle is an important uncertain parameter for possible WAIS collapse. As no (partial) WAIS collapse is induced in the simulations, we find very similar ice volumes for Last Interglacial (LIG) and present day. The spread of ice volumes among the four experiments with $\phi_{min} =$1–5° is on average 13 m SLE. ~~For now we chose~~ We choose as a reference a lower bound for the till friction angle of $\phi_{min} = 2°$ in ocean regions, as simulated deglaciation shows a good match to modern ice volume (Fig.15b, grey).

Figure 15: ~~Simulation of~~ Ice volume histories over two glacial cycles for different ~~minimal~~ parameterizations of till friction ~~angles in the marine sectors~~angle. ~~The choice~~ (a) For spatially

3.4.3 Subglacial hydrology

~~Friction at the ice sheet base is weakly constrained. A time-dependent basal substrate rheology scheme allows meltwater generated at the ice-sheet bed to saturate and weaken the subglacial till layer (de Fleurian et al., 2018) . The resulting reduced basal traction allows grounded ice to accelerate. This can, in turn, cause dynamic thinning, a reduction in driving stress and ultimately a reduced ice stream flow later on. In PISM yield stress is defined as Mohr-Coulomb criterion (Cuffey and Paterson, 2010) as in Eq. , with the hydrology-related effective pressure~~

$$N_{\text{til}} = N_0 \left(\frac{\delta P_0}{N_0} \right)^s 10^{(e_0/C_c)(1-s)},$$

~~which accounts for the overburden pressure $P_0 = \rho_i g H$ for given ice thickness H, and the fraction of effective water thickness in the till layer s, while all other parameters are constants (adopted from Bueler and van Pelt, 2015) .~~

Till water distribution

~~Till water in our PISM simulations is modeled as boundary layer with an effective thickness of water content W with respect to a maximum amount of basal water $W_{\text{til}}^{\max} = 2\,\text{m}$ and enters as fraction s in Eq. . We use a~~ The effective till water content in PISM ~~non-conserving hydrology~~ ~~model that connects W_{til} to the basal melt rate M_b, where ρ_w is the density of water and C_d is a fixed~~ scheme is a result of the balance between basal melting and a constant drainage rate,

$$\frac{\partial W_{\text{til}}}{\partial t} = \frac{M_b}{\rho_w} - C_d.$$

see Eq. (11).

PISM's default drainge rate of 1 mm/yr is smaller than the basal melting in most of the grounded Antarctic Ice Sheet regions, such that till saturates over time. Higher decay rates can effectively drain the till water in the inner ice sheet regions which generally cause less extended and more confined ice streams, less ice discharge and hence thicker ice sheets. In transient glacial cycle simulations, this relationship applies for both present-day climate conditions (see Fig. 16) and for colder-than-present climates. A till water drainage rate of 10 mm/yr can cause up to 11 m SLE additional ice volume (orange line in Fig. 17a).

Figure 16: Present-day result of glacial cycle simulation showing ice thickness anomaly to Bedmap2 (lower left) and to reference (lower right) for different till water decay rates (1 mm/yr left, 5 mm/yr middle and 10 mm/yr right column) causing different till water distributions underneath the ice sheet (upper row). For a decay rate of 1 mm/yr (reference) about 90% of ice sheet's bed is saturated, while for 10 mm/yr saturated till is only found in the coastal regions and underneath fast-flowing ice stream.

Another relevant aspect is the initial till water fraction on ocean beds that become grounded. PISM assumes that grounding line advances into dry till area $W_{\mathrm{til}} = 0$, where a till water layer can form over the following decades or centuries. If we assume a rigid till layer instead with $W_{\mathrm{til}} = W_{\mathrm{til}}^{\mathrm{max}}$ for an advancing grounding line we find slower growth of glacial ice sheet volume and much earlier deglaciation, while ice volumes are comparable to the reference case for present-day climate conditions (compare ~~green~~ orange and grey line in Fig. 17a). ~~Simulation over two glacial cycles for different till water decay rates underneath the grounded ice sheet. Higher values cause less extended ice streams, less ice discharge and hence thicker ice sheets (blue and orange). If we assume maximum till water~~

~~fraction across ocean beds, grounding line advance of marine glaciers is decelerated. Accordingly, we find less extended and thinner ice sheet at glacial periods, earlier retreat but similar present-day results, compare grey and green lines.~~

~~Overburden~~ Critical overburden pressure fraction

650 The effective pressure cannot exceed the overburden pressure, i.e., $N_{til}^{max} = P_0$ ~~(for details see Bueler and van Pelt, 2015, Sect. 3.2)~~, while in the case of saturated till layer ($s = 1$) ~~we find~~ in Eq. (11) yields a lower limit $N_{til}^{min} = \delta P_0$, with δ ~~a certain~~ being a fraction of the effective overburden pressure~~(PISM default is 2%, our reference is 4%)~~, at which the excess water will be drained into a transport system. As in large portions of the grounded Antarctic Ice Sheet, where ~~a certain~~ the maximum amount of till water

655 is abundant, the parameter δ ~~practically~~ scales the lower bound of the yield stress and hence affects the total ice volume above flotation considerably. PISM's default δ-value is 2%, while for the reference simulation we use 4%, which yields a better score in a basal parameter ensemble (Albrecht et al., 2019, Appendix A). For a doubling in δ, PISM simulations suggest almost a doubling in glacial ice volume change (see Fig. 17b). Also, for higher values of δ, the onset of deglacia-

660 tion occurs earlier.

Figure 17: ~~Volume above flotation in simulation~~ (a) Simulation over two glacial cycles for different

~~values~~ till water decay rates (a) and for different fractions of the overburden pressure (b) underneath

4 Climatic forcing

In our PISM simulations the Antarctic Ice Sheet responds to externally prescribed climatic forcings. In this section we choose reconstructions of Antarctic temperatures and sea-level variations which implicitly incorporate the past climate response to changes in orbital configurations and atmospheric CO_2 content. However, in this stand-alone mode no feedbacks of the ice sheet to the climate system are considered, but we discuss contributions of the climatic forcings to the volume evolution of Antarctic Ice Sheet.

4.1 Sea-level forcing

The Antarctic Ice Sheet, particularly in its western part, rests on a bed below the sea-level with floating ice shelves attached. The location of the grounding line in PISM is solely determined by the flotation criterion (cf. $H \leq h_f$ in Eq. (6)) and ~~therewith~~ therefore also by the current sea level height z_{sl}, for given ice thickness H and bed elevation b. ~~Glacial dynamics in the marine ice sheet sections~~ Marine ice sheet dynamics are hence sensitive to changes in sea-level, which has been 120–140 m lower than today at the Last Glacial Maximum. We neglect regional sea-level effects due to changes of the rotation of the earth or due to self-gravitation, which can have a stabilising effect on the ice sheet locally (Konrad et al., 2015). Instead, we consider global mean sea-surface heights reconstructions prescribed by the ICE-6G_C GIA model, which includes the influence of the changing surface area of the oceans (Stuhne and Peltier, 2015, 2017, courtesy Dick Peltier). To analyse the sensitivity of the model's response to the choice of the sea-level forcing ~~we compare also to a few~~, we compare our results to other reconstructions by Lambeck et al. (2014); Bintanja and Van de Wal (2008); Imbrie and McIntyre (2006); Spratt and Lisiecki (2016). Focusing on the last deglacial period, the timing of sea-level rise onset in response to the melting of the northern hemispheric land ice masses varies by a couple of thousand years among the different sea-level curves (Fig. 18)~~, e.g.~~. For instance, the reconstruction from a glacio-isostatic adjustment model simulation of eustatic sea level by Stuhne and Peltier (2015) peaks already before 25 ~~kyrs~~ kyr BP with around -130 m below present (~~blue~~grey) while the much smoother SPECMAP sea-level curve by Imbrie and McIntyre (2006) has a minimum around -18 kyr BP and a comparably late relaxation to the present-day sea-level ~~stand (orange~~(blue).

The modeled Antarctic Ice Sheet response at the Last Glacial Maximum is rather unaffected by the choice of the sea-level forcing, while in contrast the ice volume at ~~present-day ice volume~~ present-day varies by up to 2.5 m sea-level equivalent (lower right panel of Fig. 18). In particular ~~the so-called~~, the meltwater pulse 1a ~~(MWP1a Liu et al., 2016)~~ (MWP1a; Liu et al., 2016) at around 14.35 kyr BP, with a global sea-level rise of 9–15 m or more within a few hundred years (see grey vertical band in Fig. 18), is well represented as a step in the sea-level curve in the reference forcing time series of the ICE-6G_C (VM5a) model. ~~This~~ About 4 ky later, this triggers a comparably

early and quick grounding line retreat in the Ross and Weddell Sea embayment, where the large ice shelves become afloat.
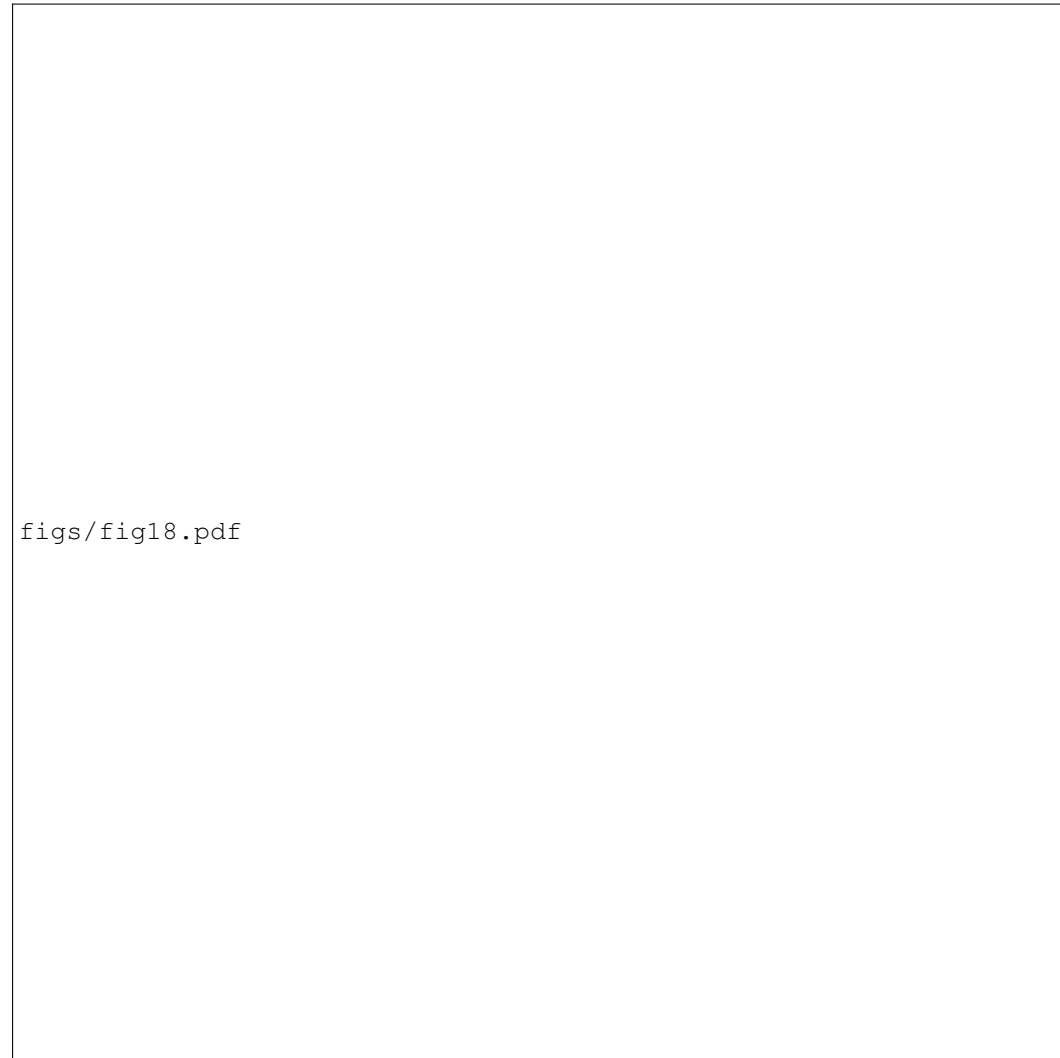
Figure 18: Time series of reconstructed sea-level change over the last 135 kyr (upper left) and the last 30 kyr (upper right) by Stuhne and Peltier (2015); Imbrie and McIntyre (2006); Lambeck et al. (2014); Bintanja and Van de Wal (2008); Spratt and Lisiecki (2016) and corresponding PISM-simulated sea-level relevant ice volume anomaly relative to observations (Fretwell et al., 2013) in lower panels. In order to approximate the effect of self-gravitation we scaled the ICE-6G forcing (Stuhne and Peltier, 2015) by 80%. For about 25 m higher sea-level stand at LGM we find almost the same modeled ice volume, while we find ~~much~~ earlier ~~and~~ but more gradual deglaciation (violet).

If self-gravitational effects were accounted for within a sea-level model, the local sea-level anomaly at the grounding line would be reduced compared with the global mean. A scaling of the sea-level forcing by 80–90% would mimic the first-order feedback of self-gravitation on grounding line mo-

tion. Interestingly, neither the ice volume at LGM nor at present-day is significantly affected, but the onset and rate of deglaciation (Fig. 18, ~~purple~~ violet line).

4.2 Surface temperature forcing

Varying surface temperatures drive ice flow changes on glacial timescales. In PISM we model the non-linear thermo-coupling via a Glen-type flow law with a generalized form of Arrhenius form. More specific, PISM's default flow law is the polythermal Glen-Paterson-Budd-Lliboutry-Duval law (Lliboutry and Duval, 1985; Aschwanden et al., 2012), where the ice softness depends on both the temperature and the liquid water fraction, so it parameterizes the (observed) softening of pressure-melting-temperature ice as its liquid fraction increases. Since vertical diffusion processes in the ice are rather slow, the corresponding response of the ice sheet to surface temperature anomalies occurs with some delay of up to a few thousand years, involving a long-lasting memory for past events (see Sect. 1.3).

On paleo time scales PISM can use temperature reconstructions from ice cores based on deuterium isotopes, such as the EPICA Dome~~C~~ C ice core (EDC, Jouzel et al., 2007) with a well resolved timeseries over the last 803 kyr (EDC3 age scale), representative for the inner East Antarctic Ice Sheet. However, most of the ice-dynamical changes on glacial timescales occur in the marine regions of the West-Antarctic Ice Sheet, ~~whereas~~ and the much closer WAIS Divide ice core provides a highly resolved temperature reconstruction (WDC, Cuffey et al., 2016), which spans only the last 67.7 kyr. As surface temperature forcing $\Delta T(t)$ we consider the temperature anomaly with respect to the year ~~2000~~ 1950 A.D. added to the parameterized temperature field of Sect. 3.1. For model periods before 67.7 kyr the temperature anomaly of EDC applies (with respect to the last 1000-years average), with a small jump of 0.2 K within variability, see upper panels in Fig. 19. The EDC temperature reconstruction shows higher variability than the WDC reconstruction.

~~As WDC temperature rise occurred somewhat earlier than at EDC the Antarctic Ice Sheet responds with higher deglaciation rate (cf. grey in blue line)~~ In our simulations, the Antarctic Ice Sheet volume responds with several thousand years delay to the surface temperature forcing. The LGM minimum in surface temperatures reconstructions happened around 22 kyr BP in the WDC data, while largest ice volume is simulated at 14 kyr BP. The main temperature rise at WDC occurred between 18 kyr and 12 kyr BP contributing to initial deglaciation at around 12 kyr BP with major retreat between 8 kyr and 4 kyr BP. At EDC location the reconstructed temperature rise happened about 1 kyr later with more variability leading to a more gradual deglaciation between 12 kyr and 2 kyr BP. Comparisons with other ice core temperature reconstructions, however, suggest a superimposed ~~effect of~~ lapse rate effect due to surface height change during deglaciation at WDC location (Werner et al., 2018). In addition, Antarctic temperature anomalies at glacial maxima with up to -10 K may be overestimated systematically (personal communication Eric Steig). We also test for a scaled temperature reconstruction from WDC with a LGM temperature of only 6 K below present (see ~~orange~~ light

blue lines in Fig. 19). Interestingly, this weaker temperature forcing results in slightly thicker glacial ice volume (probably an effect of temperature-coupled surface mass balance, see Sect. 4.4) and delayed deglaciation. We have also tested for the influence of temperature variability on the simulated ice volume (Mikkelsen et al., 2018) and found slightly earlier initial retreat for the 500-yr moving average WDC temperature forcing, while for added white noise of 1.5 K variance the present-day ice volume is more than 5 m SLE larger than the reference (compare orange, light orange and grey lines in Fig. 19).

Figure 19: Timeseries of PISM-simulated ice volume above flotation relative to observations (Fretwell et al., 2013) over last 135 kyr (lower left) and last 31 kyr (lower right) forced with three different surface temperature reconstructions (upper panels) at WDC ~~(Cuffey et al., 2016)~~ (Cuffey et al., 2016, grey) and EDC ~~(Jouzel et al., 2007)~~ (Jouzel et al., 2007, blue) leading to different ice volume histories, particularly during deglaciation period. WDC temperature reconstruction scaled by 60% cause 2 m SLE larger glacial ice volume and slower deglaciation (light blue). When WDC temperature reconstruction is smoothed, we find a slightly earlier initial retreat (orange), while added white noise leads higher ice volume at present-day (light orange)

4.3 Ocean temperature forcing

Sub-shelf melting in PISM is calculated via PICO (Reese et al., 2018) from salinity and temperature in the lower ocean layers on the continental shelf (Schmidtko et al., 2014) averaged over 18 separate basins adjacent to the ice shelves around the Antarctic continent. While salinity change over time in the deeper layers is neglected in this study, the ocean temperature responds with some delay to changes in the global mean temperature. We analyzed simulations with coupled climate model ECHAM5/MPIOM over more than 6,000 years following a four-fold increase in CO_2 forcing (courtesy Li et al., 2012) and identified the anomaly in global mean temperature, in Antarctic temperature (south of 66° S) and in Antarctic ocean temperature at depth levels between 500 and 2,500 m. After ~~the~~ a response time of about 3,000 years the ocean temperature stabilizes at about $f_o = 0.75$ of the global mean anomaly, while Antarctic surface temperature anomaly is amplified by a factor of 1.8 (see Fig. 20a). As we intend to estimate ocean temperature change from ice surface temperature change reconstructed from ice cores, we could fit the response function directly from the Antarctic mean surface temperature in the climate model data. But we prefer to use a more general definition, as response to global mean temperature change, which makes it easier to compare to other approaches. We found that, for ~~considered time scales~~ the time scales considered here, Antarctic surface temperatures respond rather ~~linearily~~ linearly with global mean temperature change (and respective amplification factor). ~~In addition, as response to global mean temperature we build on a more general definition, which is easier to compare to other approaches.~~

figs/fig20b.pdf

(a)   (b)

Figure 20: (a) Global mean temperature (green), Antarctic mean temperature south of 66°S (grey) and ocean temperature averaged over upper 500m (light blue), intermediate (500-2500m, blue) and deeper layers (below 2500m, violet) of the MPIOM model coupled to ECHAM5 forced by a CO_2 quadrupling within 140 years (Li et al., 2012). (b) Reconstructed noisy response function $R(t)$ (blue) with fitted function $R^*(t)$ (orange dashed) as in Eq. 13. For comparison fit function with $\alpha = 1$ (green dotted).

Using linear response theory (Winkelmann and Levermann, 2013) and assuming the global mean temperature anomaly $\Delta T_{GM}(t)$ via a convolution integral related to the ocean temperature as

$$\Delta T_o(t) = \int_0^t dt' \, R(t - t') \, \Delta T_{GM}(t'),$$ (11)

we reconstruct a response function $R(t)$ and a corresponding fit function with $R^*(t) \sim t^{-\alpha}$ (see Fig. 20b), which vanishes beyond the typical response time τ_r. For $\alpha = 2$ and with integration constant in the numerator yielding unit integral, such that

$$\int_0^{\tau_r} R^*(t) \, dt = f_o,$$ (12)

this yields

$$R^*(t) = f_o \cdot \frac{[t_0^{-1} - (\tau_r + t_0)^{-1}]^{-1}}{(t + t_0)^2}, \qquad 0 \le t \le \tau_r.$$ (13)

. ~~Reconstructed noisy response function $R(t)$ (blue) with fitted function $R^*(t)$ (orange dashed) as in Eq. 13. For comparison fit function with $\alpha = 1$ (green dotted).~~ The inferred response fit function convoluted with a given timeseries of global mean surface temperature anomaly (or here with the scaled ice core temperature reconstruction) hence provides an estimate for the corresponding change in ocean temperature at intermediate depth. Figure 21 shows the estimated ocean temperature anomaly curve (blue) with some delay with respect to the WDC surface temperature reconstructions ~~(Cuffey et al., 2016, , grey)~~ (Cuffey et al., 2016, grey) , here scaled by $0.75/1.8 = 5/12 = 42\%$ (purple). WDC likely ~~reflects better~~ better reflects the ocean conditions in the widely marine West Antarctic Ice Sheet than the EDC in central East Antarctica (Jouzel et al., 2007)~~.~~.

The resulting timeseries is comparably smooth with a resolution of 500 years and serves as PICO ocean temperature forcing. A comparison to reconstructions with a GCM in the TraCE-21ka project (Liu et al., 2009) [5] shows that short warming periods above present level can occur at intermediate depth, e.g. during ACR around 14 kyr BP, which can not be adequately resolved with our approach. The GCM ocean data are bounded below by the pressure melting point. As negative ocean temperature anomalies can result in unphysical values below pressure melting point, we leave it to the PICO module to assert this lower bound, such that melting vanishes and overturning circulations halts accordingly. As a consequence ocean forcing ~~is not relevant~~ becomes irrelevant for much colder-than present glacial climates. The here presented parameterization assumes that ocean water masses at depth below 500 m can access ice shelf cavities and induce melting, which is certainly very simplified regarding the complex topography flow patterns around Antarctica. Also, we used data from a simplified sensitivity experiment with ECHAM5/MPIOM, for a much warmer than present climate, which implies various model uncertainties. We had to make assumptions about a suitable

---

[5]http://www.cgd.ucar.edu/ccr/TraCE/

response function, which is fitted to model data that are averaged over certain regions and ocean
795 depths, implying further uncertainties.

Figure 21: Response of the intermediate ocean temperature (blue) to surface temperature anomaly as reconstructed from WDC (Cuffey et al., 2016, grey line) assuming a polar amplification factor of 1.8 and an equilibrium ocean scale factor of 0.75, as identified in climate model analysis for a warming scenario. Convolution yields a delayed response with respect to the forcing (compare violet and blue curve). Dots indicate bins of 500 year means. The timeseries includes the Antarctic Cold Reversal (ACR) 14.6-12.7 kyr BP (Fogwill et al., 2017). For comparison, GCM ocean temperature anomaly is shown (in olive), as reconstructed by TraCE-21ka (Liu et al., 2009), for the mid-ocean depth 600-2,800m depth and south of 66°S.

Transient PISM simulations reveal ~~effects of~~ a delayed response of the ice volume to the ocean temperature forcing ~~on the timing of deglaciation with delays of a few thousand years when compared to the scaled surface temperature forcing timeseries~~ with main deglaciation occurring when temperature anomalies reach almost present-day levels (Fig. 22, cf. upper and lower panels). When we ~~apply directly~~ directly apply the smoothed and scaled surface temperature forcing as PICO forcing we still
800 get very similar results, but a slightly earlier retreat (~~green~~orange). Simulations reveal that the power of the response function (cf. Fig. 20b) is of minor relevance for the ice sheet's response (compare

grey and blue lines), and so is the amplitude of cooling at glacial stage, here scaled by 60% (~~red~~light orange). If the ocean forcing is related to the EDC temperature reconstruction (see previous Section 4.2) we find a later warming and hence a delayed deglaciation (~~orange~~light blue). ~~As the forcing is defined as anomaly, which vanished towards~~ Ocean forcing likely plays a key role in warmer than present-climates. However, we do not see this effect in our simulations during the Last Interglacial. Although ocean temperatures rise by more than 1 K above present we find similar ice volumes as for present-day, in all our simulations. Precipitation scaling and the till properties seem to play an important role in stabilizing WAIS and preventing from collapse. However, a thorough investigation of necessary model settings for WAIS collapse during LIG would fill a separate study.

As we employ an anomaly forcing, which becomes near zero at present day, the modeled modern ice sheet configurations are rather independent of the applied ocean temperature forcing ~~applied. However, response functions require linearity, causality and stationarity.~~ (except for EDC, which is generally colder through the Holocene). Also, There is literature suggesting periods of decoupled ocean and surface temperature evolution (e.g. Antarctic Cold Reversal) with strong potential effects on the ice sheet deglaciation~~, which is discussed in Sect. A1~~. Appendix A1 provides an estimate of the effect of intermediate ocean warming events from a simple perturbation analysis with PICO.

Figure 22: Sensitivity of transient ice volume above flotation to varied ocean temperature forcing. Reference simulation (grey) is based on EDC+WDC surface temperature with fit response function of power $\alpha = 2$. The resulting ice volume change is similar for a fit response function with power $\alpha = 1$ (blue). Even if ocean temperature forcing responds immediately to surface temperature anomalies (~~green~~orange) the resulting effects on ice volume are comparably small. If different surface temperature reconstructions are used from EDC with $\alpha = 2$ (~~orange~~light blue), we find for later warming delayed deglaciation ~~accrodingly~~accordingly. If the amplitude of WDC surface temperature anomalies was 40% lower (~~red~~light orange), this would have only negligible effect on the modeled ice volume.

4.4 Precipitation forcing

820 Continental-scale precipitation change is closely related to temperature change. While colder ~~temperature~~ temperatures lead to slower ice flow and hence larger ice masses, they also lead to dryer conditions and hence to less ice mass accumulation. This effect is based on the Clausius-Clapeyron-relationship which suggests higher atmospheric moisture capacity and hence more accumulation in a warmer atmosphere. ~~Analysis~~ As average over the Antarctic continent, the analysis of ice core and mod-

825 eling data suggest ~~for the Antarctic continent~~ a linear scaling relationship between precipitation and temperature change of ~~$f_{p,l} = 5 \pm 1\,\% \, K^{-1}$ precipitation change per degree continental average temperature change~~ $f_{p,l} = 5 \pm 1\,\% \, K^{-1}$ (Frieler et al., 2015). In PISM simulations, precipitation forcing $P(t)$ is coupled directly to the temperature forcing $\Delta T(t)$ (Sect. 4.2) using an exponential relationship (Ritz et al., 1996; Quiquet et al., 2012, Eq. 2), which scales the present-day mean

830 precipitation field P_0 as

$$P(t) = P_0 \exp\left(f_p \, \Delta T(t)\right) \approx P_0 \left(1.0 + f_{p,l} \, \Delta T(t)\right). \tag{14}$$

The exponential function is hence compatible with the precipitation lapse correction (Eq.(10)) and it allows for easier comparisons with other studies that use power law relationships, e.g. with $f_p = \ln(2)/10$ for Pollard and DeConto (2009). In fact, precipitation change is depending very much on

835 the Antarctic region. In our simulations we use ~~for $\Delta T(t)$~~ a combination of temperature reconstructions from the EDC and WDC for $\Delta T(t)$ (see Sect. 4.2), for which the study by (Frieler et al., 2015) suggest slightly higher values of $f_{p,l} = 5.9 \pm 2.2\,\% \, K^{-1}$ and $f_{p,l} = 5.5 \pm 1.2\,\% \, K^{-1}$, respectively. In East Antarctica values are even slightly higher than in West Antarctica.

In glacial periods with much colder temperatures of $\Delta T = -10\,\mathrm{K}$, an exponential precipitation

840 change with $f_p = 7$–$9\,\% \, K^{-1}$ yields 50–60% less precipitation as compared to modern times. Without any temperature-scaled precipitation change our simulations suggest up to 7 m SLE thicker ice sheets at glacial maximum (cf. ~~orange and~~ grey and light blue line in Fig. 23). The reference value of $7\,\% \, K^{-1}$ precipitation change corresponds to more than 50% dryer conditions than present and about 3–4 m SLE less ice volume than for 5% K^{-1} (cf. ~~blue and grey~~ grey and blue line).

845 ~~There are also reconstructions~~ Reconstructions of precipitation at ice core sites~~available~~, e.g. at WDC (Buizert et al., 2015; Fudge et al., 2016), ~~which reveals precipitation change~~ reveal precipitation changes relative to present of up to -60% during ~~glacial maximum~~ LGM and up to 25% more precipitation through the ~~Holcene~~Holocene. Figure 23 shows the corresponding transient effects of reconstructed precipitation forcings on the ice sheet's volume above flotation ~~. The excess accumulation~~

850 (orange line). The additional accumulation during the Holocene at WDC prohibits deglaciation and causes a more than 10 m SLE larger modern ice sheet configuration. However, the reconstructed signal at WDC may be biased to some extent from a lapse-rate effect due to surface elevation changes during deglaciation (personal communication Eric Steig). ~~We hence choose 'PREC' as relevant climate forcing parameter in the large ensemble analysis in a bf companion paper~~Interestingly, we

855 find a similar ice volume response when applying no the lapse rate correction for changing surface elevation (as described in Eq. (10)), which also diminishes deglaciation (light orange in Figure 23 for the same precipitation forcing as the reference). The simulations hence suggest that the precipitation scaling parameter f_p is highly relevant for the ice sheet's extent at glacial maximum and will be considered as ensemble parameter 'PREC' in Albrecht et al. (2019) .
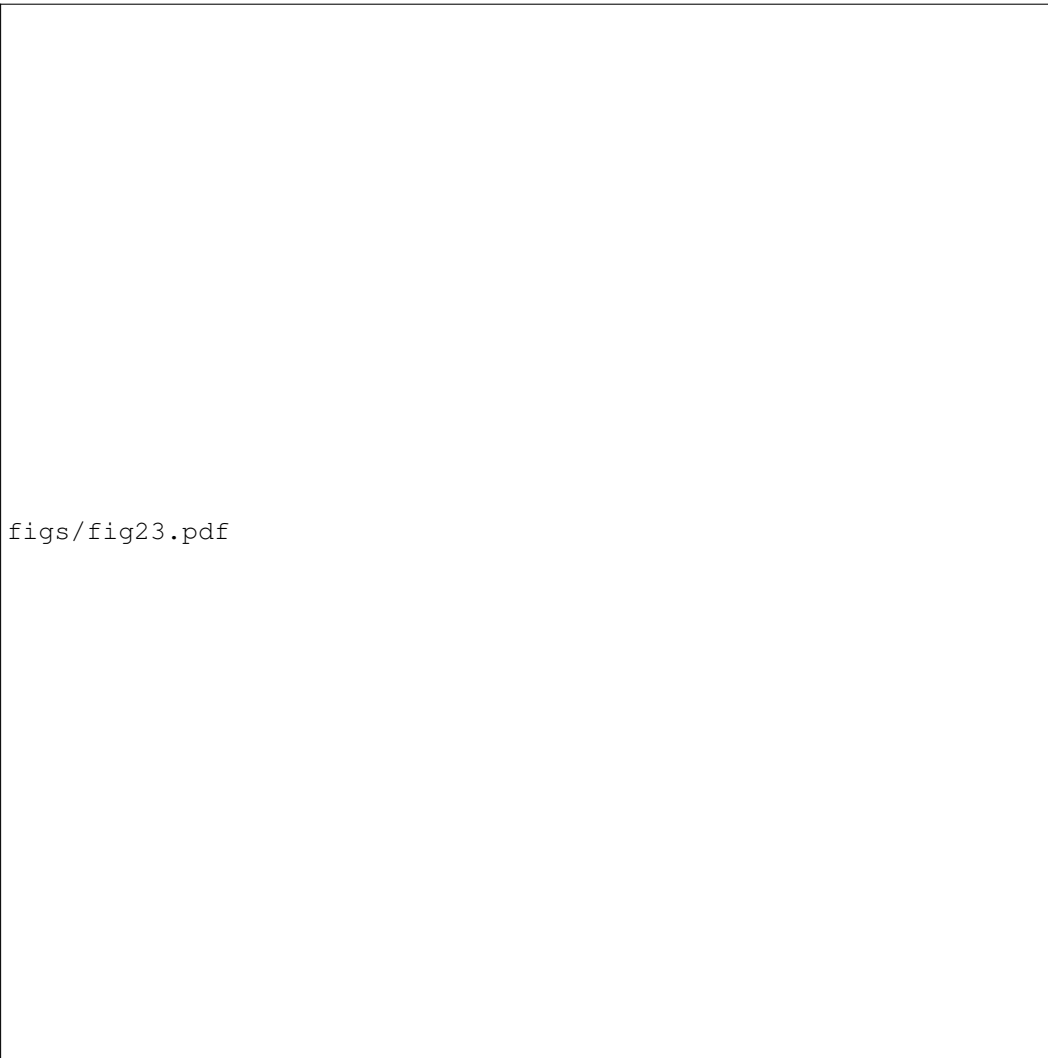
Figure 23: Sensitivity of transient ice volume above flotation to varied precipitation forcing. Grey curve is the reference with an exponential scaling factor of $7\%\,\mathrm{K}^{-1}$ with respect to WDC temperature reconstruction (Cuffey et al., 2016). Ice volume is slightly larger for $5\%\,\mathrm{K}^{-1}$ (blue) and much larger without precipitation forcing (~~orange~~light blue). Deglaciation is prohibited when using WDC accumulation reconstruction (Fudge et al., 2016) with additional accumulation during Holocene (~~green~~orange). A similar effect reveals when no lapse rate correction is applied for the precipitation (light orange).

4.5 Combined effects of climatic forcings in glacial cycle simulations

In our simulations with PISM the above described climatic forcings (Sections 4.1–4.4) have different effects on the Antarctic Ice Sheet evolution at different periods. Both, temperature and sea-level forcing reveal a periodic signature not only of the dominant 100 kyr orbital cycle, but with smaller amplitudes also of the higher-frequency cycles, e.g. MIS 3 around 57 kyr BP (Weichselian High Glacial) or the Last Glacial Maximum MIS 2 around 29 kyr BP (Lisiecki and Raymo, 2005). For glacial cycle simulations, sea-level forcing has the strongest effect on the ice volume, as it alone triggers larger glacial ice volume than in the reference simulation (see Fig. 24b, orange and grey). However, the rising sea-level during deglaciation alone induces only little ice sheet retreat. When sea-level forcing is turned off, the other forcings balance each other such that ice volume remains approximately at modern level through glacial periods (Fig. 24c). Also surface temperature forcing alone (Fig. 24b, blue) can produce glacial volumes of similar extent as sea-level forcing. If surface temperatures remain at modern level, the other forcings can still produce a glacial maximum volume that is only 3 m SLE lower than the reference. In our simulations, surface temperature anomalies also drive changes in ocean temperature and precipitation. Ocean temperatures forcing has only little effect on glacial extent, but it influences the onset of deglaciation (light orange). Without ocean forcing the interglacial (and modern) ice volume is up to 7 m SLE larger than the reference (Fig. 24c). While sea-level and temperature forcings cause a growth of ice sheets at glacial climates, precipitation forcing has an opposite effect (Fig. 24, light blue). Without precipitation the Antarctic Ice Sheet can reach glacial extents of up to 7 m SLE above the reference (coupled to the surface temperature forcing with $f_p = 7\%/K$). This result of the precipitation forcing for glacial climates also explains why the individual responses to the sea-level and the surface temperature forcing exceed the reference ice volume by about 3-4 m SLE, in which all four forcings are superimposed. We hence choose the precipitation scaling parameter 'PREC' as relevant climate forcing parameter in the ensemble analysis in Albrecht et al. (2019) .

Another recent study using the PSU-ISM ice sheet model also finds a dominance of atmospheric and sea-level forcing on the Antarctic ice volume over the last four glacial cycles (Tigchelaar et al., 2019), which together drive glacial-interglacial ice volume changes of 12–14 m SLE, while ocean temperature forcing is almost negligible, also during interglacials. Here, we do not want to go into the details of this study, which uses a comparably coarse output of an Earth System Model of intermediate complexity for the atmospheric and ocean forcing instead of a scaling with ice core temperature reconstructions. As a key result, Tigchelaar et al. (2019) find much smaller individual ice volume changes, which amount to less than half of the full ice volume response. In our simulations, however, the individual response to sea-level forcing (and surface temperature forcing) as well as the sum of all individual forcings exceed the combined response. This is partly due to the fact, that precipitation forcing (up to 50% less during glacial climate) provides a strong negative effect on the ice volume in full forcing case, which seems to be weaker in the "atm" forcing in Tigchelaar et al. (2019, ca. 15% in Fig. 8). If we consider the LGM and present-day state as rather stable states, a certain perturbation threshold need to be hit to initiate the (non-linear) transition (Termination I) into the other state. In our simulations this threshold can be reached with individual forcings, while in the other study the combined superposition is required.

5 Conclusions

In this study we have run PISM simulations of the Antarctic Ice Sheet over the last two glacial cycles~~and investigated the sensitivity of ice volume history to variations in~~. In the following we summarize the main findings of our sensitivity analysis with regard to the impact of different model parameter settings, boundary conditions and ~~climatic forcings.~~ climate forcing choices on the evolution of the Antarctic Ice Sheet. Table 2 provides a brief overview. Differences in ice volume above flotation ~~are~~ were characterized for specific periods~~of the Last Interglacial,~~, in particular for the Last Glacial Maximum (LGM) and for present day, while at Last Interglacial ice volumes were generally around 1 m SLE lower than present. During deglaciation, small perturbations can be amplified causing a strong divergence in the ice sheet response, ~~e.g. in the onset of deglaciation or in the maximum change rates. We quantify~~. We estimated the amount of model-intrinsic uncertainty ~~of up to 2~~to be around 1 m SLE for present-day climate conditions ~~, for different thermal initialization methods but otherwise identical model settings.~~ and much smaller for glacial conditions. Hence, simulated changes in interglacial ice volume due to ~~variation~~ variations in parameters or boundary conditions are considered ~~significant~~ "significant" when larger than ~~the~~ this intrinsic uncertainty.

~~We find consistent results within~~ Within this uncertainty range~~for grid resolution refinement~~, we found consistent results for the reference horizontal grid resolution of 16 km ~~or finer. Simulated ice volumes reveal only little variation for variation in SIA flow law exponent of $n_{STA} = 3 \pm 1$. However, in combination with variations of~~ and finer, while we did not find convergence for much

higher vertical resolution of to 1 m at the base. Regarding ice dynamical parameters, we found for the largest sensitivity for present day ice volume for variation of the SIA and SSA flow enhancement factors, as well as for the SSA flow law exponent~~over the same range, simulated ice volumes differ~~

925 ~~significantly by 2–7m SLE. Even more significant is the effect of the SIA enhancement factor with much thinner grounded ice for larger parameter values and a range of simulated ice volume of up to 11m SLE between ESIA=1–5. Increasing SSA enhancement factors cause faster deglaciation and hence thinner modern ice sheets with up to 7m SLE difference for the tested parameter range of ESSA=0.3–1.0, while in contrast volumes at LGM are rather unaffected. Calving parameters have~~

930 ~~only little effect on the simulated ice volume.~~, while ESIA also shows high sensitivity at LGM.

Processes at the interface of ice and bedrock are highly uncertain. For the application of different geothermal heat flux maps, we found largest sensitivities for the present-day state with more than 3 m SLE (standard deviation). Basal friction in PISM is associated with various hydrological and

935 microscale processes. ~~Basal roughness~~ Geological properties of the basal substrate expressed as till friction angle is a key parameter here. We ~~present~~ presented an optimization algorithm for till friction angle distribution to minimize the misfit to modern ~~ice thickness~~ grounded ice thickness (Sect. 3.4.2). However, ~~ice streams are reproduced~~ simulated ice streams were less confined than with a piecewise-linear parameterization dependent on bed topography. ~~Also, the procedure cannot help to constrain~~

940 ~~basal roughness on the continental shelf underneath the modern ice shelves. As modern~~ Modern ice shelf regions ~~are~~ were covered by grounded ice in glacial climates, ~~a~~ where till properties underneath the ice shelves are weakly constrained. A variation of minimal till friction angle ~~of $\phi_{\min} = 1.0°–5.0°$~~ ~~causes 3–5m SLE difference in ice volume above flotation for each degree, so in total up to 15~~ caused a simulated ice volume range of up to 8 m SLE~~difference over the tested range. Regarding~~. Also

945 variation of the hydrological model ~~part~~ parameters show large sensitivities, variations in till water decay rate and of the critical fraction of effective overburden pressure ~~within a plausible range of 1–10mm/yr and 2-8, respectively, reveal~~ revealed additional considerable uncertainties of ~~more than 10~~ up to 6 m SLE each. ~~For the effective overburden pressure, however, at least the uncertainty for modern climate conditions is much lower. Basal sliding in PISM can account for a dependence of~~

950 ~~basal shear stress and sliding velocity, varying~~ Variation of basal sliding from plastic till deformation to linear sliding ~~, expressed by the pseudo plastic exponent PPQ. Simulated ice volumes differ for this range of PPQ=0–1 by up to 10~~ in terms of the sliding exponent PPQ, also yields an ice volume uncertainty of more than 5 m SLE, ~~both for glacial and modern climate conditions~~ in particular at LIG and present day. The basal model components are consequently the least constrained and most

955 sensitive parts ~~for~~ in PISM glacial cycle simulations.

Within the coupled Earth model, ~~variations~~ an increase in mantle viscosities ~~over~~ by two orders of magnitude ~~cause~~ caused slower ice sheet growth but faster deglaciation for higher values. ~~PISM~~

~~simulations yield consistent present-day ice volumes for mantle viscosities of 5×10^{20}Pas or more.~~
~~The Earth model is interactively coupled with PISM, but it is not globally defined and has so far neglected changes of water masses around the ice sheet. We find~~ We found that the effect of changing ~~sea level~~ global mean sea level height and bed topography for the glacial isostatic adjustment and hence on grounding line migration is a relevant feedback~~amplifying~~, that amplifies the ice sheet growth for glacial climates by more than 5 m SLE. In contrast, ~~the sensitivity of ice volume evolution~~ we identified a comparably low sensitivity of glacial ice volume to variations of the elastic part of the Earth model, expressed via the parameter for flexural rigididy~~over a range of 5–100$\times10^{23}$Nm, is rather low with only a few meters SLE difference. Here we have run the latest PISM version v1.1 with a recent bug fix, revealing additional variability to glacial volume history~~.

In our study we ~~present~~ presented a parameterization for the ice surface temperature ~~close~~ fitted to modern reanalysis data, that accounts for changes in geometry and that can be easily used in combination with the PPD scheme ~~. However, PDD seems to be of minor relevance in Antarctic glacial cycle simulations. If annual-mean reanalysis temperatures are applied directly as modern boundary condition in combination with precipitation rates from the~~ (Sect. 3.1). Variation of PDD parameters or the consideration of more realistic temperature distributions from a regional climate model ~~Racmo2.3p2, both lapse corrected, we find similar ice volumes at Last Glacial Maximum, but delayed growth and somewhat earlier deglaciation. For the subsurface boundary, we find for geothermal heat flux maps from different available source comparably little difference in modeled LGM ice volume , in contrast to previous studies. The model spread of present-day ice volumes with up to 2m SLE is not significant.~~

or reanalysis data produce only insignificant changes is simulated ice volume history. In order to run glacial cycle simulations we have prescribed past external climatic ~~forcing~~ forcings for sea-level, ~~temperatures of the air and the ocean~~ surface air and ocean temperatures, and for precipitation. ~~Reconstructions of global mean sea level use different methodologies which differ both in LGM level as well as in the rate of change and timing of the last deglaciation, i.e. for the representation of meltwater pulse 1a (MWP1a). Hence, the simulated response of the Antarctic Ice Sheet can differ by up to 5~~For different reconstructions of sea-level and temperature forcing we found rather low ice volume sensitivities of below 1 ~~m SLE for different forcings.~~ m SLE at LGM and up to 2 m SLE at present day, but more than 3 m SLE for the precipitation forcing, for variation of the scaling parameter PREC. Ocean temperature change is modeled as a delayed response to changes of reconstructed air temperatures. The tested sensitivity to different response functions and air temperature reconstruction may not cover the full range of oceanic uncertainties, in particular for deglaciation and warmer than present climates. Further sensitivity experiments with focus on deglacial grounding line sensitivity, are discussed in the Appendix A). Sea level forcing is the most dominant forcing at play together with surface air temperature forcing, as each alone ~~can~~ could trig-

ger glaciation with ice volume growth of more than 12 m SLE above present. If no sea-level forcing ~~is~~ was applied, temperature and precipitation forcing balance each other and the Antarctic Ice Sheet ~~remains~~ remained at modern configuration even for glacial climate conditions ~~. Precipitation forcing in PISM can be coupled directly to temperature forcing or can be applied as fractional anomaly to reconstructed accumulation rates from WAIS Divide Core. For the latter case the Antarctic Ice Sheet does not retreat from its LGM configuration until present-day due to excess accumulation trough the Holocene. Regarding surface temperature reconstructions we compared changes with respect to the choice of available cores from EPICA Dome C or WAIS Divide Core, which show only little difference in the ice volume evolution. Even if the LGM temperatures were 40warmer, as recent discussions within the community suggest, we find similar glacial extents and a delayed but still effective deglaciation with less than 2.5m SLE difference. Ocean temperature change is modeled as delayed response to changes of reconstructed air temperatures. For different response functions and air temperature PISM-PICO simulates similar LGM states. However, the onset of deglaciation and hence present-day ice volume can differ by a few meters SLE. This means that, compared to the other forcings, ocean temperature forcing is of minor relevance for glacial cycle simulations. Hence, we have not varied PICO parameters in this study. Even if we enhance sub-shelf melting for 2,000 years at Antarctic Cold Reversal according to a 2K warming in the ocean, the Antarctic Ice Sheet responds with slightly earlier but slower retreat resulting in similar present-day states. We have identified model settings that allows for earlier deglacial retreat, among which the subglacial hydrology is the most dominant. But~~ (Sect. 4.5). However, in all simulations retreat ~~occurs~~ occured after MWP1a.

From the discussed model settings and boundary conditions~~we select~~, we select a total of four relevant parameters~~representative for each of~~, one each for the different sections ~~. Regarding~~ (Sect. 2: Ice sheet and Earth model parameters, Sect. 3: Boundary conditions and input datasets and Sect. 4: Climatic Forcing). Regarding the climatic forcing we identified the precipitation change rate PREC as ~~representative~~ the most relevant uncertain parameter within the range of 2–10%/K, for the Earth model the mantle viscosity VISC within the range of $1-100\times10^{20}$$0.1-10\times10^{21}$ Pa s, for the basal friction model the sliding exponent PPQ within the range 0.25–1.0 and for the internal ice flow dynamics the ESIA enhancement factor within the range 1–7. While ESIA and PREC are more relevant for the LGM configuration of the Antarctic Ice Sheet, VISC and PPQ determine the timing and rate of deglaciation to the present-day configuration, and are hence in particular relevant for the West Antarctic Ice Sheet. These parameter ranges define the dimensions of the ~~large ensemble~~parameter ensemble, which is presented and analyzed in the ~~companion paper .~~companion paper (Albrecht et al., 2019) .

We have shown, that PISM can be a powerful tool for paleo-simulations of Antarctic Ice Sheet evolution if ice sheet modelers take account of identified key uncertainties regarding model parameterization

and forcing choices.

1035

Author contributions

TA designed, ran and analyzed the ice sheet model experiments; TA and RW co-developed PISM and implemented processes relevant for application to the Antarctic Ice Sheet. RW and AL contributed to the interpretation of the results.

1040 ~~Code and data availability~~

Code and data availability

The PISM code used in this study can be obtained from https://github.com/talbrecht/pism_pik/tree/ pism_pik_1.0 and will be published with DOI ~~link~~reference. Results and plotting scripts are available upon request and will be published in www.PANGAEA.de. For now see jupyter notebook https:// 1045 nbviewer.jupyter.org/url/www.pik-potsdam.de/~albrecht/notebooks/paleo_paper_final.ipynb. PISM input data are preprocessed using https://github.com/pism/pism-ais with original data citations.

Competing interests

The authors declare that they have no conflicts of interest.

Supplementary Material

1050 Movie of reference PISM simulation of the Antarctic Ice Sheet over the past 210 kyr, Copernicus Publications: https://doi.org/10.5446/41779

Acknowledgements. Development of PISM is supported by NASA grant NNX17AG65G and NSF grants PLR-1603799 and PLR-1644277. Special thanks are due to Constantine Khroulev for many years of productive PISM code development and open-source maintenance. ~~PISM uses third-party PETScsolver libraries~~We also 1055 want to thank the PETSc[6] developers, who provide excellent third-party solver libraries for PISM. Also other open-source software was used in this study, in particular NumPy (www.numpy.org), CDO (https://code.mpimet. mpg.de/projects/cdo/), NCO (http://nco.sourceforge.net/) and matplotlib (https://matplotlib.org/). The authors gratefully acknowledge the European Regional Development Fund (ERDF), the German Federal Ministry of Education and Research and the Land Brandenburg for supporting this project by providing resources on the 1060 high performance computer system at the Potsdam Institute for Climate Impact Research. Computer resources for this project have been also provided by the Gauss Centre for Supercomputing/Leibniz Supercomputing Centre (www.lrz.de) under Project-ID pr94ga. T.A. is supported by the Deutsche Forschungsgemeinschaft (DFG)

---

[6]https://www.mcs.anl.gov/petsc/

in the framework of the priority program "Antarctic Research with comparative investigations in Arctic ice areas" by grant LE1448/6-1 and LE1448/7-1. We thank Melchior van Wessem for providing surface forcing

1065 data sets from RACMO2.3p2, Dick Peltier for the sea-level anomalies, Christo Buizert for the WDC temperature reconstructions before publication. We are also grateful to Xylar Asay-Davis, Thomas Kleiner, Matthias Mengel, Mark Pittard, Dave Pollard, Ronja Reese, Eric Steig, Aslak Grinsted and Pippa Whitehouse for very constructive discussions. Finally, we appreciate the helpful suggestions and comments by the reviewers Lev Tarasov and Johannes Sutter, which led us to considerable improvements of the manuscript.

References

Albrecht, T. and Levermann, A.: Spontaneous ice-front retreat caused by disintegration of adjacent ice shelf in Antarctica, Earth and Planetary Science Letters, 393, 26–30, 2014.

Albrecht, T., Winkelmann, R., and Levermann, A.: Glacial cycles simulation of the Antarctic Ice Sheet with PISM - Part 2: Parameter ensemble analysis, The Cryosphere Discussions, 2019, doi:10.5194/tc-2019-70, https://www.the-cryosphere-discuss.net/tc-2019-70/, 2019.

An, M., Wiens, D. A., Zhao, Y., Feng, M., Nyblade, A., Kanao, M., Li, Y., Maggi, A., and Lévêque, J.-J.: Temperature, lithosphere-asthenosphere boundary, and heat flux beneath the Antarctic Plate inferred from seismic velocities, Journal of Geophysical Research: Solid Earth, 120, 8720–8742, 2015.

Aschwanden, A. and Blatter, H.: Mathematical modeling and numerical simulation of polythermal glaciers, Journal of Geophysical Research: Earth Surface, 114, 2009.

Aschwanden, A., Bueler, E., Khroulev, C., and Blatter, H.: An enthalpy formulation for glaciers and ice sheets, Journal of Glaciology, 58, 441–457, doi:10.3189/2012JoG11J088, 2012.

Aschwanden, A., Fahnestock, M. A., and Truffer, M.: Complex Greenland outlet glacier flow captured, Nature communications, 7, 10 524, 2016.

Bahadory, T. and Tarasov, L.: LCice 1.0 – a generalized Ice Sheet System Model coupler for LOVE-CLIM version 1.3: description, sensitivities, and validation with the Glacial Systems Model (GSM version D2017.aug17), Geoscientific Model Development, 11, 3883–3902, doi:10.5194/gmd-11-3883-2018, https://www.geosci-model-dev.net/11/3883/2018/, 2018.

Bakker, P., Clark, P. U., Golledge, N. R., Schmittner, A., and Weber, M. E.: Centennial-scale Holocene climate variations amplified by Antarctic Ice Sheet discharge, Nature, 541, 72, 2017.

Barletta, V. R., Bevis, M., Smith, B. E., Wilson, T., Brown, A., Bordoni, A., Willis, M., Khan, S. A., Rovira-Navarro, M., Dalziel, I., et al.: Observed rapid bedrock uplift in Amundsen Sea Embayment promotes ice-sheet stability, Science, 360, 1335–1339, 2018.

Bentley, M. J., Ó Cofaigh, C., Anderson, J. B., Conway, H., Davies, B., Graham, A. G. C., Hillenbrand, C.-D., Hodgson, D. A., Jamieson, S. S. R., Larter, R. D., Mackintosh, A., Smith, J. A., Verleyen, E., Ackert, R. P., Bart, P. J., Berg, S., Brunstein, D., Canals, M., Colhoun, E. A., Crosta, X., Dickens, W. A., Domack, E., Dowdeswell, J. A., Dunbar, R., Ehrmann, W., Evans, J., Favier, V., Fink, D., Fogwill, C. J., Glasser, N. F., Gohl, K., Golledge, N. R., Goodwin, I., Gore, D. B., Greenwood, S. L., Hall, B. L., Hall, K., Hedding, D. W., Hein, A. S., Hocking, E. P., Jakobsson, M., Johnson, J. S., Jomelli, V., Jones, R. S., Klages, J. P., Kristoffersen, Y., Kuhn, G., Leventer, A., Licht, K., Lilly, K., Lindow, J., Livingstone, S. J., Massé, G., McGlone, M. S., McKay, R. M., Melles, M., Miura, H., Mulvaney, R., Nel, W., Nitsche, F. O., O'Brien, P. E., Post, A. L., Roberts, S. J., Saunders, K. M., Selkirk, P. M., Simms, A. R., Spiegel, C., Stolldorf, T. D., Sugden, D. E., van der Putten, N., van Ommen, T., Verfaillie, D., Vyverman, W., Wagner, B., White, D. A., Witus, A. E., and Zwartz, D.: A community-based geological reconstruction of Antarctic Ice Sheet deglaciation since the Last Glacial Maximum, Quaternary Science Reviews, 100, 1–9, doi:10.1016/j.quascirev.2014.06.025, 2014.

Bindschadler, R. A., Nowicki, S., Abe-Ouchi, A., Aschwanden, A., Choi, H., Fastook, J., Granzow, G., Greve, R., Gutowski, G., Herzfeld, U., et al.: Ice-sheet model sensitivities to environmental forcing and their use in projecting future sea level (the SeaRISE project), Journal of Glaciology, 59, 195–224, 2013.

Bintanja, R. and Van de Wal, R.: North American ice-sheet dynamics and the onset of 100,000-year glacial cycles, Nature, 454, 869–872, 2008.

Bons, P. D., Kleiner, T., Llorens, M.-G., Prior, D. J., Sachau, T., Weikusat, I., and Jansen, D.: Greenland Ice Sheet: Higher nonlinearity of ice flow significantly reduces estimated basal motion, Geophysical Research Letters, 45, 6542–6548, 2018.

Briggs, R., Pollard, D., and Tarasov, L.: A glacial systems model configured for large ensemble analysis of Antarctic deglaciation, The Cryosphere, 7, 1949–1970, 2013.

Briggs, R. D., Pollard, D., and Tarasov, L.: A data-constrained large ensemble analysis of Antarctic evolution since the Eemian, Quaternary Science Reviews, 103, 91–115, doi:10.1016/j.quascirev.2014.09.003, 2014.

Brondex, J., Gagliardini, O., Gillet-Chaulet, F., and Durand, G.: Sensitivity of grounding line dynamics to the choice of the friction law, Journal of Glaciology, 63, 854–866, 2017.

Bueler, E. and Brown, J.: Shallow shelf approximation as a "sliding law" in a thermomechanically coupled ice sheet model, Journal of Geophysical Research, 114, doi:10.1029/2008JF001179, 2009.

Bueler, E. and van Pelt, W.: Mass-conserving subglacial hydrology in the Parallel Ice Sheet Model version 0.6, Geoscientific Model Development, 8, 1613, 2015.

Bueler, E., Lingle, C. S., and Brown, J.: Fast computation of a viscoelastic deformable Earth model for ice-sheet simulations, Annals of Glaciology, 46, 97–105, 2007.

Buizert, C., Cuffey, K., Severinghaus, J., Baggenstos, D., Fudge, T., Steig, E., Markle, B., Winstrup, M., Rhodes, R., Brook, E., et al.: The WAIS Divide deep ice core WD2014 chronology–Part 1: Methane synchronization (68–31 ka BP) and the gas age–ice age difference, Climate of the Past, 11, 153–173, 2015.

Chen, B., Haeger, C., Kaban, M. K., and Petrunin, A. G.: Variations of the effective elastic thickness reveal tectonic fragmentation of the Antarctic lithosphere, Tectonophysics, 746, 412–424, 2018.

Cornford, S., Martin, D., Lee, V., Payne, A., and Ng, E.: Adaptive mesh refinement versus subgrid friction interpolation in simulations of Antarctic ice dynamics, Annals of Glaciology, 57, 1–9, 2016.

Cuffey, K. M. and Paterson, W. S. B.: The physics of glaciers, Academic Press, 2010.

Cuffey, K. M., Clow, G. D., Steig, E. J., Buizert, C., Fudge, T., Koutnik, M., Waddington, E. D., Alley, R. B., and Severinghaus, J. P.: Deglacial temperature history of West Antarctica, Proceedings of the National Academy of Sciences, 113, 14 249–14 254, http://www.usap-dc.org/view/dataset/600377, 2016.

de Fleurian, B., Werder, M. A., Beyer, S., Brinkerhoff, D. J., Delaney, I., Dow, C. F., Downs, J., Gagliardini, O., Hoffman, M. J., Hooke, R. L., et al.: SHMIP The subglacial hydrology model intercomparison Project, Journal of Glaciology, 64, 897–916, 2018.

DeConto, R. M. and Pollard, D.: Contribution of Antarctica to past and future sea-level rise, Nature, 531, 591–597, 2016.

Dee, D. P., Uppala, S., Simmons, A., Berrisford, P., Poli, P., Kobayashi, S., Andrae, U., Balmaseda, M., Balsamo, G., Bauer, d. P., et al.: The ERA-Interim reanalysis: Configuration and performance of the data assimilation system, Quarterly Journal of the royal meteorological society, 137, 553–597, 2011.

Depoorter, M. A., Bamber, J., Griggs, J., Lenaerts, J., Ligtenberg, S. R., Van den Broeke, M., and Moholdt, G.: Calving fluxes and basal melt rates of Antarctic ice shelves, Nature, 502, 89, 2013.

Doake, C., Corr, H., Rott, H., Skvarca, P., and Young, N.: Breakup and conditions for stability of the northern Larsen Ice Shelf, Antarctica, Nature, 391, 778, 1998.

Edwards, T. L., Brandon, M. A., Durand, G., Edwards, N. R., Golledge, N. R., Holden, P. B., Nias, I. J., Payne, A. J., Ritz, C., and Wernecke, A.: Revisiting Antarctic ice loss due to marine ice-cliff instability, Nature, 566, 58, 2019.

Falcini, F. A., Rippin, D. M., Krabbendam, M., and Selby, K. A.: Quantifying bed roughness beneath contemporary and palaeo-ice streams, Journal of Glaciology, 64, 822–834, 2018.

Feldmann, J. and Levermann, A.: Collapse of the West Antarctic Ice Sheet after local destabilization of the Amundsen Basin, Proceedings of the National Academy of Sciences, p. 201512482, doi:10.1073/pnas.1512482112, http://www.pnas.org/lookup/doi/10.1073/pnas.1512482112, 2015.

Feldmann, J. and Levermann, A.: From cyclic ice streaming to Heinrich-like events: the grow-and-surge instability in the Parallel Ice Sheet Model, The Cryosphere, 11, 1913–1932, 2017.

Feldmann, J., Albrecht, T., Khroulev, C., Pattyn, F., and Levermann, A.: Resolution-dependent performance of grounding line motion in a shallow model compared with a full-Stokes model according to the MISMIP3d intercomparison, Journal of Glaciology, 60, 353–360, doi:10.3189/2014JoG13J093, 2014.

Fogwill, C., Turney, C., Golledge, N., Etheridge, D., Rubino, M., Thornton, D., Baker, A., Woodward, J., Winter, K., Van Ommen, T., et al.: Antarctic ice sheet discharge driven by atmosphere-ocean feedbacks at the Last Glacial Termination, Scientific reports, 7, 39 979, 2017.

Fowler, A.: A theoretical treatment of the sliding of glaciers in the absense of cavitation, Phil. Trans. R. Soc. Lond. A, 298, 637–681, 1981.

Fox Maule, C., Purucker, M. E., Olsen, N., and Mosegaard, K.: Heat Flux Anomalies in Antarctica Revealed by Satellite Magnetic Data, Science, 309, 464–467, doi:10.1126/science.1106888, 2005.

Fretwell, P., Pritchard, H. D., Vaughan, D. G., Bamber, J. L., Barrand, N. E., Bell, R., Bianchi, C., Bingham, R. G., Blankenship, D. D., Casassa, G., Catania, G., Callens, D., Conway, H., Cook, A. J., Corr, H. F. J., Damaske, D., Damm, V., Ferraccioli, F., Forsberg, R., Fujita, S., Gim, Y., Gogineni, P., Griggs, J. A., Hindmarsh, R. C. A., Holmlund, P., Holt, J. W., Jacobel, R. W., Jenkins, A., Jokat, W., Jordan, T., King, E. C., Kohler, J., Krabill, W., Riger-Kusk, M., Langley, K. A., Leitchenkov, G., Leuschen, C., Luyendyk, B. P., Matsuoka, K., Mouginot, J., Nitsche, F. O., Nogi, Y., Nost, O. A., Popov, S. V., Rignot, E., Rippin, D. M., Rivera, A., Roberts, J., Ross, N., Siegert, M. J., Smith, A. M., Steinhage, D., Studinger, M., Sun, B., Tinto, B. K., Welch, B. C., Wilson, D., Young, D. A., Xiangbin, C., and Zirizzotti, A.: Bedmap2: improved ice bed, surface and thickness datasets for Antarctica, The Cryosphere, 7, 375–393, doi:10.5194/tc-7-375-2013, https://secure.antarctica.ac.uk/data/bedmap2/, 2013.

Frieler, K., Clark, P. U., He, F., Buizert, C., Reese, R., Ligtenberg, S. R. M., van den Broeke, M. R., Winkelmann, R., and Levermann, A.: Consistent evidence of increasing Antarctic accumulation with warming, Nature Climate Change, 5, 348–352, doi:10.1038/nclimate2574, 2015.

Fudge, T., Markle, B. R., Cuffey, K. M., Buizert, C., Taylor, K. C., Steig, E. J., Waddington, E. D., Conway, H., and Koutnik, M.: Variable relationship between accumulation and temperature in West Antarctica for the past 31,000 years, Geophysical Research Letters, 43, 3795–3803, http://www.usap-dc.org/view/dataset/601004, 2016.

Fürst, J. J., Durand, G., Gillet-Chaulet, F., Tavard, L., Rankl, M., Braun, M., and Gagliardini, O.: The safety band of Antarctic ice shelves, Nature Climate Change, 6, 479, 2016.

Gasson, E., DeConto, R., and Pollard, D.: Antarctic bedrock topography uncertainty and ice sheet stability, Geophysical Research Letters, 42, 5372–5377, 2015.

1190 Gillet-Chaulet, F., Durand, G., Gagliardini, O., Mosbeux, C., Mouginot, J., Rémy, F., and Ritz, C.: Assimilation of surface velocities acquired between 1996 and 2010 to constrain the form of the basal friction law under Pine Island Glacier, Geophysical Research Letters, 43, 2016.

Gladstone, R., Schäfer, M., Zwinger, T., Gong, Y., Strozz, T., Moore, J., Mottram, R., and Boberg, F.: Importance of basal processes in simulations of a surging Svalbard outlet glacier., Cryosphere Discussions, 7,

1195 2013.

Gladstone, R. M., Payne, A. J., and Cornford, S. L.: Parameterising the grounding line in flow-line ice sheet models, The Cryosphere, 4, 605–619, doi:10.5194/tc-4-605-2010, 2010.

Gladstone, R. M., Payne, A. J., and Cornford, S. L.: Resolution requirements for grounding-line modelling: sensitivity to basal drag and ice-shelf buttressing, Annals of glaciology, 53, 97–105, 2012.

1200 Gladstone, R. M., Warner, R. C., Galton-Fenzi, B. K., Gagliardini, O., Zwinger, T., and Greve, R.: Marine ice sheet model performance depends on basal sliding physics and sub-shelf melting, The Cryosphere, 11, 319–329, 2017.

Goelzer, H., Coulon, V., Pattyn, F., de Boer, B., and Van De Wal, R. S.: Brief communication: On calculating the sea-level contribution in marine ice-sheet models, The Cryosphere Discussions, 2019.

1205 Goldsby, D. and Kohlstedt, D.: Superplastic deformation of ice: Experimental observations, Journal of Geophysical Research: Solid Earth, 106, 11 017–11 030, 2001.

Golledge, N. R., Menviel, L., Carter, L., Fogwill, C. J., England, M. H., Cortese, G., and Levy, R. H.: Antarctic contribution to meltwater pulse 1A from reduced Southern Ocean overturning, Nature Communications, 5, doi:10.1038/ncomms6107, 00000, 2014.

1210 Golledge, N. R., Kowalewski, D. E., Naish, T. R., Levy, R. H., Fogwill, C. J., and Gasson, E. G.: The multi-millennial Antarctic commitment to future sea-level rise, Nature, 526, 421–425, 2015.

Golledge, N. R., Keller, E. D., Gomez, N., Naughten, K. A., Bernales, J., Trusel, L. D., and Edwards, T. L.: Global environmental consequences of twenty-first-century ice-sheet melt, Nature, 566, 65, 2019.

Gomez, N., Pollard, D., and Mitrovica, J. X.: A 3-D coupled ice sheet–sea level model applied to Antarctica

1215 through the last 40 ky, Earth and Planetary Science Letters, 384, 88–99, 2013.

Gomez, N., Pollard, D., and Holland, D.: Sea-level feedback lowers projections of future Antarctic Ice-Sheet mass loss, Nature communications, 6, 8798, 2015.

Halberstadt, A. R. W., Simkins, L. M., Anderson, J. B., Prothro, L. O., and Bart, P. J.: Characteristics of the deforming bed: till properties on the deglaciated Antarctic continental shelf, Journal of Glaciology, 64, 1014–

1220 1027, 2018.

Hay, C. C., Lau, H. C., Gomez, N., Austermann, J., Powell, E., Mitrovica, J. X., Latychev, K., and Wiens, D. A.: Sea level fingerprints in a region of complex Earth structure: The case of WAIS, Journal of Climate, 30, 1881–1892, 2017.

Huybrechts, P. and de Wolde, J.: The dynamic response of the Greenland and Antarctic ice sheets to multiple-

1225 century climatic warming, Journal of Climate, 12, 2169–2188, 1999.

Imbrie, J. D. and McIntyre, A.: SPECMAP time scale developed by Imbrie et al., 1984 based on normalized planktonic records (normalized O-18 vs time, specmap.017), 10.1594/PANGAEA.4417068, 2006.

Jouzel, J., Masson-Delmotte, V., Cattani, O., Dreyfus, G., Falourd, S., Hoffmann, G., Minster, B., Nouet, J., Barnola, J. M., Chappellaz, J., Fischer, H., Gallet, J. C., Johnsen, S., Leuenberger, M., Loulergue, L., Luethi, D., Oerter, H., Parrenin, F., Raisbeck, G., Raynaud, D., Schilt, A., Schwander, J., Selmo, E., Souchez, R., Spahni, R., Stauffer, B., Steffensen, J. P., Stenni, B., Stocker, T. F., Tison, J. L., Werner, M., and Wolff, E. W.: Orbital and Millennial Antarctic Climate Variability over the Past 800,000 Years, Science, 317, 793–796, doi:10.1126/science.1141038, 2007.

Kingslake, J., Scherer, R., Albrecht, T., Coenen, J., Powell, R., Reese, R., Stansell, N., Tulaczyk, S., Wearing, M., and Whitehouse, P.: Extensive retreat and re-advance of the West Antarctic ice sheet during the Holocene, Nature, 558, 430, 2018.

Kleiner, T., Rückamp, M., Bondzio, J. H., and Humbert, A.: Enthalpy benchmark experiments for numerical ice sheet models, The Cryosphere, 9, 217–228, doi:10.5194/tc-9-217-2015, https://www.the-cryosphere.net/9/217/2015/, 2015.

Konrad, H., Sasgen, I., Pollard, D., and Klemann, V.: Potential of the solid-Earth response for limiting long-term West Antarctic Ice Sheet retreat in a warming climate, Earth and Planetary Science Letters, 432, 254–264, 2015.

Lambeck, K., Rouby, H., Purcell, A., Sun, Y., and Sambridge, M.: Sea level and global ice volumes from the Last Glacial Maximum to the Holocene, Proceedings of the National Academy of Sciences, 111, 15 296–15 303, doi:10.1073/pnas.1411762111, 2014.

Larour, E., Seroussi, H., Morlighem, M., and Rignot, E.: Continental scale, high order, high spatial resolution, ice sheet modeling using the Ice Sheet System Model (ISSM), Journal of Geophysical Research: Earth Surface, 117, 2012.

Levermann, A., Albrecht, T., Winkelmann, R., Martin, M., Haseloff, M., and Joughin, I.: Kinematic first-order calving law implies potential for abrupt ice-shelf retreat, The Cryosphere, 6, 273–286, 2012.

Li, C., Storch, J.-S. v., and Marotzke, J.: Deep-ocean heat uptake and equilibrium climate response, Climate Dynamics, 40, 1071–1086, doi:10.1007/s00382-012-1350-z, 2012.

Lingle, C. S. and Clark, J. A.: A numerical model of interactions between a marine ice sheet and the solid earth: Application to a West Antarctic ice stream, Journal of Geophysical Research: Oceans, 90, 1100–1114, 1985.

Lisiecki, L. E.: Links between eccentricity forcing and the 100,000-year glacial cycle, Nature geoscience, 3, 349, 2010.

Lisiecki, L. E. and Raymo, M. E.: A Pliocene-Pleistocene stack of 57 globally distributed benthic δ18O records, Paleoceanography, 20, 2005.

Liu, J., Milne, G. A., Kopp, R. E., Clark, P. U., and Shennan, I.: Sea-level constraints on the amplitude and source distribution of Meltwater Pulse 1A, Nature Geoscience, 9, 130–134, doi:10.1038/ngeo2616, 2016.

Liu, Z., Otto-Bliesner, B., He, F., Brady, E., Tomas, R., Clark, P., Carlson, A., Lynch-Stieglitz, J., Curry, W., Brook, E., et al.: Transient simulation of last deglaciation with a new mechanism for Bølling-Allerød warming, Science, 325, 310–314, 2009.

Lliboutry, L. and Duval, P.: Various isotropic and anisotropic ices found in glaciers and polar ice caps and their corresponding rheologies: Ann Geophys V3, N2, March–April 1985, P207–224, in: International Journal of Rock Mechanics and Mining Sciences & Geomechanics Abstracts, vol. 22, p. 198, Pergamon, 1985.

Ma, Y., Gagliardini, O., Ritz, C., Gillet-Chaulet, F., Durand, G., and Montagnat, M.: Enhancement factors for grounded ice and ice shelves inferred from an anisotropic ice-flow model, Journal of Glaciology, 56, 805–812, http://www.ingentaconnect.com/content/igsoc/jog/2010/00000056/00000199/art00006, 2010.

1270   Maris, M., De Boer, B., Ligtenberg, S., Crucifix, M., Van De Berg, W., and Oerlemans, J.: Modelling the evolution of the Antarctic ice sheet since the last interglacial, The Cryosphere, 8, 1347–1360, 2014.

Martin, M. A., Winkelmann, R., Haseloff, M., Albrecht, T., Bueler, E., Khroulev, C., and Levermann, A.: The Potsdam Parallel Ice Sheet Model (PISM-PIK) – Part 2: Dynamic equilibrium simulation of the Antarctic ice sheet, The Cryosphere, 5, 727–740, doi:10.5194/tc-5-727-2011, http://www.the-cryosphere.net/5/727/2011/,

1275   2011.

Martos, Y. M., Catalán, M., Jordan, T. A., Golynsky, A., Golynsky, D., Eagles, G., and Vaughan, D. G.: Heat flux distribution of Antarctica unveiled, Geophysical Research Letters, 44, 2017.

Mengel, M. and Levermann, A.: Ice plug prevents irreversible discharge from East Antarctica, Nature Climate Change, 4, 451–455, doi:10.1038/nclimate2226, http://www.nature.com/doifinder/10.1038/nclimate2226,

1280   2014.

Mengel, M., Feldmann, J., and Levermann, A.: Linear sea-level response to abrupt ocean warming of major West Antarctic ice basin, Nature Climate Change, 6, 71–74, 2016.

Mikkelsen, T. B., Grinsted, A., and Ditlevsen, P.: Influence of temperature fluctuations on equilibrium ice sheet volume, The Cryosphere, 12, 39–47, 2018.

1285   Morlighem, M., Williams, C. N., Rignot, E., An, L., Arndt, J. E., Bamber, J. L., Catania, G., Chauché, N., Dowdeswell, J. A., Dorschel, B., et al.: BedMachine v3: Complete bed topography and ocean bathymetry mapping of Greenland from multibeam echo sounding combined with mass conservation, Geophysical research letters, 44, 2017.

Nowicki, S. M., Payne, A., Larour, E., Seroussi, H., Goelzer, H., Lipscomb, W., Gregory, J., Abe-Ouchi, A.,

1290   and Shepherd, A.: Ice Sheet Model Intercomparison Project (ISMIP6) contribution to CMIP6, Geoscientific Model Development, 9, 4521, 2016.

Pattyn, F.: The paradigm shift in Antarctic ice sheet modelling, Nature communications, 9, 2728, 2018.

Pattyn, F., Perichon, L., Durand, G., Favier, L., Gagliardini, O., Hindmarsh, R. C., Zwinger, T., Albrecht, T., Cornford, S., Docquier, D., et al.: Grounding-line migration in plan-view marine ice-sheet models: results of

1295   the ice2sea MISMIP3d intercomparison, Journal of Glaciology, 59, 410–422, 2013.

Pittard, M., Galton-Fenzi, B., Roberts, J., and Watson, C.: Organization of ice flow by localized regions of elevated geothermal heat flux, Geophysical Research Letters, 43, 3342–3350, 2016.

Pollard, D. and DeConto, R.: Description of a hybrid ice sheet-shelf model, and application to Antarctica, Geoscientific Model Development, 5, 1273, 2012a.

1300   Pollard, D. and DeConto, R. M.: Modelling West Antarctic ice sheet growth and collapse through the past five million years, Nature, 458, 329–332, 2009.

Pollard, D. and DeConto, R. M.: A simple inverse method for the distribution of basal sliding coefficients under ice sheets, applied to Antarctica, The Cryosphere, 6, 953–971, doi:10.5194/tc-6-953-2012, http://www.the-cryosphere.net/6/953/2012/, 2012b.

1305 Pollard, D., Chang, W., Haran, M., Applegate, P., and DeConto, R.: Large ensemble modeling of the last deglacial retreat of the West Antarctic Ice Sheet: comparison of simple and advanced statistical techniques, Geosci. Model Dev., 9, 1697–1723, doi:10.5194/gmd-9-1697-2016, 2016.

Pollard, D., Gomez, N., and Deconto, R. M.: Variations of the Antarctic Ice Sheet in a Coupled Ice Sheet-Earth-Sea Level Model: Sensitivity to Viscoelastic Earth Properties, Journal of Geophysical Research: Earth
1310 Surface, 122, 2124–2138, 2017.

Purucker, M.: Geothermal heat flux data set based on low resolution observations collected by the CHAMP satellite between 2000 and 2010, and produced from the MF-6 model following the technique described in Fox Maule et al.(2005), 2013.

Quiquet, A., Punge, H. J., Ritz, C., Fettweis, X., Gallée, H., Kageyama, M., Krinner, G., Salas y Mélia, D.,
1315 and Sjolte, J.: Sensitivity of a Greenland ice sheet model to atmospheric forcing fields, The Cryosphere, 6, 999–1018, doi:10.5194/tc-6-999-2012, https://www.the-cryosphere.net/6/999/2012/, 2012.

Reese, R., Albrecht, T., Mengel, M., Asay-Davis, X., and Winkelmann, R.: Antarctic sub-shelf melt rates via PICO, The Cryosphere, 12, 1969, 2018.

Ritz, C., Fabre, A., and Letréguilly, A.: Sensitivity of a Greenland ice sheet model to ice flow and ablation
1320 parameters: consequences for the evolution through the last climatic cycle, Climate Dynamics, 13, 11–23, 1996.

Schmidtko, S., Heywood, K. J., Thompson, A. F., and Aoki, S.: Multidecadal warming of Antarctic waters, Science, 346, 1227–1231, 2014.

Schoof, C.: The effect of cavitation on glacier sliding, in: Proceedings of the Royal Society of London A:
1325 Mathematical, Physical and Engineering Sciences, vol. 461, pp. 609–627, The Royal Society, 2005.

Schoof, C.: Variational methods for glacier flow over plastic till, Journal of Fluid Mechanics, 555, 299–320, 2006.

Schoof, C.: Marine ice-sheet dynamics. Part 1. The case of rapid sliding, Journal of Fluid Mechanics, 573, 27, doi:10.1017/S0022112006003570, 2007a.

1330 Schoof, C.: Ice sheet grounding line dynamics: Steady states, stability, and hysteresis, Journal of Geophysical Research, 112, doi:10.1029/2006JF000664, http://doi.wiley.com/10.1029/2006JF000664, 2007b.

Schoof, C.: Coulomb friction and other sliding laws in a higher-order glacier flow model, Mathematical Models and Methods in Applied Sciences, 20, 157–189, 2010.

Shapiro, N. M. and Ritzwoller, M. H.: Inferring surface heat flux distributions guided by a global seismic model:
1335 particular application to Antarctica, Earth and Planetary Science Letters, 223, 213–224, 2004.

Siegert, M. J., Jamieson, S. S., and White, D.: Exploration of subsurface Antarctica: uncovering past changes and modern processes, Geological Society, London, Special Publications, 461, 1–6, 2018.

Simmons, A.: ERA-Interim: New ECMWF reanalysis products from 1989 onwards, ECMWF newsletter, 110, 25–36, 2006.

1340 Spratt, R. M. and Lisiecki, L. E.: A Late Pleistocene sea level stack, Climate of the Past, 12, 1079, 2016.

Stuhne, G. and Peltier, W.: Assimilating the ICE-6G_C Reconstruction of the Latest Quaternary Ice Age Cycle Into Numerical Simulations of the Laurentide and Fennoscandian Ice Sheets, Journal of Geophysical Research: Earth Surface, 122, 2324–2347, 2017.

Stuhne, G. R. and Peltier, W. R.: Reconciling the ICE-6G_C reconstruction of glacial chronology with ice sheet dynamics: The cases of Greenland and Antarctica, Journal of Geophysical Research: Earth Surface, 120, 2015JF003 580, doi:10.1002/2015JF003580, 2015.

Sun, S., Cornford, S., Liu, Y., and Moore, J. C.: Dynamic response of Antarctic ice shelves to bedrock uncertainty, The Cryosphere, 8, 1561–1576, 2014.

Sutter, J., Fischer, H., Grosfeld, K., Karlsson, N. B., Kleiner, T., Van Liefferinge, B., and Eisen, O.: Modelling the Antarctic Ice Sheet across the mid-Pleistocene transition–implications for Oldest Ice, The Cryosphere, 13, 2023–2041, 2019.

The PISM authors: PISM, a Parallel Ice Sheet Model: User's Manual, http://pism-docs.org/sphinx/, based on revision stable v.1.0 edn., 2017.

Tigchelaar, M., Timmermann, A., Friedrich, T., Heinemann, M., and Pollard, D.: Nonlinear response of the Antarctic Ice Sheet to late Quaternary sea level and climate forcing, The Cryosphere, 13, 2615–2631, doi:10.5194/tc-13-2615-2019, https://www.the-cryosphere.net/13/2615/2019/, 2019.

Tulaczyk, S., Kamb B., and Engelhardt, H.F.: Basal mechanics of Ice Stream B, West Antarctica 1. Till mechanics, Journal of Geophysical Research, 105, 463–481, 2000.

Van de Berg, W., Van den Broeke, M., Reijmer, C., and Van Meijgaard, E.: Characteristics of the Antarctic surface mass balance, 1958–2002, using a regional atmospheric climate model, Annals of Glaciology, 41, 97–104, 2005.

Weber, M. E., Clark, P. U., Kuhn, G., Timmermann, A., Sprenk, D., Gladstone, R., Zhang, X., Lohmann, G., Menviel, L., Chikamoto, M. O., Friedrich, T., and Ohlwein, C.: Millennial-scale variability in Antarctic ice-sheet discharge during the last deglaciation, Nature, 510, 134–138, doi:10.1038/nature13397, 00002, 2014.

Werner, M., Jouzel, J., Masson-Delmotte, V., and Lohmann, G.: Reconciling glacial Antarctic water stable isotopes with ice sheet topography and the isotopic paleothermometer, Nature communications, 9, 3537, 2018.

Wessem, J. M. v., Berg, W. J. v. d., Noël, B. P., Meijgaard, E. v., Amory, C., Birnbaum, G., Jakobs, C. L., Krüger, K., Lenaerts, J., Lhermitte, S., et al.: Modelling the climate and surface mass balance of polar ice sheets using RACMO2–Part 2: Antarctica (1979–2016), The Cryosphere, 12, 1479–1498, 2018.

Whitehouse, P. L.: Glacial isostatic adjustment modelling: historical perspectives, recent advances, and future directions, Earth Surface Dynamics, 6, 401–429, 2018.

Whitehouse, P. L., Bentley, M. J., Milne, G. A., King, M. A., and Thomas, I. D.: A new glacial isostatic adjustment model for Antarctica: calibrated and tested using observations of relative sea-level change and present-day uplift rates, Geophysical Journal International, 190, 1464–1482, 2012.

Whitehouse, P. L., Gomez, N., King, M. A., and Wiens, D. A.: Solid Earth change and the evolution of the Antarctic Ice Sheet, Nature communications, 10, 503, 2019.

Winkelmann, R. and Levermann, A.: Linear response functions to project contributions to future sea level, Climate dynamics, 40, 2579–2588, 2013.

Winkelmann, R., Martin, M. A., Haseloff, M., Albrecht, T., Bueler, E., Khroulev, C., and Levermann, A.: The Potsdam Parallel Ice Sheet Model (PISM-PIK) – Part 1: Model description, The Cryosphere, 5, 715–726, doi:10.5194/tc-5-715-2011, 2011.

Winkelmann, R., Levermann, A., Ridgwell, A., and Caldeira, K.: Combustion of available fossil fuel resources sufficient to eliminate the Antarctic Ice Sheet, Science advances, 1, e1500 589, 2015.

1385 Yu, H., Rignot, E., Morlighem, M., and Seroussi, H.: Iceberg calving of Thwaites Glacier, West Antarctica: full-Stokes modeling combined with linear elastic fracture mechanics, The Cryosphere, 11, 1283–1296, 2017.

Appendix A: Perturbation experiments

A1   Ocean forcing pulse at Antarctic Cold reversal

Recent studies of coupled ice sheet and ocean dynamics (e.g. Golledge et al., 2014; Fogwill et al., 2017) suggest
the idea of a positive feedback mechanism causing episodes of accelerated ice-sheet recession as
result of enhanced sub-shelf melt, in particular in an ocean warming event during the Antarctic
Cold Reversal coincident with meltwater pulse 1A. For comparably small changes in ocean forcing
(≈ 0.25 K) Golledge et al. (2014) find a three-fold mass loss from the Antarctic Ice Sheet (up to
$6\,\mathrm{mm\,yr^{-1}}$). We ran a similar sensitivity experiment with an additional ocean temperature forcing of
$1\,\mathrm{K}$ and $2\,\mathrm{K}$ entering the PICO module causing enhanced sub shelf melt. This range covers the
anomaly found in GCM ocean temperature reconstructions from TraCE-21ka (Liu et al., 2009),
averaged over 600-2,800m depth and south of 66°S.

Compared to our reference run with only $0.25\,\mathrm{m}$ SLE contribution during the period of two
millenia (grey), we detect enhanced melt during ACR (see grey bar and dotted vertical lines in
Fig. A.1) with a change in volume above flotation of $0.5\,\mathrm{m}$ SLE (blue) and $1.6\,\mathrm{m}$ SLE (orange) in
the sensitivity experiments, which corresponds to a mean sea-level contribution rate of $0.25\,\mathrm{mm\,yr^{-1}}$
and $0.82\,\mathrm{mm\,yr^{-1}}$, respectively. Even though the ocean temperature forcing in the sensitivity experiments
exceeds present-day level (with melt rates in the Ross and Weddell Sea above $1\,\mathrm{m\,yr^{-1}}$), its effect
on ice volume seems comparably small, as grounding lines extended to the shallow edge of the
continental shelf with rather small ice shelves attached. Accordingly, PICO responds with less
overturning and melt as it would for a modern configuration of the Antarctic Ice Sheet and ice
shelves. For stronger ocean forcing early in the deglaciation phase ($1\,\mathrm{K}$ and $2\,\mathrm{K}$) we find a more
gradual ice volume retreat later in the Holocene and a 1-$2\,\mathrm{m}$ SLE larger present-day ice volume.

Figure A.1: Simulation over two glacial cycles (only last 20 kyr shown here) with different ocean temperature forcing increased by 1 K or 2 K in the two-millenia phase (14.6-12.7 kyr BP) of the Antarctic Cold Reversal after MWP1a (upper panel). Within this range, for comparison, the reconstructed GCM ocean temperature data from TraCE-21ka is shown as average over 600-2,800m depth and south of 66°S (green). The additional melt causes a doubling or even 6-fold increase in early ice volume losses, respectively, but most of the ice sheet retreat is somewhat delayed.

A2   Grounding line sensitivity

It remains an open question how much Antarctic deglaciation contributed to the the MWP1a. A timeseries of well-dated sediment data of iceberg-rafted debris (Weber et al., 2014) suggest that the main retreat of the Antarctic Ice Sheet occurred at 14.6 kyr BP, synchronously with MWP1a, while the RAISED Consortium concluded on an a later retreat with a relatively small Antarctic contribution

to MWP1a (Bentley et al., 2014) . Yet, in our reference simulation the main retreat occurs not before 10 kyr BP. From our sensitivity experiments we can identify relevant model parameters and boundary conditions that affect the stability of the grounding line and hence the onset of the last deglaciation.

In PISM the location of the grounding line is determined by the flotation condition (cf. $H = h_f$ in Eq. (6)), while at the same time it affects the overall stress balance and hence the ice sheet evolution. PISM simulates sub-grid basal friction according to interpolated grounding line location between grounded ice sheet and floating ice shelf (Gladstone et al., 2010) . Hence, grounding-line migration can be reasonable well represented in PISM (compared to full Stokes), even for coarse resolutions (Pattyn et al., 2013; Feldmann et al., 2014) . The sensitivity of grounding line motion also depends on applied boundary conditions. The availability of sub-glacial or sub-shelf melt water in the vicinity of the grounding line may enhance ice flow or thinning, respectively. These model choices can induce some additional uncertainty, as has been indicated in Golledge et al. (2015) .

Saturated till at the grounding line hampers grounding line advance and amplifies grounding line retreat (see Fig. A.2, orange and light orange vs. grey). A more slippery grounding line, as often been enforced in PISM simulations in previous studies (e.g. Golledge et al., 2015) , appears to have similar effect as the model improvement described in Sect. 3.4.3. Both show slower ice sheet growth and much earlier deglaciation from a less extended glacial state. PISM can interpolate basal melt across the grounding zone boundary using the same interpolation scheme as for the basal shear stress (Sect. 1.1). In the reference simulation, the interpolation has been not applied correctly, such that the effect of basal melting as calculated from PICO was underestimated. We find earlier deglaciation from a similar glacial state as in the reference simulation, when the melt interpolation is not applied or applied correctly[7] (blue and light blue in Fig. A.2, respectively). Be aware that PICO melt rates are only defined underneath the ice shelf and interpolation to the grounded ice sheet may jeopardize energy and mass conservation within PICO. Another aspect that can potentially affect till water content and hence sliding in ice stream regions is related to the temperate ice thermal conductivity ratio. This parameter is used to simulate a physical jump condition in the enthalpy gradient for temperate ice at the base, such that the energy at the base is balanced by the basal melting (Kleiner et al., 2015) . In the reference simulation we use a very low temperate ice thermal conductivity ratio of CR=1×10^{-5} as suggested by Kleiner et al. (2015) . However, this ratio does not seem to affect the cold-temperate transition surface and hence the ice volume history in PISM much, even when varied over four orders of magnitude (default value CR=0.1, see light orange line in Fig. A.2).

---

[7] https://github.com/pism/pism/pull/441

Figure A.2: Sensitivity of transient ice volume above flotation to varied conditions at the grounding line. Grey curve is the reference with applied sub-grid basal shear stress and old basal melt interpolation, which generally underestimates melting at the grounding line. Without basal melt interpolation (blue) or with fixed basal melt interpolation (light blue), deglaciation occurs hence earlier than in the reference, while glacial maximum extent is comparable. Glacial ice sheet growth is even slower for enforced saturated till conditions along the marine sections of the grounding line, landward (orange) or on the ocean side of the grounding line (light orange). The much higher sensitivity of the ice sheet volume to oceanic forcing yields a smaller glacial ice volume and much earlier deglaciation. The effect of variation of the temperate ice conductivity ratio over four orders of magnitude has only little effect, with slightly larger interglacial ice volumes for larger ratios (purple).

~~Physical constants and parameter values.~~

~~Parameter~~ **Name**	~~Value Units Physical~~ **Parameter** meaning ~~ρ_τ~~	~~910~~ **Range**	~~kg m^{-3}~~ **Unit**
~~ρ_w~~	~~1000~~	~~kg m^{-3}~~	~~Water density g~~
~~A_o~~	~~3.61×10^{14}~~ reference simulation	~~m^2~~	~~Surface area of world ocean c_a~~
~~f_o~~	~~0.75~~ enthalpy spin-up (Fig.1)	climate	~~Amplification factor ocean to global mean temperature f_s~~
~~τ_τ height~~ E_{SIA} **(ESIA)**	~~3000~~ **SIA flow enhancement** (Fig.3)	yr ~~1–5~~	~~Typical response time in intermediate ocean temperature K~~
~~H_{cr}~~ E_{SSA}	~~0–225 (75~~ SSA flow enhancement (Fig.3)	~~m~~ 0.3–1.0	~~Thickness calving threshold~~
~~n~~ n_{SIA}	~~2–4 (3~~ SIA flow law exponent (Fig.4)	~~2–4~~	~~Exponent in Glen's flow law~~
~~E_{SSA}~~ n_{SSA}	~~0.3–1.0 (0.6~~ SSA flow law exponent (Fig.4)	~~2–4~~	~~Enhancement factor for SSA stress balance~~
~~E_{SIA} (ESIA)~~ dz	~~1–7 (2~~ vertical resolution (Fig.5)	~~1–40~~	~~Enhancement factor for SIA stress balance~~ m
~~f_p (PREC)~~ K	~~2–10 (7~~ Eigencalving parameter (Fig.6)	~~K^{-1}~~ 10^{16}-10^{18}	~~Relative precipitation change with air temperature~~ m s
~~η (VISC)~~ H_{cr}	~~1–100 (5) $\times 10^{19}$~~ calving thickness (Fig.6)	~~Pas~~ 75–225	~~Earth upper mantle viscosity~~ m
~~D height~~ η **(VISC)**	~~5–100 (50) $\times 10^{23}$~~ **upper mantle viscosity** (Fig.7a)	~~0.1–10 $\times 10^{21}$~~	N m
~~ϕ_{min}~~ D	~~0.5–5 (2~~ flexural rigidity (Fig.7b)	~~$^\circ$~~ 0.5–10 $\times 10^{24}$	~~Minimal till friction angle in marine parts~~ Pa s
q ~~(PPQ)~~ **(PPQ)**	**pseudo plastic exp.** (Fig.13)	0–1 ~~(~~	
ϕ	till friction angle (Fig.15a)	~~param~~	~~Basal friction exponent in Eq.~~ u_0 $^\circ$
~~N_0~~ ϕ_{min}	~~1000~~ min till friction angle (Fig.15b)	~~Pa~~ 1–5	~~Reference effective pressure~~ $^\circ$
~~δ~~ C_d	~~0.02–0.1 (0.04~~ till water decay (Fig.17a)	1–10	~~Parameter determining effective overburden pressure δP_0 e_0~~ mm yr^{-1}
~~C_c~~ δ	~~0.12~~ fr. eff. overburden pres. (Fig.17b)	2–8	~~Till compressibility W_{max}~~ %
~~C_d~~ G	~~0.001–0.01 (0.001)~~ geothermal heatflux (Fig.12a)	~~m yr^{-1}~~ datasets	~~Till drainage rate~~ mW m^{-2}
~~b~~ f_p **(PREC)**	**precipitation scaling** (Fig.23)	0-7	~~m~~ % K^{-1}
~~H~~ σ_{PDD}	stnd of daily temp. (Fig.10)	~~m~~ 0–5	~~Ice thickness~~
~~z_{sl}~~ T_s	temperature forcing (Fig.10)	datasets	~~m~~
~~τ_c~~ Δz_{sl}	sea-level forcing (Fig.18)	datasets	m
ΔT_s	surface temp. forcing (Fig.19)	icecores	K
ΔT_o	ocean temp. forcing (Fig.22)	param	K

5 ~~Perturbation experiments~~

4.1 ~~Energy spin-up procedure and intrinsic memory~~

~~In the introduction to PISM (Sect. 1.1) we have briefly described a spin-up procedure, which results in a three-dimensional enthalpy field that is in balance with the modern climate boundary conditions (see Sect. 3). We assume hereby that present-day conditions have been similar to those in the penultimate interglacial (210kyr BP). As the three-dimensional enthalpy field carries the memory of past climate conditions, a more realistic spin-up climatic boundary condition may be achieved when the temperature reconstruction of the previous glacial cycles (EDC, see Sect. 4.2) or the long-range mean is used as anomaly forcing, while the ice sheet geometry remains fixed at present-day observations (Bedmap2; Fretwell et al., 2013). Here we investigate to what extent the choice of the temperature forcing in the enthalpy field spin-up can affect subsequent full-dynamics simulations over the last two glacial cycles until present.~~

~~Simulations are conducted with identical model settings and climate forcing but different initial energy states. The modeled ice volumes converge at glacial maxima with less than 0.2m SLE difference among the three simulations. As deglaciation can be delayed by a few thousand years modern ice volume can differ by up to 2m SLE (see Fig. 1 around time 0 BP). Also the full-physics spin-up over four glacial cycles reveals comparable differences to the reference (Fig. ??). In order to evaluate to what extent the sensitivity of the simulation results to changes in the energy initialization method is related to a memory effect (that should vanish) or to deterministic chaos, we continues the simulations for the same glacial climate forcing (but now different geometries), such that simulations ran for 420kyr and 630kyr in total. Interestingly, simulated ice volumes diverge to some extent during interglacial states. As deglaciation reveals nonlinear threshold behavior it can amplify small differences at glacial maxima. Ice thickness variations of up to 1000m are found mainly in the large ice shelf basins of Ross (Siple Coast), Amery and Ronne-Filchner (Bungenstock), see Fig. 2, mostly determined by the location of the migrating grounding line. Hence, the remaining deviations can be interpreted as model-internal uncertainty and should be kept in mind when comparing and evaluating ensembles of Antarctic ice volume reconstructions. Comparably small differences in initial conditions could be also related to numerical settings, such as number of CPU. Simulations over two last glacial cycles (repeated three times in a row, indicated by vertical dotted lines) with identical parameter settings but based on different spin-up procedures with prescribed initial ice sheet geometry, in which the three-dimensional ice enthalpy field (and basal melt pattern) adjusts to climatic boundary conditions. In grey initialization method as used in reference simulations. Present-day maximum ice thickness difference of three simulations after three rounds of two-glacial-cycle simulations with identical model settings, but for different initial enthalpy states (cf. final state in Fig. 1). In particular Siple Coast and Amery trough show most variations of more than 1km ice thickness. Simulation over last four glacial cycles (423kyr) compared to reference simulation over last two glacial cycles (210kyr) with identical parameters.~~

4.1 ~~Ocean forcing pulse~~ 70 ~~at Antarctic Cold reversal~~

~~Recent studies of coupled ice sheet and ocean dynamics (e.g. Golledge et al., 2014; Fogwill et al., 2017) suggest the idea of a positive feedback mechanism causing episodes of accelerated ice-sheet recession as result of enhanced sub-shelf melt, in particular in an ocean warming event during Antarctic Cold Reversal coincident with meltwater pulse 1A. For comparably small changes in ocean forcing (≈ 0.25K) Golledge et al. (2014) find a three-fold mass loss from the Antarctic Ice Sheet (up to 6mmyr^{-1}). We ran a similar sensitivity experiment with~~